3364

NAME OF AUTHOR.....LI-TSUN CHEN...........................

TITLE OF THESIS...Primordia of the lymphoid organs of..

...the chicken.................................

UNIVERSITY.........University of Alberta, Edmonton..........

DEGREE....Ph.D...............YEAR GRANTED...1968..........

Permission is hereby granted to THE NATIONAL

LIBRARY OF CANADA to microfilm this thesis and to

lend or sell copies of the film.

The author reserves other publication rights,

and neither the thesis nor extensive extracts from

it may be printed or otherwise reproduced without

the author's written permission.

(Signed).......................

PERMANENT ADDRESS:

.11252-59.Avenue..

Edmonton, Alberta

Canada

DATED..December.20..1968

NL-91

THE UNIVERSITY OF ALBERTA

PRIMORDIA OF THE LYMPHOID ORGANS OF THE CHICKEN

by

(C) LI-TSUN CHEN

A THESIS

SUBMITTED TO THE FACULTY OF GRADUATE STUDIES IN
PARTIAL FULFILMENT OF THE REQUIREMENTS FOR THE
DEGREE OF

DOCTOR OF PHILOSOPHY

DEPARTMENT OF ZOOLOGY

EDMONTON, ALBERTA

Date .*Oct. 25 1968.*..

UNIVERSITY OF ALBERTA

FACULTY OF GRADUATE STUDIES

The undersigned certify that they have read,
and recommend to the Faculty of Graduate Studies for
acceptance, a thesis entitled Primordia of the Lymphoid
Organs of the Chicken submitted by Li-tsun Chen in
partial fulfilment of the requirements for the degree of
Doctor of Philosophy.

Date.. Oct 21, 1968 ....

External Examiner

ABSTRACT

The thymus and the bursa of Fabricius are the first
lymphoid organs of the chicken. They appear on the fifth
day of incubation as proliferatio s of endodermal epithelia.
The bursa appears in the caudal half of the urodeal membrane.
The bursa appears as a median chain of intercellular
vesicles subjacent to the ectoderm and just within the
endoderm. These vesicles enlarge and fuse to become the
lumen of the bursa. The surrounding endodermal cells
proliferate to form the lining of the bursa. The electron
micrographs suggest that the urodeal ectoderm ingests
extracorporeal fluid by pinocytosis and transfers it to
the endoderm which releases it into the intercellular space
to form the vesicles.

The thymus appears as four separate proliferations.
These arise from the dorsal, lateral extremes of Pharyngeal
Pouches III and IV. Each of these proliferations lies just
dorsad and mediad to the medial end of a small, transverse
membrane connecting the pharyngeal pouch to the corresponding
branchial groove. The dorsal part of Membrane III is a tube
of ectoderm which intrudes mediad from Groove III and the
ventral part is a tube of endoderm which protrudes laterad
from the ventral part of Pouch III. The contact of ectoderm
with endoderm is continuous from just beneath the body sur-
face to a point just ventral and lateral to Thymus III.
Membrane IV does not have a ventral, endodermal part. The
contact of ectoderm with endoderm is restricted to the area
just ventral and lateral to Thymus IV. There is no chain

of vesicles and no indication of extracorporeal pinocytosis
and internal secretion in Membranes III and IV.

The urodeal membrane, and Membranes III and IV, con-
tain the debris of many dead cells. The acid phosphatase
activity of these membranes is high, which supports the
morphological evidence for cell deterioration and cell
death. The activity is high in (a) the urodeal ectoderm,
the urodeal endoderm, and the lymphoid follicles of the
bursa, and in (b) the ectoderm of Membranes III and IV,
the endoderm of Membranes III and IV, and the endodermal
epithelium of the developing thymus. The significance of
this activity is unknown excepting its frequent association
with cell deterioration and cell death, whether in the
epithelia or at sites of active lymphopoiesis.

The morphological indications of cell deterioration
and cell death are particularly noticeable in the urodeal
ectoderm and the branchial extoderm, and are remarkable
in the ectoderm of the branchial groooves. Here, as in
the thymus, the debris of epithelial cells is discharged
into the surrounding mesenchyme where it is phagocytized.
There is no indication that mesenchymal cells invade the
epithelia. The extreme deterioration of the ectoderm is
followed by rapid proliferation of the bursa and the thymus.
Despite the intimate contact of ectoderm with endoderm
it has not been possible to trace ectodermal cells into
either organs.

ACKNOWLEDGMENTS

TABLE OF CONTENTS

Page

I. INTRODUCTION

Although the lymphoid tissue of adult amniotes is distributed throughout the body it appears in the avian embryo in two small organs, the thymus and the bursa of Fabricius, before it can be detected elsewhere. This has been interpreted to mean: (1) all vertebrate leukocytes are descendants of the epithelial cells of the thymus (Beard, 1900), (2) the leukocytes are descendants of mesenchymal cells which invade the thymus and proliferate there (Maximow, 1909), (3) some of the lymphocytes are descendants of the epithelial cells of the bursa (Ackerman and Knouff, 1959), (4) the antibody-producing cells are probably derived from the endodermal epithelia of the thymus and the bursa (Ruth, 1960), (5) the first lympho-cytes of the thymus are descendants of the epithelial cells of the thymus (Auerbach, 1961), and (6) the lymphocytes of the thymus and the bursa and all other lymphocytes are descendants of blood cells which invade the bursa and the thymus (Moore and Owen, 1966 and 1967). All of these argu-ments suffer from a lack of detailed information about the origins of the bursa and the thymus. Even if the arguments about the origins of the lymphocytes are set aside, a de-tailed examination of the primordial epithelia may go some distance toward the redefinition of questions relevant to the differentiation of lymphocytes and the acquisition of immunological competence. One of the principal questions

is "What do the epithelia of the bursa and the thymus have in common which sets them apart from other derivatives of the gut?"

Grossly, the bursa and the thymus are unusual by their locations near the opposite ends of the gut. The epithelial parts arise from endoderm which connects with ectodermal epithelium of the body surface. This raises the possibility that the epithelial primordia of the bursa and the thymus may arise from the contact of ectoderm with endoderm. Because the anatomical relationship of the ectoderm and the endoderm have been disputed this has been re-investigated. The relationship is intimate.

The intimate contact of ectoderm with endoderm raises the possibility that ectodermal cells may be included in the thymus and the bursa. This is not a new question. The older literature includes many references to this possibility although the more recent literature tends to ignore or dismiss it. Ultrastructural studies were undertaken in the hope of providing some basis for resolving this question. These studies place the question in a different context. The primordia and the adjacent epithelia undergo extensive degeneration. This circumstance changed the immediate question from one of cell lineage to one of establishing the extent of autolysis and the relationship of autolysis to the formation of the bursa and the thymus.

II. MATERIALS AND METHODS

All tissues were taken from F1 hybrids of two highly inbred lines of White Leghorns maintained by the Hy-Line Poultry Farms, Johnston, Iowa. The anatomical and ultrastructural studies are based on many four to six day embryos and a few embryos of other ages. The histochemical studies include a wide range of ages.

Light and Electron Microscopy

Whole embryos are shown in Figs. 1 to 3. Figures 4 to 6 indicate the locations of the lymphoid anlagen. For anatomical and ultrastructural studies, the embryos were cut in half (Fig. 7) and hardened in fixative for 10 to 20 minutes. Two fixatives were used. These were Palade's (1952) and that of Sabatini et al. (1962). The tissues were dehydrated in ethanol and embedded in Araldite 502 or Epon modified from Luft (1961). The tissues were oriented in gelatine capsules by placing the tissues on two drops of polymerizing resin. The branchial region was oriented for frontal sectioning and the urodeal region was oriented for sagittal sectioning. For anatomical studies by light microscopy, 7 to 10u sections were cut with a steel knife and mounted in resin. Phase contrast photographs were taken on Agepe FF film (Agfa).

For ultrastructural studies it was necessary to orient the tissue more precisely. This was done by examining 7 to

10 u sections with the phase microscope, identifying the exact position and plane of the pharyngeal and cloacal complexes, and further trimming and positioning of the block. Sections were cut at 600 to 1000 $\overset{o}{A}$ with glass or diamond knives, floated on a 15% solution of acetone in water.

The sections were picked up on 150 or 200 mesh coated or uncoated copper grids and stained by floating the grids face down on a drop of saturated uranyl acetate (Watson, 1958) at room temperature. The sections were washed briefly and blotted dry. The sections were examined in a Phillips EM 100 B operated at 60 KV with a 25 micra aperature. The photographs were taken on 35 mm Kodak film (P 426) at magnifications of 1000 to 5000.

Acid Phosphatase Localization

For light microscopic localization of acid phosphatase activity, the whole embryo or part of the embryo was fixed in ice cold formaldehyde-calcium fixative for 24 hours, and infiltrated with cold gum-sucrose (Holt, 1958), and frozen in isopentane at a temperature below -100°C. The whole 5 day embryo, the anterior and posterior halves of the 6 day embryo, and the neck and tail of the 7 to 14 day embryos were frozen and embedded in O.C.T. compound (Lab-Tek, Westmount, Illinois). Sections (8 u) were cut at -15°C, frontal sections for the thymus and sagittal sections for the bursa (Figs. 8 and 9).

The sections were mounted on gelatin coated slides and dried in air at room temperature. Within one week of sectioning, slides were washed in distilled water and incubated in fresh Barka's medium (1960). After incubation for 10 to 30 minutes at room temperature, the slides were cleared and mounted in Permount. The counterstain was 1% methyl green at pH 4.0.

For electron microscopic localization of acid phosphatase activity, the bursa of Fabricius was removed from the 20 day embryo and cut into halves. The tissue was spread on filter paper, luminal side up and placed in cold 3% glutaraldehyde in 0.05M sodium cacodylate buffer at pH 7.2 for 80 minutes. Fixed tissues were washed in cold (sodium cacodylate) buffered 10% sucrose for 4 hours and cut into small pieces. These were incubated at $37^{o}C$ in Gomori's (1952) medium for 90 minutes.

The incubation medium was prepared immediately before use by dissolving 0.24 gm lead nitrate in 200 ml 0.05M sodium acetate buffer at pH 5.0 containing 7.5% sucrose and then slowly adding 20 ml of a 3% solution of sodium-glycerophosphate. Then the mixture was warmed at $60^{o}C$ for one hour cooled to room temperature, and filtered before incubation (Miller and Palade, 1964).

The tissue blocks were washed twice (10 minutes each) in a cold solution of 0.05M sodium acetate buffer (pH 5.0), 7.5% sucrose, and 4% formaldehyde (Holt and Hicks, 1961), with a 10 minute rinse in 2% acetic acid between the washes

of acetate-buffered formaldehyde.

The tissue blocks were post fixed in 1% OsO_4 veronal-acetate buffer (pH 7.3) at 0-4°C for 60 minutes, dehydrated in ethanol, and embedded in Epon 812 (Luft, 1961).

For both Barka and Gomori methods, the controls were the omission of substrate and the inclusion of 0.01M NaF in the incubation medium.

Feulgen Reaction for DNA Demonstration

Frozen sections, prepared as mentioned before, were used for demonstrating Feulgen-positive pyknotic nuclei. The preparation of Schiff reagent was after Barger and de Lamater (1948). The stained sections were counterstained with luxol fast blue (Margolis and Pickett, 1956). Both normal nuclei and pyknotic nuclei stain red in the Feulgen reaction preparation. The Feulgen-positive pyknotic nuclei are readily distinguishable from the normal nuclei by their deeper color.

Colcemid Treatment

Colcemid (CIBA Co. Ltd., Dorval, Quebec) was given to 5 day embryos. The optimal dose, 0.2 μg, was high enough to arrest all dividing cells at metaphase and low enough to allow embryos to survive until hatching. The addition of Colcemid to the embryos was carried out as follows: The 5 day embryos were candled with ultraviolet light. Only embryos having yolk sacs close to the air chamber of the egg were chosen for this experiment. A 5 mm^2 shell win-

dow was made on the blunt end of the egg, i. e., the air
chamber side. In order to avoid hemorrhage during the ap-
plication of Colcemid to embryos, a small slit was made
in the inner shell membrane lying on the chorionic membrane
and the primitive yolk sac. Colcemid solution of 0.1 ml
was then added drop by drop to the slit of the shell membrane
and it immediately spread to the chorionic membrane and the
primitive yolk sac. After this the shell window was sealed
with masking tape. The embryos were returned to the incu-
bator for another six hours incubation, and then fixed in
formol calcium fixative. The fixed embryos were embedded in
paraffin. Sections cut at 7u were stained with Ehrlich
haematoxylin.

III. OBSERVATIONS

The Bursa of Fabricius

The bursa of Fabricius is an unusual lymphoid organ.
The medulla of each follicle is separated from its cortex
by a basement membrane (Fig. 10). This is continuous with
the basement membrane of the non-lymphoid epithelium which
connects the follicles (Figs. 11 and 12). The epithelium
is endodermal. The basement membrane can, therefore, be
regarded as the fundamental demarcation between a modified
endodermal medulla and a mesenchymal cortex (Figs. 11 and
12) without implying that all the cells of the medulla are
endodermal derivatives. The histological distinction is
recognizable in the distribution of the vascular capillaries.

These surround the medulla closely, but do not penetrate it.
In consequence, erythrocytes may be found close to the medul-
la, but not in it (Fig. 13).

Cell degeneration and cell death are common in the me-
dulla (Fig. 14 to 16). Since degeneration is associated
with the activity of lysosomal enzymes, the activity of the
most definitive of these was examined. The acid phosphatase
activity of the 12 day, pre-lymphoid, bursa is concentrated
in small groups of cells scattered through the tunica pro-
pria (Fig. 17). The appearance of follicles at 13 days is
accompanied by the appearance of high, punctate activity in
the epithelium, particularly at the follicles (Fig. 18).
The punctate distribution is more evident in the epithelium
and the follicles at 14 days (Fig. 19). At 19 days, the
tunica propria and the epithelium are not very reactive,
but the medullae of the follicles contain many punctate
centers of activity (Fig. 20). At all ages the punctate
centers of the epithelium and the follicles are not as
large as the largest punctate centers of the tunica propria
and this difference has a fundamental basis.

The punctate activity of the 12, 13, and 14 day tunica
propria (Figs. 17 to 19) corresponds in size and distribu-
tion to groups of immature heterophils (Figs. 21 and 22).
At 19 days, there are fewer punctate centers in the tunica
propria (compare Fig. 20 with 23 and 24) and fewer groups of
immature heterophils. Two kinds of granulocytes, eosinophils

and heterophils, may contribute to the activity of the 19 day tunica propria (Figs. 25 and 26), but only heterophils are present at 12, 13 and 14 days. Neither eosinophils nor heterophils are present in the epithelium and the follicles. The punctate activity of these two structures must be due to other cells. It is presumed that the activity is indigenous to the endodermal cells of the epithelium and the agranulocytes of the follicles for lack of evidence to the contrary.

The acquisition of acid phosphatase activity by the 13 day epithelium does not mean that activity is negligible throughout earlier development. The epithelium is very active at 14 days (Fig. 27) and 13 days (Fig. 28), inactive at 12, 11, 10 and 9 days (Figs. 29 to 32), and very active at 7 days.(Fig. 34). The 7 day epithelium is the urodeal membrane. The epithelium of the bursa develops in this membrane and as it develops it separates (Figs. 34 and 33, in that order) and loses activity (Fig. 32). The urodeal membrane retains activity (Figs. 35, 37 and 38). The times at which the epithelium of the bursa has high activity are the times of active differentiation: the formation of the definitive epithelium, and its transformation into follicles.

The anatomy of the urodeal membrane is quite complex, but the principal features can be learned from serial sections. It is easiest to do this with para-sagittal sections

(Figs. 39 to 44). These show the 4 day proctodaeum on the right, the urodeal membrane in the center, and the cloaca on the left. The proctodaeum is lined with ectoderm which is fused through the urodeal membrane to the endoderm which lines the cloaca.

The ectoderm and endoderm are not demarcated. This continuity of ectoderm with endoderm represents a persistence of the median, sagittal continuity of the epiblast and hypoblast formed during gastrulation. The continuity persists as the 'anal plate' which is displaced to the ventral side of the embryo during the formation of the tail or caudal body fold and the elongation of the dorsal, axial skeleton. By the fourth day the anal plate has thickened to become the urodeal membrane.

The proctodaeum points toward the head which lies far outside the right margin of the figures (Figs. 39 to 44). The most caudal part of the urodeal membrane is seen in Fig. 39 and the successive, para-sagittal sections show more of the anterior membrane. It is difficult to align the sections so that they are perfectly sagittal or para-sagittal and these figures may represent sections which are tilted and twisted. For instance, the cloacal fenestra (Fig. 40) marks the midline of the posterior cloaca and the tip of the proctodaeum (Fig. 44) marks the midline of the anterior cloaca. The location of these two structures in different sections suggests that the sections are twisted

or rotated on the dorsal-ventral axis. The fact that the urodeal membrane is defined less sharply and the ventral wall of the cloaca is thicker in Figs. 42 and 43 suggests that these structures are cut tangentially which might suggest that the sections are tilted or rotated on the anterior-posterior axis. It is apparent, however, that part of the asymmetry is contributed by the embryo. This is recognized more easily in the 5 day embryos.

Sections which cut the neural tube, the notochord, the aorta, and the tip of the proctodaeum (Fig. 45) show that the tail of the embryo curves laterad, away from the plane of the section. This is most easily recognized by the presence of somites in the figure just above the amnion. The sections are twisted on the dorsal-ventral axis with respect to the cloaca, but the sections are not twisted with respect to the torso. In reality, the urodeal membrane extends from the tip of the proctodaeum to a point just beyond the left margin of the small rectangle (Fig. 45). The cavity of the cloaca appears at two points: inside the rectangle just above the tip of the proctodaeum, and above the left margin of the rectangle. The cloacal cavity is really continuous from right to left and so is the urodeal membrane which separates it from the proctodeal ectoderm. Frequently, the curve of the urodeal membrane and the cloacal cavity is exaggerated in that sections may cut through the front and rear of the urodeal membrane, but not through its center.

The posterior part of the urodeal membrane probably represents the eventual opening of the bursa into the procto-daeum and the anterior part represents the eventual opening of the embryonic cloaca. The early, incidental and temporary convolutions make the anatomical study more tedious, but are not fundamental to the contact of the ectoderm with the endoderm. There are morphological characteristics of greater relevance.

Much cell debris is present in the tip of the procto-deal ectoderm (Figs. 41 to 44) and in the anterior part of the urodeal membrane (Fig. 44). Cell debris is found, however, throughout the adjacent ectoderm, including the ectoderm in contact with the posterior part of the urodeal membrane (Fig. 41). The extent and intensity of cell degeneration may reach a peak during the fourth day (Figs. 46 to 51). At this time a mass of cells and debris protrudes into the cloacal cavity. The protrusion resembles ectoderm, but it may not be ectoderm. The protrusion is not obvious in 5 day embryos (Figs. 52 to 57), but this may be due to the great growth of the urodeal membrane which expands over the region in which the protrusion was formed (Figs. 56 and 57). Numerous vesicles appear in the urodeal membrane subjacent to the ectoderm. They form a rough arc from the rear (Fig. 53) to the front (Fig. 57) of the membrane. Some are deep within the membrane. The fate of these vesicles is more evident in 6 day embryos.

The vesicles seem to fuse. This is suggested by the bulges of some (Figs. 59, 61 and 63), the close contact of others (Figs. 58, 60 and 62), and the constriction of a few large vesicles (Figs. 61 and 62). The number and size of the vesicles suggests that active secretion of fluid occurs throughout the urodeal membrane. Their clarity indicates that they are not deposits of cell debris. These vesicles fuse to form the lumen of the bursa. The vesicles at the anterior of the urodeal membrane may not contribute to the lumen of the bursa (Figs. 33 to 31, in that order).

The anatomical study suggests that the ectoderm plays an important role in the formation and development of the urodeal membrane. The ectoderm in and near the membrane is peculiar in at least two ways: it produces much debris and this is followed by the formation of extracellular vesicles. Electron micrographs show that the production of debris is accompanied by the formation of intercellular spaces which may be the forerunners of the extracellular vesicles. The most superficial of the intercellular spaces are separated from the proctodeal cavity by just one layer of cells (Fig. 64). The proctodeal surface of these cells has many indentations and small vesicles suggestive of active pinocytosis. Small and large vesicles are scattered throughout the cytoplasm. The cells are linked by tight junctions, desmosomes (Fig. 65), and interdigitations. The cells may look healthy, but they contain masses of lipid and membrane-bound debris,

which may resemble organelles. The free mitochondria contain the distinctive cristae, but these may be incomplete and irregularly spaced. There are many irregular, osmiophilic bodies, presumably lipid, throughout the cytoplasm. Golgi-like vesicles are present, but few if any multivesicular bodies are found in the superficial cells.

Cells beneath the superficial cells may contain long, clear membrane-bound spaces which resemble tubular endoplasmic reticulum (Fig. 65). The diameters of these are comparable to the diameters of the larger, rounded vesicles of the superficial cells. It is conceivable, therefore, that the rounded vesicles of the superficial cells may represent cross-sections of tubular reticulum. If so, the arrangement of the tubular reticulum is highly ordered in a manner not reflected in the arrangement of the tubular mitochondria. Tubular reticulum is common in the internal cells, but has not been recognized in the superficial cells.

The boundaries of internal cells may lead into areas of unusual opacity. These may be diffuse near the proctodeal cavity (Fig. 65), but the deeper ones have distinct interdigitations, condensations near the cell surfaces, and thickenings of the cell surfaces (Fig. 73). The diffuse areas are presumed to be early stages in the formation of the more distinct areas.

The nuclei of urodeal cells have typical nuclear envelopes; the space between the membranes is slightly irregular,

but the two membranes join at the pores (Fig. 66). There
are small groups of Golgi-like vesicles near the nucleus.
Multivesicular bodies are found near the nucleus. These
are more common in the deeper cells. A few ribosomes are
attached to the intracytoplasmic membranes, but this is not
the usual location in young embryos. Most occur in groups
of four or more scattered through the cytoplasm (Fig. 66);
nuclear granules are not grouped this way.

The cell surfaces which border the intercellular spaces
may show interruptions. Sharp, dark cell membrane may be in-
terrupted by streams of cytoplasm which enter the intercel-
lular space (Fig. 66). This is not necessarily an artifact
of fixation. Spaces, so close to each other that they must
have experienced similar changes during preparation, may
differ; one may have the interrupted, dark boundary and the
other may have a continuous, light boundary (Fig. 66). The
latter resembles the cell membranes at the proctodeal and
cloacal surfaces and the former resembles the cell membranes
around the extracellular vesicles (Figs. 64, 72 and 73).
If the granular contents of the cytoplasm do enter the inter-
cellular spaces and these fuse to form the extracellular
vesicles, this would account for the presence of granular
material in the extracellular vesicles (Figs. 71 to 73).

Deeper within the urodeal membrane, the Golgi vesicles
are more numerous (Fig. 67). The nucleoli may contain dense
linear segments suggestive of the nucleolemna. Intercellular

spaces are frequent. Large clumps of debris occur (Figs. 67 and 68). These may represent dead cells. The debris is found next to apparently healthy cells which may or may not have a vesicular cytoplasm. The debris seems therefore to represent real degeneration in normal development rather than some artifact of fixation. The same interpretation should apply to the membranes which enclose the debris or delimit cytoplasmic vesicles.

The urodeal membrane is heterogeneous. The foci of degeneration are not large and are not far from cells of very different composition (Fig. 69). In some of these the tubular endoplasmic reticulum may be prominent and may possess many attached and proximate ribosomes. The outer nuclear membrane may be raised in numerous blebs, and there is some indication that ribosomes may attach to it. The cytoplasmic membranes to which ribosomes are not attached are those of the Golgi, the multivesicular bodies, and the cell surface. A few ribosomes lie at the cell membrane, but there are no groups of ribosomes aligned on this membrane.

The Golgi of the deeper cells differs from the Golgi of superficial cells by the presence of cisternae and more vesicles (Fig. 70). These may be close to multivesicular bodies. The cisternae have terminal blebs suggestive of the formation of Golgi vesicles and the multivesicular bodies may have appended vesicles suggestive of fusion with Golgi vesicles. There is no indication of the attachment

of ribosomes to these three membranous structures which
would seem to set them apart from the general reticulum.
The location of elaborate Golgi in cells close to de-
generating cells (Figs. 67, 70 and 71) prompts the pos-
sibility that there may be some meaning to this proximity.
For instance, in Fig. 70 the Golgi and the multivesicular
bodies are found in a cell which is firmly attached to
another cell, the proximate region of which shows signs of
dissolution. Instead of the distinct groups of ribosomes
found elsewhere in the cell there is an arc of rather amor-
phous material. The nearest multivesicular body is perfor-
ated and a series of small vesicular bodies extends through
this and along the outside wall of the multivesicular body.
The coincidence of the various structures may be nothing
more than coincidence or artifact, but it raises the pos-
sibility that an adjacent cell may play a role in the degene-
ration of another cell by means other than direct phagocy-
tosis. This may involve the Golgi and multivesicular bodies
of the viable cells. Figure 70 is reproduced as part of Fig.
71.

The borders of the extracellular or bursa vesicles may
be lined by long extensions of cytoplasm bearing long or
numerous tight junctions (Fig. 71). These are common and
are similar to extensions which border the cavity of the
cloaca (Fig. 73). The tight coupling of these cells and the
symmetry of the vesicles (Fig. 73) suggest that the fluid of

the vesicles is under pressure. The flattening of the cells reduces the distance between cell membrane and nuclear envelope. The nuclear blebs may come close to the cell membrane and may be difficult to distinguish from it and from intracytoplasmic membranes (Fig. 72). The cell membrane bordering the extracellular vesicles may show the dark-light alteration described previously. Again, there is the hint that the light segments may be portals through which amorphous and granular cytoplasm enters the vesicles (Fig. 72). The dark segments seem to be darker than the nuclear and intracytoplasmic membranes.

Extracellular vesicles are found close to the cloaca, but no indication of fusion with the cavity of the cloaca has been seen. If fusion occurs it might be difficult to detect. The contrast between the contents of the extracellular vesicles and the cavity of the cloaca, as shown in Fig. 73, is practically invariant. The former always contains visible material and the latter never does. Complex arrays of tight junctions are more common near the cloaca (Fig. 73). The complex tight junctions are less common in areas which lack extracellular vesicles, but interdigitations and desmosomes are common throughout the urodeal membrane (Fig. 74).

Another feature of the membrane is the widespread occurrence of cytolysomes (Fig. 75). These are largest near

the proctodaeum (Figs. 67 and 68). Perhaps these represent phagocytosis, but typical phagocytes were not seen. Degeneration is remarkably discrete away from the proctodaeum. Death seems to come to the urodeal cells individually by mechanisms which are either internal or involve only the dying cell and those adhering to it.

The urodeal membrane is demarcated from mesenchyme by a basement membrane (Fig. 76). No cells were seen to broach this. The cells along the basement membrane are healthy, and contain multivesicular bodies, nuclear blebs, and many cytoplasmic vesicles, but little debris. These are the most uniform of the urodeal cells. Most are polarized with the nucleus located toward the basement membrane and the bulk of the cytoplasm and its organelles located away from the basement membrane. As in the follicles of the lymphoid bursa (Figs. 10, 13, and 14), the basement membrane of the urodeal membrane is simple and continuous and serves as a useful histological marker. This contrasts with the basement membrane of the thymus.

The Thymus

Unlike the follicles of the bursa, the cortex and medulla of a thymus follicle are not separated by a basement membrane. The original basement membrane of the thymus corresponds in position to the outer surface of the cortex, i.e. to its demarcation from free mesenchyme (Chan and Sainte-Marie, 1968). Even this original demarcation doesn't mean much because the vascular capillaries penetrate deeply

into the cortex and the medulla in company with mesenchyme.
To its center, the mature thymus must be regarded as an
organ of mixed origin, a mesenchymal-endodermal organ.
The epithelium is demonstrable in mammals, after treat-
ments which deplete the organ of its lymphocytes, as a
complex, convoluted, and tenous tissue (R. N. Baillif,
1948). The basement membrane may persist around the epi-
thelial cells, but its demonstration in the normal thymus
as a continuous, histological boundary is formidable for
topological reasons if it is, in fact, continuous.

Unlike that of mammals, the thymus of birds does not
fuse into one median organ. It persists as two unconnected
bilateral organs. Each is formed of many lobes arranged on
either side of the esophagus and trachea. The lobes take
cervical positions very early and can be seen under the
surface of the neck on the 13th day (Fig. 77). At this age
the thymus contains a little punctate acid phosphatase
activity (Fig. 78) which is less abundant than that of
the bursa.

The positions of the lobes at 12 days are not much
different (Figs. 78 and 79). At 11 days the lobes are thin-
ner, but still lymphoid (Figs. 81 and 82). At 10 days the
thymus is in transition from the pre-lymphoid, epithelial
condition (Figs. 83 and 84). At 8 days some lobules are
epithelial and some are beginning the histological transi-
tion (Figs. 85 and 86). At 7 days the thymus is wholly

epithelial (Figs. 87 and 88). The thymus undergoes two morphological changes between the 7th and 8th days: it separates into segments and these send out lateral lobules. These penetrate the mesenchyme at about the time the cytological transition to lymphoblasts begins (Ackerman and Knouff, 1964).

The 7 day thymus represents a great elongation of the 6 day thymus (Figs. 89 and 90). Thymus III contributes most of this. The upper or cranial tip of Thymus III (Figs. 89 and 90) is the most dorsal part. This is derived from the lateral part of the thymus primordium and presumably from its associated ectoderm and the caudal tip is derived from the medial part of the thymus primordium and the broken connection to Pharyngeal Pouch III. By analogy with the mammalian thymus, the center and the caudal tip of Thymus III should extend caudad to form the elongated thymus of day 7 (Figs. 87 and 88).

The 5 day thymus is connected mediad to the pharynx through the pharyngeal pouch and laterad it touches a mass of ectoderm (Figs. 91 to 94). In some 5 day embryos this mass is continuous with the ectoderm of Branchial Groove III and through it to the ectoderm of Branchial Groove IV, a small part of which is attached to Thymus IV (attachment not shown).

The 5 day thymus is connected to the pharynx through the pharyngeal pouch (Figs. 91 to 94). The thymus arises

as a dorsal protrusion from the crescentic lateral end of Pouch III (Fig. 92) and similarly from Pouch IV. A small mass of ectoderm which abuts Thymus III has detached from the branchial groove. This mass of ectoderm is fused to the endoderm. Its fate will require detailed studies, but its presence adjacent to the thymus primordium is evidence that ectodermal cells are sufficiently close to the thymus to contribute to it.

An earlier stage of development shows the thymus as a distinct dorsal protrusion of Pouch III (Figs. 95 to 98). At this stage the pharyngeal cavity extends into the thymus primordium (Figs. 97 and 98). The acid phosphatase reaction is intense (Figs. 99 and 100). Enzyme activity is concentrated in a band about one third of the distance from the lumen to the mesenchyme, but there are many other foci of activity in the epithelium. These other foci include debris which is at the edge of the epithelium and is, presumably, being expelled into the mesenchyme (Figs. 99 and 100). The proof of this must await electron micrographs which intercept points of extrusion. Cell deterioration and death and high acid phosphatase activity are not restricted to the thymus. Related epithelial areas, which may or may not contribute to the thymus primordium, also show deterioration and high activity (Fig. 101).

More ventral sections trace the primordium to the caudal wall of the lateral end of the pharyngeal pouch (Fig.

102). The ectoderm intrudes to a point just under the
lateral extreme of the primordium (Fig. 103). In this in-
stance the ectoderm can be traced directly to the super-
ficial branchial ectoderm of Groove III (Fig. 103). Suc-
ceeding ventral sections cut a lateral protrusion of the
ventral endoderm of the pouch (Figs. 104 to 106). This
reaches to the branchial groove. The differences between
Figs. 91 to 94 and Figs. 95 to 98 indicate a difference
in maturity; the thymus shown in Figs. 91 to 94 is slightly
more advanced. The comparison also indicates one of the
practical problems in studies of this kind. The age or
stage of an embryo is not an exact guide to the morphology
of the thymus primordium. Figs. 91 to 94 represent the
right Thymus III and Figs. 95 to 98 represent the left
Thymus III of one 5 day embryo. The left thymus is the
better for showing the intrusion of ectoderm and the later-
al extension of endoderm, but the right thymus is the bet-
ter for showing the intimate contact of ectoderm with the
thymus primordium. The differences are not restricted to
Thymus III and its associated membranes. The right Thymus
IV (Figs. 93 and 94) is more advanced than the left Thymus
IV (Figs. 106 to 108), which is just beginning its protru-
sion from Pouch IV. The differences between the right Thy-
mus III and IV and the left Thymus III and IV are real
and are not explained by tilting of the sections. Rarely,

if ever, are the two sides symmetrical. The different shape
and the greater maturity of Thymus III as compared with
Thymus IV is expected, but the different maturities of the
two sides is the more fundamental contrast.

Cell degeneration is very common throughout the epi-
thelial complexes from which the thymus is formed (Figs.
102 to 108). It is extreme medial to the thymus, where the
connection to the pharynx will break, and lateral to the
thymus, where the connection to the branchial groove will
break (Figs. 109 and 110). It is profound in the external
ectoderm which lines the grooves and the adjacent surfaces
(Fig. 110). This is an area which will be enclosed by
overgrowth of the hyoid arch and the surface is destined
therefore to become internal. Since most of the enclosed
epithelium will disappear, it seems that the degeneration
of the external epithelium anticipates its inclusion with-
in the body and cannot be viewed as a consequence of in-
clusion.

Intense acid phosphatase activity is found throughout
the epithelia (Figs. 111 and 112). This may be compared
with the acid phosphatase activity of the urodeal membrane
(Fig. 113). The reality of degeneration is confirmed by
the intense uptake of dye at the surface of the branchial
grooves (Figs. 114 and 115). Three branchial areas take up
the dye: Grooves II, III, and IV. Nearby, but separate, is
the large, seemingly homogeneous (see legend, Fig. 114),

degenerating area of the wing. This area is the subject
of the best description of amniote degeneration (Saunders
et al., 1962). Comparison of this area with the punctate
staining of the branchial grooves confirms the morpho-
logical and histochemical evidence of degeneration at the
external surfaces of the grooves. The maximal intensities
are about the same. The apparent homogeneity of the stain-
ed area of the wing is an artifact. The plane of focus
intercepts the branchial ectoderm, but not the stained area
of the wing. It is not practical to apply this technique
to the internal membranes, but it seems safe to assume that
the internal epithelia would stain in those areas which show
morphological and histochemical evidence of degeneration.

The surface of Groove III is an area of profound de-
generation (Fig. 116). The montage shows a mixture of dark,
intermediate, and light cells plus debris within the epi-
thelium, and phagocytes just outside the epithelium. Some
of the light cells contain masses of very dark debris (Figs.
117 and 118) like those of the mesenchymal phagocytes (Fig.
116). Some dark cells have membranous whorls (Fig. 117) in-
dicative of membrane destabilization and cell damage (Chen
and Ruth, 1966; Carr, 1967). The dark cells may be degen-
erating cells and the light cells may be healthy phagocytes.

Intercellular spaces are present. These are irregular
and are not accompanied by tight intercellular junctions,

desmosomes, or interdigitations (Fig. 119), in contrast to those of the urodeal membrane. The nucleoli of the dark cells are heterogeneous and contain structures which resemble the nucleolemna; this resemblance may be an accident of degeneration. The nucleoli of light cells are more homogeneous. Some are regular arrays of heavy granules (Figs. 118 and 119). The outer nuclear membrane of light cells is separated from the inner by the familiar, irregular space (Figs. 117 to 119). That of dark cells is close to the inner nuclear membrane (Fig. 119). The nuclear envelope of dark cells is indented or crenated and that of the light cells is smoother. The crenation of the dark nuclei is accompanied by a crenation of the whole cell(Figs. 116 and 119). This suggests that the opacity of dark cells is enhanced by dehydration. The crenation is, however, accompanied by a more subtle departure from normal than simple dehydration or shrinkage.

The ribosomes and the nuclear granules of light cells are larger, more opaque, and more clustered than those of dark cells (Figs. 119 and 120). The smaller and lighter granules of dark cells are scattered more evenly and do not form clusters, excepting those aligned on the endoplasmic reticulum or intracytoplasmic membranes (Fig. 120). It seems that the granules of dark cells have dissociated to give the entire cell a relatively greater and more uniform opacity. This may be a consequence or a cause of dehydration, but

these observations only indicate that two characteristics, cell shrinkage and dissociation, go together.

The impression that it is the dark, not the light, cells which are degenerate is substantiated by differences in the lipid bodies of the two cells. The lipid bodies of dark cells may have crista-like membranes (Fig. 120). Other lipid bodies in the same cells may be transitional between these and distinct, if abnormal, mitochondria (Fig. 120). The lipid bodies of light cells are relatively homogeneous (Fig. 120), there are no transitional lipid bodies, and their mitochondria look more normal (Fig. 120). This suggests that the mitochondria of dark cells degenerate into lipid bodies which contribute to those of the light cells by direct phagocytosis and modification or by dissolution and absorption of the lipid.

Similar signs of degeneration are present at the internal contacts of ectoderm with endoderm (Fig. 121). The mixed population of light and dark cells extends inward as far as these contacts. The primordium of the endodermal thymus is distinguished by the high proportion of healthy cells (Fig. 122). These are partially separated from the mesenchyme by a basement membrane (Fig. 122). Despite the presence of many healthy cells the thymus also contains many signs of degeneration (Figs. 123 and 124) and the

mesenchymal cells may contain much debris (Figs. 123 and 126). Mesenchymal cells and phagocytes have not been identified within the epithelium of the thymus primordium. This agrees with the indications in the light micrographs (Figs. 99 and 100) that the debris leaves the epithelium and is phagocytized in the mesenchyme.

The thymus primordium contains many myelin figures. One of these has not been seen in the endoderm away from the thymus, in the surrounding mesenchyme, or in the branchial ectoderm. This is the nuclear whorl (Fig. 127). Some protrude into the intercellular space (Fig. 128). Similar, but smaller, whorls have been interpreted as developing mitochondria (Pannese, C., 1966), but it is more likely that they represent destabilization of the nuclear envelope or discard of excess envelope. Small alterations of the nuclear envelope are seen in other tissues, e.g. bursa lymphocytes, but the distinctive whorls are peculiar, in this study, to the primordium of the thymus. They are interpreted as evidence of membrane instability associated with differentiation or degeneration. Since similar whorls occur in spermiogenesis (Anderson et al., 1967) it is unlikely that their presence is a necessary indication of cell death, although they may accompany a decrease in nuclear functions.

Myelin degeneration is not restricted to the nuclear envelope of the thymus cells. It is found in mitochondria (Figs. 127, 129 and 130), and in all parts of the cytoplasm.

The degeneration seen in the electron micrographs of internal epithelia, including the primordium of the thymus, must involve cell death as well as cell differentiation.

Although mitotic cells have been seen in the thymus they are not frequent. Yet mitosis or migration from contiguous epithelia or mesenchyme must occur in order for the thymus to grow. It is difficult to exclude cell migration, but somewhat easier to test the intensity of mitosis. Colcemid blocks mitosis and leaves the condensed metaphase chromosomes in the center of the cell as a large clump. Many such arrested metaphases may be seen in the 5 day thymus six hours after treatment of the embryo (Figs. 136 to 141). These are not distributed uniformly. In more ventral sections the arrested metaphases are separated by areas of degeneration and debris (Figs. 137 to 141). The distribution of the arrested metaphases is distinctly different from that in the pharyngeal pouches which have a zone of arrested metaphases adjacent to the lumen (Fig. 142).

IV. DISCUSSION

The immediate purpose of the work is to describe the earliest development of the primary lymphoid anlagen. The chicken embryo was selected because it has two principal lymphoid anlagen and the ages of the embryos can be controlled.

Histological and cytological methods have been used because the components of the anlagen are too small to be easily identified by any other means and too fragile for dissection.

The principal point of the observations may be stated directly. There is an intimate contact of ectoderm and endo-derm in the immediate vicinity of the anlagen of the thymus and the bursa of Fabricius. Both organs begin as masses of endodermal epithelium. A direct contribution of ectoderm is not evident, but is not excluded by our observations. The regions of ectodermal-endodermal contact and the adjacent anlagen are areas of massive cell degeneration and cell death.

The occurrence of small vesicles in the urodeal membrane is the first indication of the formation of the primordium of the bursa of Fabricius. These vesicles, in most cases, are found in the 5-day chick embryo, although occasionally a very few vesicles can be identified in the 4-day embryo. In 1880 Stieda mentioned that Bornhaupt (1867) had described the ap-pearance of the bursal vesicles on day 7 or 8 at a time when the rectum has not yet connected with the anal canal. Gasser (1880), however, maintained that the primary development of the bursa occurs earlier - its presence being evident on day 6. Wenckebach (1888) reported the occurrence, in the 5-day old embryo of Gallus , of many small cavities in a narrow crest of epithelial tissue in the posterior portion of the cloaca. In 1915 Jolly indicated that bursal vesicles are seen on the sixth day of incubation. However, vesicles appear to be

visible in his picture of the 5-day embryo (Fig. XXII, p. 398). Pera (1958) described the presence, in 5-day embryos, of numerous small and irregular cavities, separated from each other by a fairly thin epithelial wall; these appeared along with the initial development of the bursa. In 1964 Ruth et al. reported that small vesicles were present at the point of contact of the urodeal membrane and the proctodaeum in the 4-day chick embryo, and were more obvious the 5-day embryo. The present study confirms that the development of the bursal primordium of the chick embryo is evident on the fifth day of incubation.

The bursal vesicles of the 5-day embryo are most frequent in the endoderm which contacts ectoderm. They are less numerous near the cloacal lumen and do not appear in the dorsal side of the cloacal lining. These observations lead to the supposition that the ectoderm plays some role in the early development of the bursa primordium. Pera (1958) has discussed the contributions of the germ layers to the bursa of Fabricius. Many agreed that the bursa is endodermal; a view exemplified by the work of Huscke (1838), Bornhaupt (1867), Stieda (1880), Wenckeback (1888), Marshall (1893), Pomayer (1902), Boyden (1922) and others. However, other workers such as Koëlliker (1879), Retterer & Balfour (1876), Vialleton (1911) considered the bursa to be ectodermal. Pera himself supported the view that the bursa is endodermal, and suggests that those workers who

considered it ectodermal probably studied the organ at too
advanced a stage of development (8-9 days of incubation);
that is, when the potential bursa does not show any con-
nection with the posterior cloacal wall. Moreover, at
this stage, the cavity of the bursa communicates with the
proctodaeum. The separation from the cloaca and the ac-
quisition of a secondary connection to the proctodaeum
are the probable basis for the erroneous concept that the
bursa is ectodermal.

Boyden (1922) reported that the regression of the
caudal intestine is greatly complicated by the disintegra-
tion of the adjacent cloacal wall, the latter process re-
sulting in the formation of the cloacal fenestra. The
active disintegration begins at about 2 days and 18 hours
of incubation. Jolly (1915) mentioned that the post-anal
intestine (caudal intestine) undergoes regression on the
third or fourth days. No caudal intestine was seen in 4-
or 5-day embryos used in the present study. The regression
of the caudal intestine is not related to the formation of
the urodeal membrane: the latter grows by fusion of the
two cloacal walls starting from the floor of the cloaca im-
mediately adjacent to the proctodeal lumen and extending
to the posterior end of the cloaca. The fact that the
bursal vesicles appear in the urodeal membrane close to
the proctodeal lumen and (later) along the boundary between
the urodeal membrane and the mesenchyme indicates that the

bursa does not develop from the caudal intestine. However, Stieda (1880) and Jolly (1915) described work supporting the conclusion that the bursa comes from the caudal intestine. In 1880 Stieda wrote "The epithelium of the bursa of Fabricius develops from the epithelial elements which originally belong to the caudal intestine". In 1915 Jolly presented evidence that the first primordium of the bursa exactly occupies the position of the post-anal intestine (caudal intestine) and is oriented in the same way. He added that one might even say that this primordium is identical with what remains of the post-anal intestine, and one might consider the bursa as representing the remainder of the caudal intestine which arises posteriorly, turns towards the head, and undergoes a subsequent development to form a true cloacal caecum.

Pera (1958) writes in his discussion "In the embryos of _Gallus_ _domesticus_ the bursa starts growing in that narrow region of the posterior cloacal wall, from which at an earlier stage, the caudal intestine protruded. More precisely, some nests of epithelial cells are observed in embryos 3 days and 2 hours and 3 days and 18 hours old, when the caudal intestine has almost regressed to a small thin cord. These nests proliferate actively and generate a small ovoid, epithelial protuberance in embryos of 4 days and 4 days and 4 hours. This protuberance represents the potential bursa of Fabricius". The protuberance, described by Pera as extending from the

floor of the cloaca toward the proctodeal lumen (Fig. 18,
Pera, 1958) has not been seen in the present study (see
Figs. 39-42). The urodeal membrane seen between the floor
of the cloaca and the proctodeal lumen is easily demonstrated
in 4-day chick embryos (Figs. 39-42), and the protuberance
seen by Pera may be just a part of the newly formed urodeal
membrane.

Many papers dealing with the development of the bursa of
Fabricius were published in the late 19th century and early
20th century. However, there were very few of these accounts
which dealt with the problem of how the bursa vesicles are
formed. No doubt this was partly due to the limitations
of the light microscope. In 1880 Stieda mentioned that the
atrophy of cells in the center of the solid spherical body,
which he thought to be the first primordium of the bursa,
forms a small cavity, which later communicates with the anal
canal. The present studies show that cell degeneration
occurs in the urodeal membrane and the proctodeal ectoderm,
but the vesicles are not simply the spaces vacated by dying
cells. Many distended intercellular spaces are seen with the
electron microscope. These distended intercellular spaces
coalesce to form larger spaces or bursa vesicles, the latter
being large enough to be seen with the light microscope.
Cell debris is not present in the distended intercellular
spaces or bursal vesicles, and it seems clear that cell deaths
do not result in the formation of the bursal vesicles.

Conversely, the vesicles seem to be produced by secretion of fluid by healthy cells. This may be accompanied by the release of fluid cytoplasm (Fig. 66).

The exact function of the bursa is not clear. Because the development of the bursa is inverse to that of the gonads - full-grown before sexual maturity and involuted at sexual maturity - some authors have attempted to relate the bursa to reproduction. Jolly (1928) reported that castration retards the involution of the bursa in the male chicken. In 1943 Selye reported that injection of sexual hormones accelerates the involution of the bursa in the cock. Kirkpatrick and Andrews (1944) obtained the same result in the pheasant. It was, however, the work of Glick et al. (1956) which assigned an important function to the bursa as an immune organ. The chick bursectomized within two weeks of hatching and the chick embryo treated with androgen to prevent development of the bursa show serious impairment of antibody production (Mueller et al., 1960).

The primordia of the chicken thymus arise from thickenings of the third and fourth pharyngeal pouches. A thickening of the epithelium of the dorsal part of the second pouch was mentioned by Kastschenko (1887). This epithelial thickening was again reported by Scothorne in 1957 in six other species of birds. Since the thickening disappears without undergoing any specific differentiation and is the anatomical homologue of Thymus II of lower vertebrates, it has been

termed an abortive thymus.

Mall (1887) described the endoderm of the third pharyn-geal pouches as the only anlagen of the chicken thymus, but Verdun (1898) reported that the primordium of the chick thymus develops from the third and fourth pharyngeal pouches. The dual origin from the third and fourth pouches is generally accepted and is confirmed in this study. The two anlagen on each side combine to form a thymus on each side of the animal (Hammond, 1954).

On the basis of his observation that the second clos-ing membrane of a visceral cleft forms laterad to the original closing membrane, Kastschenko (1887) concluded that the ectodermal epithelia of the third and fourth branchial grooves probably contribute to the formation of the chick thymus. This has been tested by Schrier and Hamilton (1952) and Hammond (1954). Schrier and Hamilton (1952) described experiments in which carbon particles, placed on the branchial surface, found their way to the thymus and parathyroids. They concluded that the ectoderm may contribute to the formation of the thymus anlagen. Hammond observed (1) a marked reduction in the development of the thymus following the removal of the branchial ecto-derm, even when the wound closes over well enough to permit attachment of the pouches to the reconstituted ecto-derm, and (2) that rudiments of the thymus cannot be found if the pouches fail to attach to ectoderm. He claimed that

the thymus in the chick is a derivative of the branchial
ectoderm related to the dorsal part of Pharyngeal Pouches
III and IV, and that the pharyngeal pouches do not give
rise to the thymus if the branchial ectoderm and the pouches
do not make proper contact. Hammond is probably correct in
pointing out that the thymus development requires the normal
relation between the pouches and their respective branchial
ectoderm. The branchial ectoderm could, however, be re-
quired for the normal development of its respective pouch,
but might not be essential to the formation of the deriva-
tives of the thymus rudiments. The removal of branchial
ectoderm interferes with the normal development of the
pouches and this alone might explain the absence of the
thymus rudiment. The base of the major thymus rudiment
arises from the endodermal cells of the pouches just at
the discernible limit of the branchial ectoderm. The ecto-
dermal part of Branchial Membrane III separates from the
body surface, but remains attached to Thymus III. Thus
ectodermal cells of Membrane III may contribute to the
formation of Thymus III, but it is clear that the greater
portion of the rudiment arises from the dorsal part of the
pouch. Thymus IV behaves in a similar way.

The function of the thymus remained obscure for a long
time. The situation changed about 1950 when systematic re-
moval of various organs showed that thymectomy of the young
mouse blocks the onset of lymphatic leukemia (Ruth et al.,

1965). Beginning in 1957, Fichtelius and his colleagues published a series of isotopic studies which indicated that immunologically competent cells may emigrate from the thymus as they differentiate (Ruth, 1960). Additionally, the thymus may play a continuing role in the humoral control of lymphoid homeostasis (Miller, 1964; Metcalf, 1964). The initial indication of this is seen in the early invasion of the thymus by blood-borne cells which proliferate within the organ (Moore and Owen, 1967).

The present study differs from previous studies by inclusion of electron micrographs of the earliest anlagen of the bursa and the thymus. These confirm the impression of cell degeneration and death evident in light micrographs. Numerous lipid droplets of irregular shapes are observed in the proctodeal ectoderm, urodeal membrane, and the area of contact between branchial ectoderm and pharyngeal endoderm. The significance of this is not clear. Kremer also noted that degenerating cells often contain fat (Glucksmann, 1951). The proctodeal ectoderm, the urodeal membrane and the cloacal endoderm contain cell debris and numerous foci of cytoplasmic degradation similar to those found in the branchial ectoderm and the pharyngeal endoderm. Foci of cytoplasmic degradation are morphologically similar to the autophagic vacuoles of de Duve (1963) and cytolysomes of Novikoff (1960). What is the significance of focal cytoplasmic degradation? Evidence is available to show that cytolysomes or autophagic vacuoles

contain hydrolytic enzymes (de Duve, 1959; Novikoff et al., 1960) and are sites of digestion. The varied appearance of these cytolysomes is due to differences in the stages of their degradation and to the presence of different cell organelles in them. In the present study, some of them, in an advanced stage of degradation, are seen occupying the major part of the cell. The occurrence of cytolysomes and cell debris is indicative of cell degeneration. (Cytolysomes are frequent in cells injured experimentally, Hruban et al., 1963; Swift et al., 1964; Novikoff et al., 1964; Miller et al., 1964). Hruban et al. (1963) have suggested that focal cytoplasmic degradation involves the enclosure of small portions of cytoplasm in smooth membranes within which digestion occurs. Novikoff et al. (1964) also suggested that autophagic vacuoles originate from the endoplasmic reticulum.

The multivesicular bodies and the Golgi apparatus of the bursa primordium may be related to the formation of lysosomes. The appearance of multivesicular bodies close to the Golgi apparatus and the similarity of the inner vesicles of the multivesicular body to the Golgi vesicles are suggestive of an intimate relationship. Novikoff et al. (1964) proposed that Golgi vesicles may contribute to the formation of multivesicular bodies, and may be considered to be the primary lysosomes. The inner vesicles of multivesicular bodies frequently resemble Golgi vesicles in size and appearance. The individual vesicles of multivesicular bodies

of rat cells possess acid phosphatase activity. It may be that the multivesicular body receives acid hydrolases from the Golgi vesicles, some of which appear intact within the body.

Bruni and Porter (1965) observed multivesicular bodies in the early stage of their formation. The vesicles are identical in size and content to the vesicles released from the Golgi lamellae, and Golgi vesicles are very close to and even attached to the multivesicular bodies. They propose that vesicles are released from the Golgi apparatus, lose their surface coating, and fuse into aggregates which transform into multivesicular bodies. It might be expected that Golgi vesicles would also transport lysosomal hydrolases to autophagic vacuoles, but thus far no observations suggestive of this have been encountered.

A distention of the nuclear envelope or nuclear blebbing has been seen occasionally in the cells from the urodeal membrane (Fig. 72). Small vesicles or granules were seen in the nuclear blebs (Figs. 65 and 76). These vesicles differ from Golgi vesicles and MVB vesicles. Possibly, they contribute to the intracellular bursa vesicles. The bursa vesicles seem to exert pressure on the surrounding cells as though these cells form the bursa vesicles by actively secreting fluid which cannot escape. The electron micrographs show the tight junctions between the cells which enclose the bursa vesicle. The tight junctions are seen only near the luminal aspect of the apposed cell surfaces.

In contrast to the urodeal membrane and other epithelia, the cells in the growing tip of the thymus are loosely packed together. The numerous, irregular, intercellular spaces are penetrated by many long, slender cytoplasmic protrusions. The thymus is partly separated from the surrounding mesenchyme by an incomplete basement membrane and fluffy extracellular substance (Fig. 122). Cells are actively proliferating as shown by the large number of blocked metaphases in Colcemid-treated embryos. Ovoid nuclei with large nucleoli are seen in the dorsal part of the thymus (Fig. 122). Nuclei with irregular outline are found in the ventral part of the thymus (Fig. 123). Tubular endoplasmic reticulum and mitochondria are moderately frequent. Cell debris is common and phagocytes containing cell debris are seen close to or beside the thymus. Free cell debris also occurs close to the thymus. This supports light microscopic indications that some cell debris is expelled from the thymus and other epithelia into the mesenchyme where it is phagocytized by mesenchymal cells.

The thymus contains many myelin figures connected to the nuclear envelope as whorls. Other myelin figures are connected to mitochondria, endoplasmic reticulum, Golgi membrane, and plasma membrane. Myelin figures may be indicative of membrane destabilization or membrane degeneration, and may be a step in the elimination of excess membrane. Nuclear whorls similar to those of the thymus appear during spermiogenesis (Nicander and Bane, 1962; Fawcett and Ito, 1965; Anderson et al., 1967)

and in the spinal ganglia of the chick embryo (Pannese, 1966). Myelin figures have been found in normal cells as well as in degenerating or experimentally treated cells (Cecio, 1964). Although myelin figures are demonstrated more readily in glutaraldehyde-osmium tetroxide fixed materials than in other fixatives (Carr, 1967), they are also found in the materials fixed in osmium tetroxide alone (Cecio, 1964) or in permanganate (Stoeckenius, 1958; Campiche, 1960). For example, myelin figures connected with the nuclear envelope have been found in spermatozoa fixed in osmium tetroxide alone (Nicander and Bane, 1962; Fawcett and Ito, 1965). Richter and Moize (1966) reported that myelin figures were present in the bladders of all adult mice but were not seen in bladders of the rat, guinea pig, rabbit, dog, cat or human. They were always present in the intermediate layer of epithelial cells but never in the basal or superficial layers. They did not occur in newborn mice but appeared by 10 to 14 days of age. Myelin figures are not, therefore, a simple artifact of glutaraldehyde fixation. They must be present before fixation or they must arise during fixation as a consequence of a physical peculiarity of the membranes which is expressed during fixation as nuclear whorls or myelin figures.

Two types of cells have been observed in the region of contact of the branchial ectoderm and the endoderm of the pharyngeal pouch: light and dark cells (Figs. 116 and 121). The recognition of two types is based on the profound alteration of the electron-scattering potential of the nuclear and

cytoplasmic matrices of entire cells. Light and dark cells
are also found in the liver parenchymal cells under various
experimental conditions: after ligation of the common bile
duct in the liver of rat (Steiner et al., 1962); after the
administration to rats of toxic agents such as ethionine
(Herman et al., 1962) and carcinogens such as napthyliso-
thiocyanate (Steiner and Baglio, 1963). Steiner and Baglio
(1963) did not consider the occurrence of light and dark
cells to be due to an artifact produced by the buffer used
in the preparation of the fixative. There is as yet no
acceptable explanation, although it seems clear that light
and dark cells mainly appear when tissues or cells are not in
normal condition. In the normal developing embryo their oc-
currence may be due to tissues or cells undergoing some special
alteration.

The cytoplasmic granules of dark cells are more evenly
distributed than those of light cells, which suggests that
polyribosomal clusters are present in light cells, but absent
from dark cells. The smaller size of the granules of dark
cells indicates that the ribosomes have dissociated into their
subunits. Such dissociation is thought to occur whenever the
ribosome loses its attachment to messenger RNA (Guthrie and
Nomura, 1968). Thus the appearance of the dark cell can be
interpreted to mean that it is not synthesizing protein. For
this and other reasons, the dark cell is regarded as a degen-
erating cell and the light cell is regarded as metabolically

active.

Cell deaths are encountered in: (1) the pharyngeal
pouch and contact of the branchial ectoderm and the pharyn-
geal pouch during the development of the thymus primordia;
(2) proctodeal ectoderm and the urodeal membrane during the
development of the bursa primordium; (3) the posterior part
of the cloaca during its regression; and (4) the fusion of
the amniotic folds. The occurrence of the degenerating cells
is so apparent that it cannot be accidentally or artifactually
produced during the tissue preparation. The appearance of
the degenerating cells was noted during the examination of
the tissues with the phase contrast microscope and was fur-
ther confirmed by electron microscopic and histochemical
observations. There is no reason, therefore, to doubt their
actual existence.

The fact that cell death accompanies differentiation
suggests that cell degeneration is a consequence, or a
necessary accompaniment of morphogenesis. A comprehensive
review of cell death in normal embryonic development has
been made by Glucksmann (1951) who classified the cell degen-
erations according to their developmental functions into
three groups - morphogenetic, histiogenetic and phylogenetic
degenerations. Many reports on observations of degenerating
cells during embryogenesis and organogenesis are listed in
Glucksmann's review (1951). The cell degeneration observed
in the present study can be considered as a morphogenetic

degeneration, according to Glucksmann's classification.
Saunders et al. (1962) have also pointed out the role of
cell death in the shaping of the upper arm and forearm dur-
ing morphogenesis of the avian wing.

As for the explanation for the death of embryonic cells
Glucksmann (1951) and Ernst (1926) have different viewpoints.
Ernst (1926) has suggested that endogenous and exogenous
factors might cause the death of embryonic cells. He thought
that the life energy of embryonic cells might become exhausted
like that of adult blood cells, epidermal cells, and die.
Glucksmann (1951) considered that Ernst's comparison is not
very apt, since embryonic cells are able to rejuvenate
themselves by division while the differentiated adult cells
are incapable of division. Experimental embryological and
genetic observation suggests that certain stimuli for the
proliferation and differentiation of organs are active for
limited periods only, and it is thus reasonable to assume
that when these stimuli cease, cells fail to divide and
complete their specialization, thereby aging and subsequently
dying (Glucksmann, 1951). With regard to exogenous factors
Ernst (1926) has considered the pressure of neighboring mito-
tic cells and the displacement of cells by changes in the
shape of organs which may lead to nutritional disturbances,
and result in death. Glucksmann (1951) thought that although
Ernst's view may apply in a few instances, it certainly would
not account for the majority of morphogenetic degenerations.

Some previous reports (Hamburger and Levi-Montalcini, 1949; Hamburger, 1958; Gasseling and Saunders, 1961) appear to support the view that cell death is the result of certain tissue interactions (Saunders et al., 1962). In general, however, the causation of the morphogentic degenerations is still obscure. Cell degeneration mentioned above is presumably under genetic control, but this is not defined. However, some cases apparently depend on particular genes (Gluecksohn-Schoenheimer, 1942, 1945).

The cell degeneration evident in the urodeal membrane during the formation of bursa vesicles is accompanied by intensive acid phosphatase activity. When the bursa separates from the urodeal membrane the enzyme activity decreases and the signs of cells degeneration are greatly reduced. The enzyme activity reappears in the bursa epithelium during the formation of the follicles and the follicles show signs of cell deterioration. This parallel between acid phosphatase activity, cell deterioration, and differentiation, during the formation of the bursa epithelium and later during the formation of the follicles, suggests that the three processes are intimately, if not necessarily, related.

The cell degeneration in the ectodermal branchial grooves, the endodermal pharyngeal pouches and the thymus primordium is closely associated with acid phosphatase activity. The enzyme activity in the thymus decreases greatly after the

seventh day of incubation. The release of the acid phospha-
tase or other lysosomal hydrolases is not necessarily the
cause of cell death. The lysosomes may become activated
after the cells die. The time at which lysosomal hydrolases
begin to act in cell degeneration is unknown. The cell
debris appears to be phagocytized or absorbed by neighbor-
ing epithelial cells or extruded into the mesenchyme and
phagocytized by the mesenchymal cells.

The fact that the mitotic cells of the pharyngeal pouch
appear along the inner lining of the pouch, as revealed by
the Colcemid method (Fig. 142) and the fact that acid phos-
phatase activity is concentrated basal to the mitotic fig-
ures of the pouch (Figs. 99 and 100) suggest that the acid
phosphatase activity may be associated with cell division
rather than cell degeneration. De Duve and Wattiaux (1966)
emphasize the perinuclear rearrangement of the lysosomes
during mitosis (Dougherty, 1964; Robbins and Ganatas, 1964;
Kent et al., 1965) and the activation of lysosomes in lympho-
cytes by phytohemagglutinin (Hirschhorn et al., 1964) as
indicative that acid phosphatase may play a role in mitosis.
Nevertheless, the acid phosphatase activity of the branchial
and cloacal epithelia is always intense in areas of cell
degeneration and is particularly intense around visible
debris. Unless this association with debris represents an
artifact of enzyme localization it is more likely that

intense acid phosphatase activity in the branchial and cloacal epithelia is related primarily to the formation and disposal of debris. This is substantiated by the intense activity in mesenchymal cells which contain debris and the weak activity in proliferating lymphoid tissue.

V. SUMMARY

1. The thymus and the bursa of Fabricius, the first lymphoid organs of the chicken, appear on the fifth day of incubation as proliferations of endodermal epithelia.

2. The bursa appears in the caudal half of the urodeal membrane. The urodeal membrane is a small, thin partition between the right and left halves of the body in the region ventral to the caudal end of the gut. The dorsal part of the urodeal membrane is cloacal endoderm and the ventral part is proctodeal ectoderm. The bursa appears as a median chain of intercellular vesicles subjacent to the proctodeal ectoderm and just within the endoderm. These vesicles enlarge and fuse to become the lumen of the bursa. The surrounding endodermal cells proliferate to form the lining of the bursa. The vesicles at the anterior of the urodeal membrane may not contribute to the lumen of the bursa. The posterior part of the urodeal membrane probably represents the eventual opening of the bursa into the proctodaeum and the anterior part represents the eventual opening of the embryonic cloaca.

3. The number and size of the bursa vesicles suggest that active secretion of fluid occurs throughout the urodeal membrane. Their light microscopic clarity indicates that they are not deposits of cell debris. The borders of the bursa vesicles are lined by numerous tight junctions. The tight

coupling of these cells and the symmetry of the vesicles suggest that the fluid of the vesicles is under pressure. The enlarged and fused bursa vesicles form a bursa sac caudad to the urodeal membrane and the cloaca. The blind end of the bursa sac expands dorsally towards the vertebral column. The bursa lymphoid follicles first appear in the bursa epithelium on the 13th day of incubation.

4. Cell degeneration and cell death are common in the proctodeal ectoderm and the urodeal membrane. Since degeneration is associated with the activity of lysosomal enzymes, the activity of the most definitive of these was examined through the early development of the bursa. The acid phosphatase activity of the bursa epithelium is very active at 7 days, 13 days and 14 days, and inactive at 9, 10, 11, and 12 days. The times at which the epithelium of the bursa has high activity are the times of active differentiation: the formation of the definitive bursa epithelium and its transformation into follicles. The high activity in the proctodeal ectoderm and the subjacent urodeal membrane is associated with the formation of the anus and the bursa stalk.

5. The acid phosphatase activity in the tunica propria is mainly attributed to the immature heterophil granulocytes and partly to the mesenchymal cells.

6. The thymus appears as four separate proliferations. These arise from the dorsal, lateral extremes of pharyngeal

pouches III and IV. Each of these proliferations lies just
dorsal and medial to the medial end of a small, transverse
membrane connecting the pharyngeal pouch to the correspond-
ing branchial groove. The dorsal part of Membrane III is
a tube of ectoderm which intrudes mediad from Groove III
and the ventral part is a tube of endoderm which protrudes
laterad from the ventral part of Pouch III. The contact
of ectoderm with endoderm is continuous from just beneath
the body surface to a point just ventral and lateral to
Thymus III. Membrane IV does not have a ventral, endodermal
part. The contact of ectoderm with endoderm is restricted
to the area just ventral and lateral to Thymus IV. There
is no chain of vesicles.

7. Cell degeneration is very common throughout the epi-
thelial complexes from which the thymus is formed. It is
extreme medial to the thymus, where the connection to the
pharynx will break, and lateral to the thymus, where the
connection to the branchial groove will break. Intense
acid phosphatase activity is found throughout the epithelium
and in the early thymus, but not in the thymus after the
seventh day of incubation. The reality of degeneration is
confirmed by the intense uptake of dye at the surface of the
branchial groove. The branchial areas which take up dye
are Grooves II, III, and IV.

8. The Colcemid-treated embryos show that cell proliferation
is concurrent with cell degeneration in the early thymus

primordium.

9. Two types of cells have been observed in the region of contact of the branchial ectoderm and the endoderm of the pharyngeal pouch: light and dark cells.
The recognition of two types is based on the profound alteration of the electron-scattering potential of the nuclear and cytoplasmic matrix of entire cells.

10. In thymus cells, nuclear whorls are commonly seen. Myelin figures appear in connection with mitochondria, endoplasmic reticulum and Golgi membrane. Nuclear whorls and myelin figures are an indication of membrane degeneration.

BIBLIOGRAPHY

Ackerman, G. A., and R. A. Knouff. 1959. Lymphocytopoiesis in the bursa of Fabricius. Am. J. Anat., 104: 163-206.

Ackerman, G. A., and R. A. Knouff. 1964. Lymphocyte formation in the thymus of the embryonic chick. Anat. Rec., 149: 191-216.

Anderson, W. A., A. Weissman and R. A. Ellis. 1967. Cytodifferentiation during spermiogenesis in Lumbricus terrestris. J. Cell Biology, 32: 11-26.

Auerbach, R. 1961. Experimental analysis of the origin of cell types in the development of the mouse thymus. Dev. Biol., 3: 336-354.

Baillif, R. N. 1949. Thymic involution and regneration in the albino rat following injection of acid colloidal substances. Am. J. Anat., 84: 457-510.

Barger, J. D., and E. D. De Lamater. 1948. The use of thionyl chloride in the preparation of Schiff's reagent. Science, 108: 121.

Barka, T. 1960. A simple azo-dye method for histochemical demonstration of acid phosphatase. Nature, 187: 248-249.

Beard, J. 1900. The source of leucocytes and the true function of the thymus. Anat. Anzeiger, 18: 550-561.

Beard, J. 1900. The thymus placode of the spiracle of Raja batis. Anat. Anzeiger, 18: 359.

Bornhaupt, T. 1867. Untersuchungen uber die Entwicklung der Urogenitalsystems beim Hühnchen. In Diss., Riga. (Quoted from Stieda, 1880).

Boyden, E. 1922. The development of the cloaca in birds, with special reference to the origin of the bursa of Fabricius, the formation of a urodeal sinus, and the regular occurrence of a cloacal fenestra. Amer. J. Anat. 30: 163-202.

Bruni, C., and K. R. Porter. 1965. The fine structure of the parenchymal cell of the normal rat liver. Amer. J. Pathol. 46:691.

Campiche, M. 1960. Les inclusions lamellaires des cell alveolaires dans le poumon du raton. Relations entre l'ultrastructure et la fixation. J. Ultrastructure Res. 3: 302-312.

Carr, I. 1967. Nuclear membrane whorls. Zeitschrift für Zellforschung. 80: 140-144.

Cecio, A. 1964. Electron microscopic observations of young rat liver. I. Distribution and structure of the myelin figures. Zeitschrift fur Zellforschung, 62: 717-743.

Chan, C., and G. Sainte-Marie. 1968. Distribution and morphology of the subcapsular and reticular cells of the ten-week-old rat thymus. J. Anat., 102: 477-491.

Chen, L. T., and R. F. Ruth. 1966. Nuclear structure in lymphoid primordia. Nature, 209: 381-383.

De Duve, C. 1959. Lysosomes, a new group of cytoplasmic particles. In "Subcellular Particles". T. Hayashi (ed.), Ronald, New York. P. 128.

De Duve, C. 1963. The lysosome concept. In "Ciba Foundation Symposium on Lysosomes". De Reuck, A.V.S., and M. P. Cameron (eds.). Little, Brown & Co., Boston. Pp. 1-31.

De Duve, C., and R. Wattiaux. 1966. Functions of lysosomes. Ann. Rev. of Physiology, 28:435.

Dougherty, W. J. 1964. Fate of Gogi complex, lysosomes, and microbodies during mitosis of rat hepatic cells. J. Cell Biol. 23: 25A.

Ernst, M. 1926. Uber Untergang von Zellen während der normalen Entwicklung bei Wirbeltieren. Z. ges. Anat. I. Z. Anat. Entw. Gesch., 79:228.

Fawcett, D. W., and S. Ito. 1965. The fine structure of bat spermatozoa. Amer. J. Anat., 116: 567-609.

Gasseling, M. T., and J. W. Saunders, Jr. 1961. Effects of the apical ectodermal ridge on growth of the versene-stripped chick limb bud. Dev. Biol., 3: 1-25.

Gasser, P. 1880. Die Entstehung der Kloakenoffnung bei Huhnerembryonen. Arch. f. Anat. u. Entwick., S. 297-319. (Quoted from Boyden, 1922).

Glick, B., T. S. Chang, and R. G. Jaap. 1956. The bursa
of Fabricius and antibody production. Poultry Science,
35: 224-225.

Glucksmann, A. 1951. Cell deaths in normal vertebrate
ontogeny. Biol. Rev., 26, 59-86.

Gluecksohn-Schoenheimer, S. 1942. The morphological
manifestation of a dominant mutation affecting tail
and urogenital systems. Genetics, 28: 341-348.

Gluecksohn-Schoenheimr, S. 1945. The embryonic development
of mutants of the Sd-strain in mice. Genetics 30: 29-
38.

Gomori, G. 1952. In "Miscroscopic Histochemistry, Principles
and Practice". University of Chicago Press. P. 193.

Guthrie, C., and M. Nomura. 1968. Initiation of protein
synthesis: a critical test of the 30S subunit model.
Nature, 219:232.

Hamburger, V., and R. Levi-Montalcini. 1949. Proliferation,
differentiation and degeneration in the spinal ganglia
of the chick embryo under normal and experimental con-
ditions. J. Exptl. Zool., 111: 457-502.

Hamburger, V. 1958. Regression versus peripheral control
of differentiation in motor hypoplasia. Amer. J.
Anat. 102: 365-410.

Hammond, W. S. 1954. Origin of thymus in the chick embryo.
J. Morphol. 95: 501-521.

Herman, L., L. Eber, and P. J. Fitzgerald. 1962. Liver
    cell degeneration with ethionine administration. In
    "Electron Microscopy, Fifth International Congress".
    Vol. 2, VV-6. S. S. Breese, Jr. (ed.), Academic
    Press, New York.

Hirschhorn, R., G. Kaplan, K. Hirschhorn, and G. Weissmann.
    1964. Appearance of lysosomes before mitosis induced
    in human lymphocytes by phytohemaglutinin. Clin. Res.
    12:449.

Holt, S. J. 1958. Indigogenic staining methods for este-
    rases. In "General Cytochemical Methods". J. F.
    Danielli (ed.), Academic Press, New York.

Holt, S. J., and R. M. Hicks. 1961. Studies on formalin
    fixation for electron microscopy and cytochemical
    staining purposes. J. Biophys. Biochem. Cytol.
    11: 31 and 47.

Hruban, Z., B. Spargo, H.Swift, R. W. Wissler, and R. G.
    Kleinfeld. 1963. Focal cytoplasmic degradation.
    Amer. J. Pathol. 42:657-683.

Jolly, J. 1915. La bourse de Fabricius et les organs
    lymphoepitheliaux. Arch. d'anat. micr. T. 16: 363-
    547.

Jolly, J., and A. Pezard. 1928. Castration retards the
    involution of the bursa Fabricius. C. R. de la Societe
    de Biologie, 98: 379-380.

Kastschenko, N. 1887. Das Schlundspaltengluet des
     Hühnchens. Arch. Anat. Phy., Anat. Abt. S. 258-300.
     (Quoted from Hammond, 1954).

Kent, G., O. T. Minik, E. Orfei, F. I. Volini, and F.
     Madera-Orsini. 1965. The movement of iron-laden
     lysosomes in rat liver cells during mitosis. Amer.
     J. Pathol., 46:803.

Kirkpatrick, C. M., and F. N. Andrews. 1944. The influ-
     ence of the sex hormones on the bursa of Fabricius
     and the pelvis in the ring-necked pheasant. Endo-
     crinology, 34: 340.

Luft, J. H. 1961. Improvements in epoxy resin embedding
     methods. J. Biophs. Biochem. Cytol., 9: 409-414.

Mall, F. P. 1887. Entwicklung der Branchial Bogen und
     Spalten des Hühnchens. Arch. Anat. Phys., Anat.
     Abt. S. 1-34. (Quoted from Hammond, 1954).

Margolis, G., and J. P. Pickett. 1956. New application
     of luxol fast blue myelin stain. Lab. Investigation,
     5:459.

Maximow, A. A. 1909. Untersuchungen über Blut und Binde-
     gewebe 2. Uber die Histogenese der Thymus bei Säu-
     getieren. Arch. mikroskop. Anat. u. Entwicklungs-
     mech. 74:525-621.

Miller, F., and G. E. Palade. 1964. Lytic activities in
     renal protein absorption droplets. J. Cell Biol.,
     23: 519-552.

Moore, M. A. S., and J. J. T. Owen. 1966. Experimental studies on the development of the bursa of Fabricius. Devel. Biol. 14: 40-51.

Moore, M. A. S., and J. J. T. Owen. 1967. Experimental studies on the development of the thymus. J. Exptl. Med. 126:715.

Mueller, A., H. R. Wolfe, and R. K. Meyer. 1960. Precipitin production in chickens. XXI. Antibody production in bursectomized chickens and in chickens injected with 19-nortesosterone on the fifth day of incubation. J. Immunol., 85: 172-179.

Nicander, L., and A. Bane. 1962. Fine structure of boar spermatozoa. Zeitchr. Zellforsch. 57: 390-405.

Novikoff, A. B. 1960. Biochemical and staining reactions of cytoplasmic constituents. In "Developing Cell Systems and Their Control". Pp. 167-203. D. Rudnick (ed.), Ronald Press, New York.

Novikoff, A. B., and E. Essner. 1960. The liver cell. Some new approaches to its study. Amer. J. Med., 29: 102-131.

Novikoff, A. B., E. Essner, and N. Quintana. 1964. Golgi apparatus and lysosomes. Fed. Proc. 23: 1010.

Palade, G. E. 1952. A study of fixation for electron microscopy. J. Exptl. Med., 95: 285-297.

Pannese, E. 1966. Structures possibly related to the formation of new mitochondria in spinal ganglion neuroblasts. J. Ultrastructure Res., 15: 57-65.

Patten, B. M.   1951.   Early embryology of the chick.   4th
    ed. The Blakiston Co., Philadelphia.

Pera, L. 1958.   Morfologia e sviluppo della bursa di
    Fabrizia in Gallus domesticus.   Archivio Italiano di
    Anatomia e di Embriologia.   63: 407-444.

Richter, W. R., and S. M. Moize.   1966.   Myelin figures in
    mouse transitional epithelium.   Fed. Proc. 25:534.

Robbins, E., and N. K. Gonatas.   1964.   The ultrastructure
    of a mammalian cell during the mitotic cycle.   J.
    Cell Biol. 21:429.

Ruth, R. F.   1960.   Ontogeny of the blood cells.   Fed. Proc.
    19: 579-585.

Ruth, R. F., C. P. Allen, and H. W. Wolfe.   1964.   The
    effect of thymus on lymphoid tissue.   In "The Thymus
    in Immunobiology".   R. A. Good and A. E. Gabrielsen
    (eds.) Harper and Row, Philadelphia.

Ruth, R. F., E. O. Hohn, and G. R. J. Law.   1965.   Onto-
    geny of the lymphoid tissue.   Scand. J. Haematol. 8:29.

Sabatini, D. D., K. G. Bensch, and R. J. Barrnett.   1962.
    New fixatives for cytological and cytochemical studies.
    In "Proceedings of Fifth International Congress for
    Electron Microscopy".   2:L3.   S. S. Breese, Jr. (ed.),
    Academic Press, New York.

Saunders, J. W., Jr., M. T. Gasseling, and L. C. Saunders.
    1962.   Cellular death in morphogenesis of the avian wing.
    Devel. Biol. 5:147-178.

Schrier, J. E., and H. L. Hamilton. 1952. An experi-
    mental study of the origin of the parathyroid and
    thymus glands in the chick. J. Exptl. Zool. 119:165.

Scothorne, R. J. 1957. Observation on the so-called
    Thymus II of birds. J. Anat., 91: 13-24.

Selye, H. 1943. Morphological changes in the fowl fol-
    lowing chronic overdosage with various steroids.
    J. Morph. 73:401-418.

Steiner, J. W., J. S. Carruthers, and S. R. Kalifat.
    1962. Observations on the fine structure of rat
    liver cells in extrahepatic cholestasis. Zeitchr. Zell-
    forsch. 58: 141.

Steiner, J. W., and C. M. Baglio. 1963. Electron
    microscopy of the cytoplasm of parenchymal liver
    cells in alpha-naphthylisothiocyanate-induced cirrhosis.
    Lab. Invest. 12: 765-790.

Stieda, L. 1880. Uber den Bau and die Entwickelung der
    Bursa Fabricii. Zeitschr. f. Wiss. Zool., Bd. 34,
    S. 296-309.

Stoeckenius, W. 1958. Fixierung von Myelinfiguren aus
    Phosphatiden und Eiweiß mit OsO_4 und $KMnO_4$. Fourth
    Int. Conf. E. M., Berlin. 2: 174-177.

Swift, H. and Z. Hruban. 1964. Focal degradation as a
    biological process. Fed. Proc. 23: 1026-1037.

Verdun, P. 1898. Sur les derives branchiaux du poulet.
    C. R. Soc. Biol., Paris. 5: 243-244. (Quoted from
    Hammond, 1954).

Watson, M. L. 1958. Staining of tissue sections for
    electron microscopy with heavy metals. J. Biophy.
    Biochem. Cytol., 4: 475-478.

Wenckebach, K. F. 1888. De Ontwikkeling en de Bouw der
    Bursa Fabricii. Proefschrift. Leiden. (Quoted
    from Boyden, 1922).

Fig. 1. Dextral view of a 4-day chick embryo. A few drops
         of two percent osmium tetroxide solution have been
         added to the embryo in order to increase the
         contrast. This treatment is also applied to the
         embryos illustrated in Figs. 2 and 3.
         X 7.8

Fig. 2. Dextral view of a 5-day chick embryo.
         X 6

Fig. 3. Dextral view of a 6-day chick embryo.
         X 7

Fig. 4. A diagram of the dextral view of a 4-day chick
         embryo. The locations of the primordia of the
         thymus (TH) and the bursa of Fabricius (BF) are
         shown in the stippled rectangles.
         X 16

Fig. 5. A diagram of the dorsal view of a 5-day chick
         embryo. The locations of the primordia of the
         thymus (TH) and the bursa of Fabricius (BF) are
         shown in the stippled rectangles.
         X 9

TH

BF

④

TH

BF

⑤
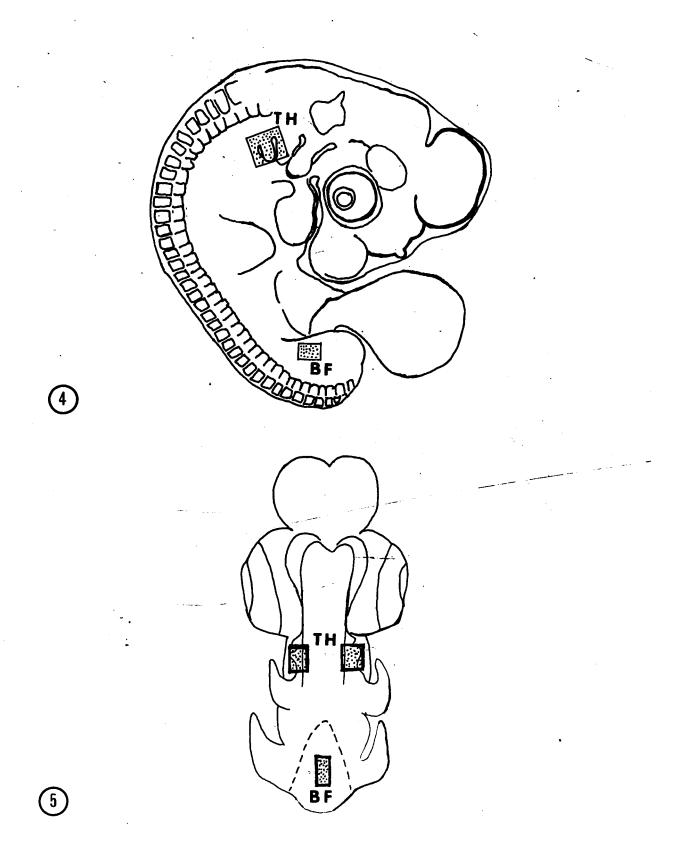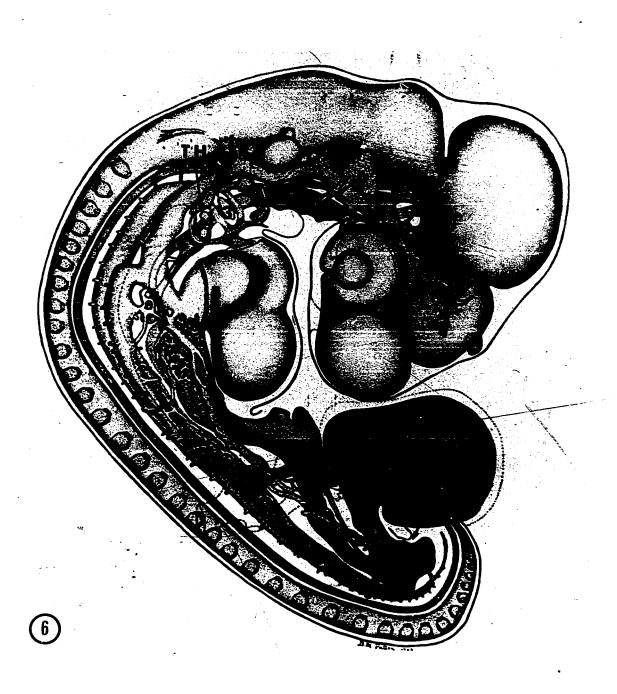
Fig. 6. Internal organs of a 4-day chick embryo drawn

from a wax-plate reconstruction after Patten

(1958) to show the locations of the primordia

of the thymus (TH) and the bursa of Fabricius

(BF).

X 25

TH

6

TH

BF

6
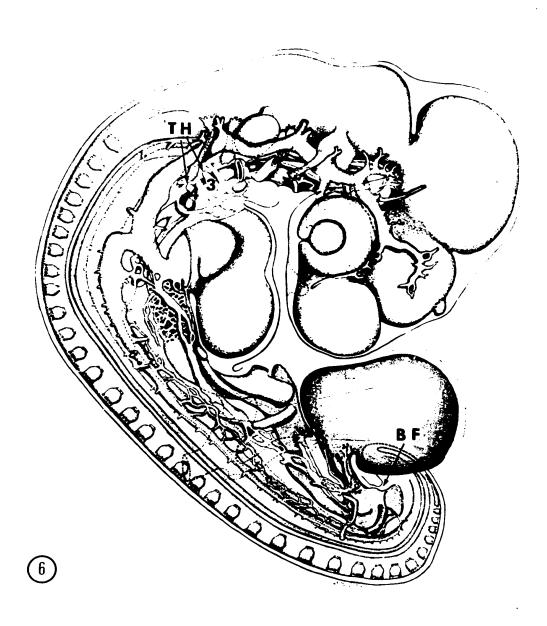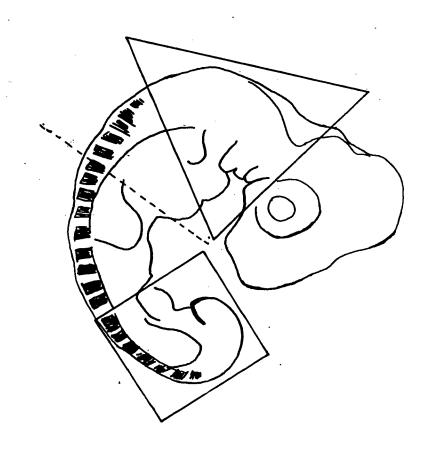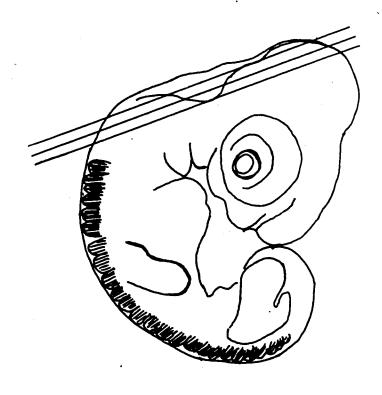
Fig. 7.   A diagram of the dextral view of a 4-day chick
          embryo.   The embryo is cut in halves (broken line)
          after brief fixation (to harden the embryo) and
          the branchial region (triangle) and the cloacal
          region (square) are cut out and fixed for
          microscopy.

⑦
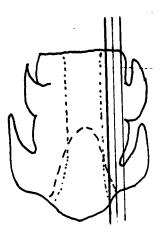
Fig. 8.   A diagram of the dextral view of a 5-day chick
          embryo to indicate the planes of the sections
          through the branchial region. The uppermost
          line indicates the plane of the first section
          which is perpendicular to the page. The
          sections are frontal with respect to the pharynx.
          X 10

Fig. 9.   A diagram of the dorsal view of the posterior
          part of a 5-day chick embryo to indicate the
          planes of the sections through the cloacal region.
          The sections are parasagittal, or sagittal, with
          respect to the axis of the body. The diagram
          does not indicate the slight curvature of the
          tail to the right.
          X 10

⑧

⑨
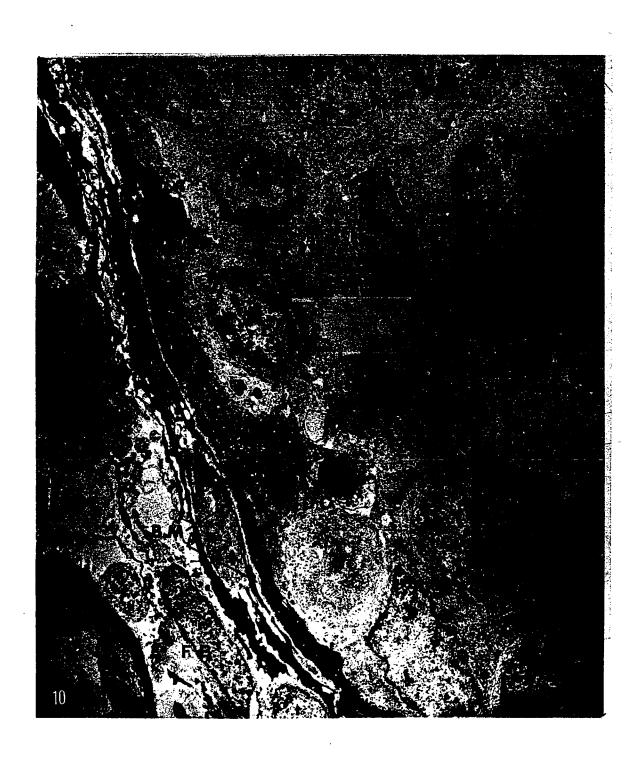
Fig. 10. Part of a bursa lymphoid follicle of the 19-day
chick embryo showing a part of a degenerating cell.
(DC) in the medulla of the lymphoid follicle. The
medulla is separated from the cortex by the basement
membrane (BM). The medulla is at the right of the
figure, the cortex at the left. Note the dark
reticular cells along the basement membrane.

   BM: basement membrane

   DC: degenerating cell   FB: fibroblast

Glutaraldehyde-osmium tetroxide, Epon,

and uranyl acetate.

X 9,600

Figs. 11-12.   Phase contrast photomicrographs of parts of
        the bursa of Fabricius of a 13-day chick embryo.
        Note that numerous cells which are darker than
        epithelial cells are distributed evenly through-
        out the tunica propria. Lymphoid follicles (LF)
        appear to be composed of two parts: the medulla
        (M) and the cortex. The boundary between the
        medulla and cortex of follicle is recognizable.
        B: boundary between medulla and cortex of
              lymphoid follicle   CA: bursal lumen
        C: cortex of follicle   M: medulla of follicle
        MU: muscularis   TP: tunica propria
        Osmium tetroxide, Araldite, and unstained.
        X 198
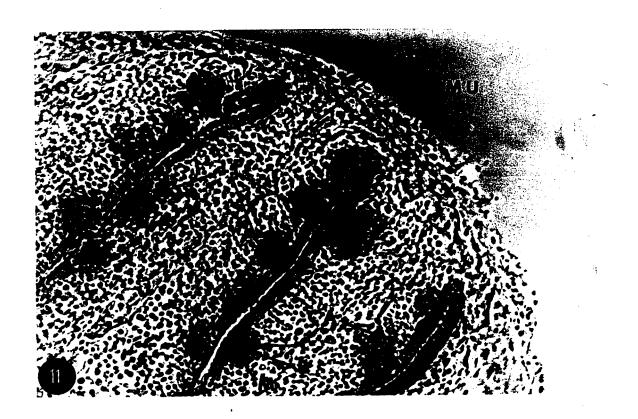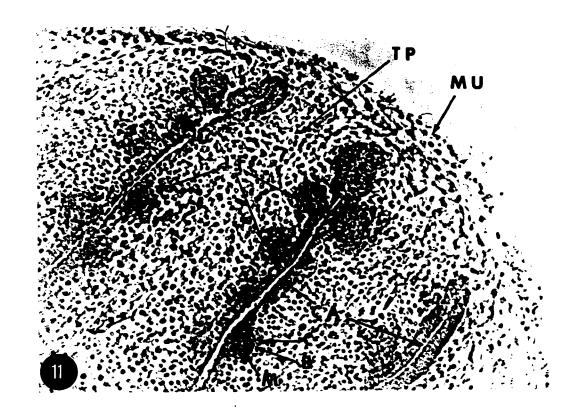
11

TP

12
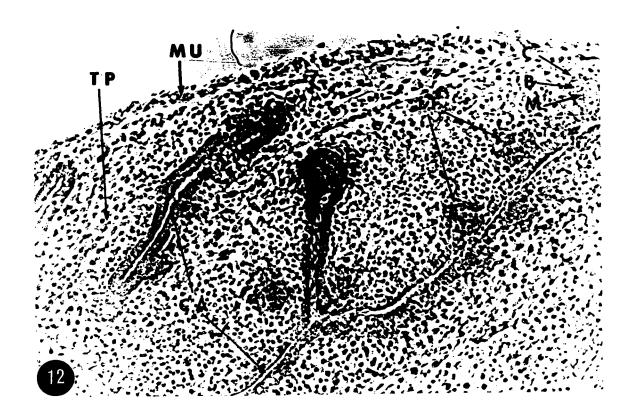
Fig. 13. Part of a bursa lymphoid follicle of the 19-day
chick embryo showing a lymphoblast surrounded by
a dark reticular cell (RC). A lymphocyte is seen
in the upper right hand corner. An erythrocyte
(ER) is shown at the lower left hand corner.
The basement membrane (BM) separates the medulla
of the lymphoid follicle (upper half) from the
cortex (lower half).

BM: basement membrane   LM: lymphocyte

EC: erythrocyte   N: nucleus

LB: lymphoblast

Glutaraldehyde-osmium tetroxide, Epon, and
uranyl acetate.

X 21,000

LM

RC

LB

N

BM

EC

13
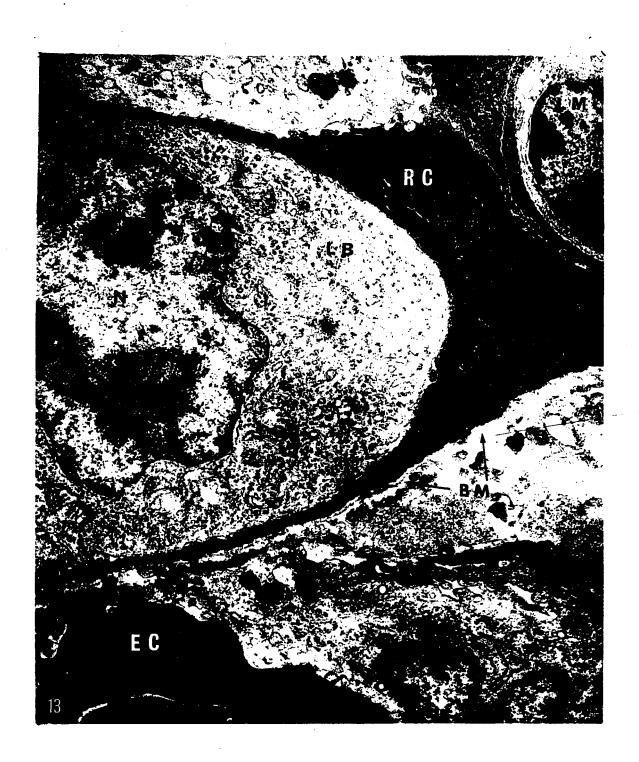
Fig. 14. A part of a lymphoid follicle of the bursa of
         Fabricius of a 19-day chick embryo showing the
         medulla of the lymphoid follicle (upper half of
         the figure) separated from the cortex (lower half)
         by the basement membrane (BM). A pyknotic nucleus
         (PN) and a desmosome are seen in the medulla.

   BM: basement membrane (basal lamina)

    D: desmosome

   PN: pyknotic nucleus

Glutaraldehyde-osmium tetroxide, Epon, and uranyl

acetate.

X 21,000

P N

B. M.

14
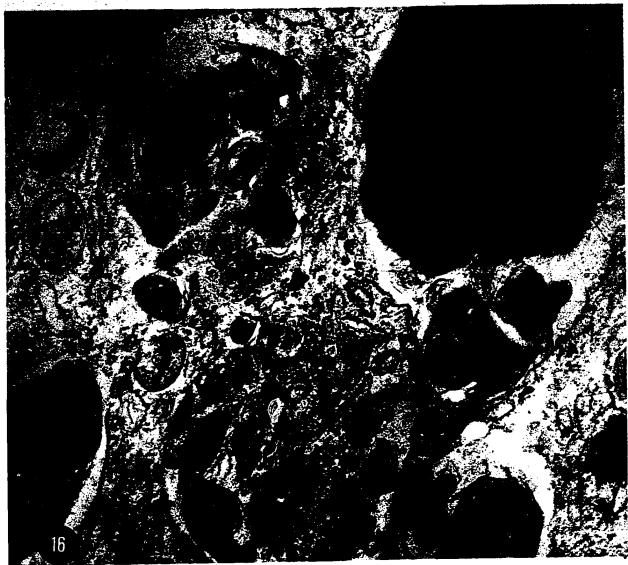
Figs. 15-16. Part of the medulla of a bursa lymphoid
follicle of a 19-day chick embryo showing two
cytolysomes (Fig. 15) and a degenerating cell
(Fig. 16). Many myelin figures are seen in
the cytoplasm of the degenerating cell.
Glutaraldehyde-osmium tetroxide, Epon, and
uranyl acetate.
X 36,000

15

16
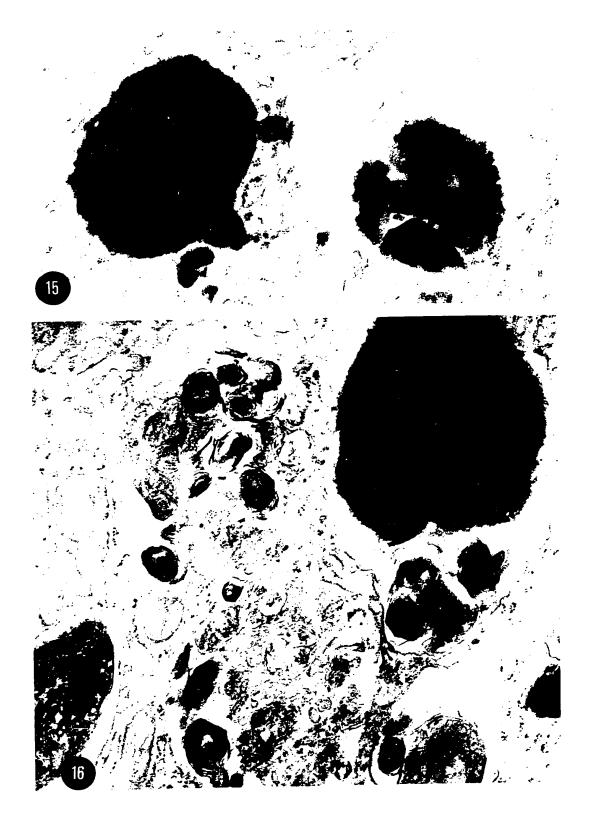
Fig. 17. The acid phosphatase activity of clusters of granu-
          locytes (arrows) in the tunica propria (TP) of a
          12-day bursa.
              TP: tunica propria   BL: lumen
          Barka medium for acid phosphatase, no counterstain.
          X 235

Fig. 18. The acid phosphatase reaction in the epithelium,
          the tunica propria, and the lymphoid follicles (LF)
          of a 13-day bursa.
          Section preparation as in Fig. 17.
          X 235

Fig. 19. High acid phosphatase activity in the lymphoid
          follicles and the tunica propria of a 14-day bursa.
          Section preparation as in Fig. 17 plus methyl green
          counterstain.
          X 235

Fig. 20. Moderate acid phosphatase activity in the lymphoid
          follicles of a 19-day bursa.
          Section preparation as in Fig. 19.
          X 110
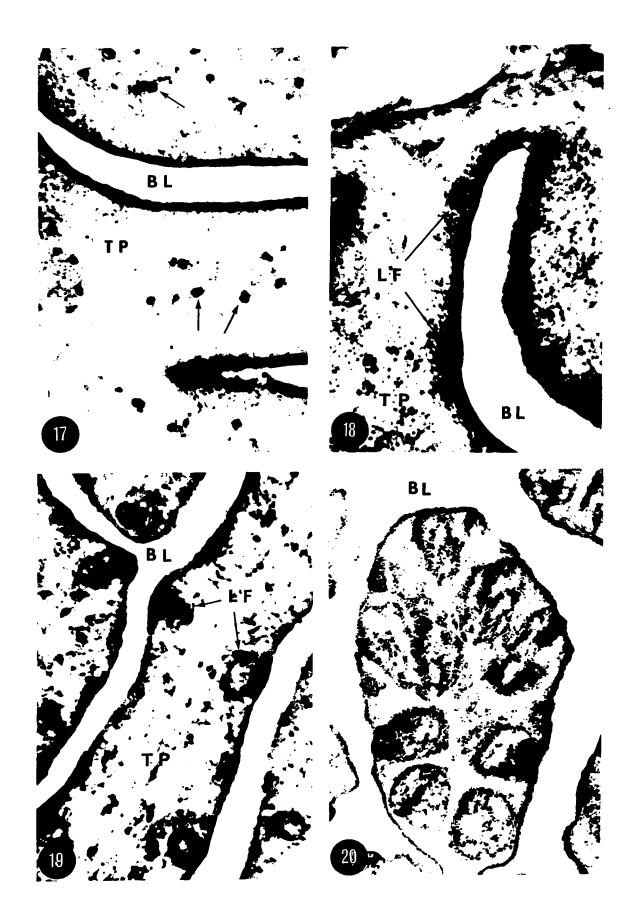
Fig. 21. Mature granulocytes in the 14-day bursa. The

immature granulocytes are larger than mature

ones and have, instead of pink to red, purple

cytoplasmic granules. A small area of the

tunica propria is shown at higher magnification

in Fig. 22.

Frozen section, Giemsa stain, color photomicro-

graph.   X 110

Fig. 22. Part of the tunica propria of the bursa shown in

Fig. 21. A cluster of immature granulocytes

with purple cytoplasmic granules is seen close to

the blood vessel in the center of this figure.

Some immature granulocytes have a mixture of

purple and red granules. (Mature granulocytes

contain red cytoplasmic granules.) The nuclei

stain pale blue.

Frozen section, Giemsa stain, color photomicro-

graph.   X 600
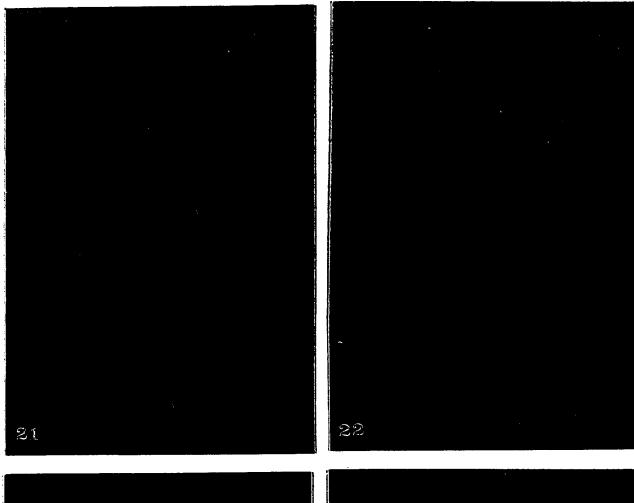
Fig. 23. Acid phosphatase activity in the lymphoid

follicles and in the tunica propria of a 14-day

bursa.

Barka medium, no counterstain.   X 110
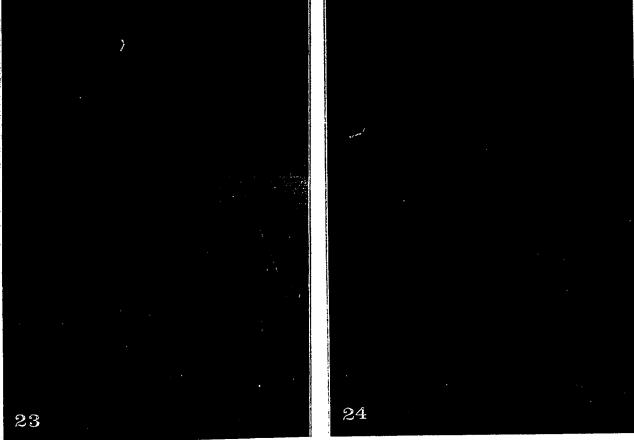
Fig. 24. Acid phosphatase in a lymphoid follicle (upper
left) and in the granulocytes. Some mature
granulocytes have low activity.
Barka medium for acid phosphatase, no counter-
stain.
X 600

21 22

23 24
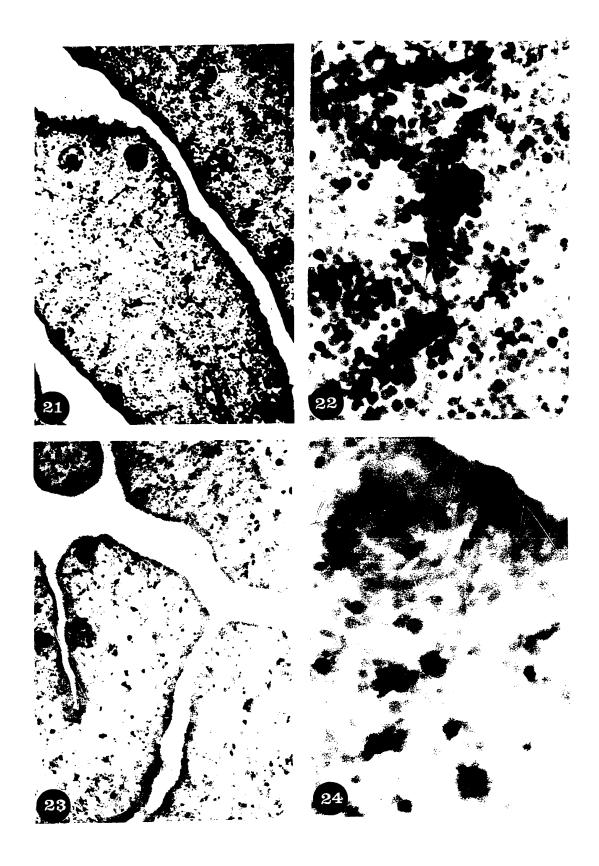
Fig. 25. A heterophil granulocyte in the tunica propria
of a 19-day bursa. There are three types of
ovoid, membrane-bound granules: "a" granules
which are full of dense, fine micro-granules
and are identical with the azurophil granules
seen after Wright staining; "b" granules which
have fewer and larger micro-granules and may
represent a transition from "a" to "c"; and
"c" granules which have less dense, smaller
micro-granules and may be the specific granules
of Wright preparations.
Glutaraldehyde-osmium tetroxide, Epon, and
uranyl acetate.
X 36,000

25

Fig. 26. Two eosinophils in the tunica propria of the 20-
         day bursa. Some granules contain an excentric
         spherical core. The acid phosphatase reaction
         produces lead phosphate deposits in the granule
         and on its limiting membrane (a).

                    N: nucleus

         Glutaraldehyde, Gomori's medium, post-fixation in
         osmium tetroxide, Epon, and unstained.
         X 21,600

26
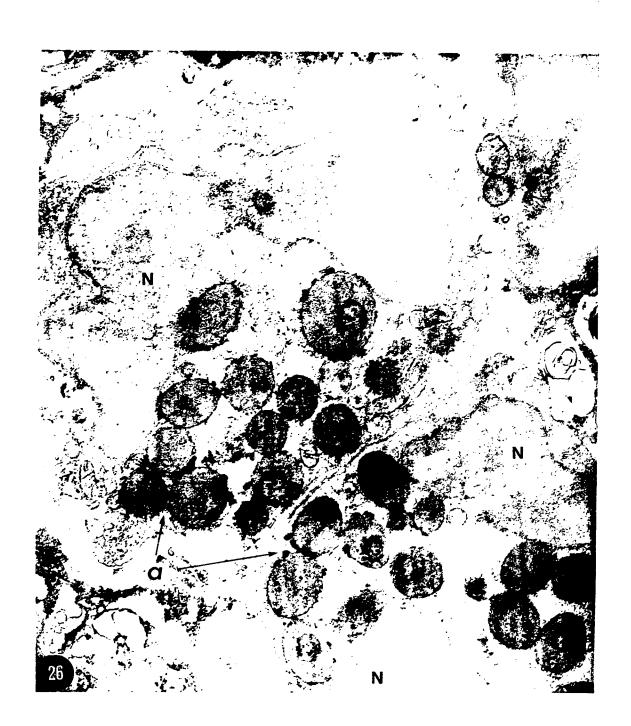
Fig. 27. Acid phosphatase in a 14-day bursa when follicles
          are abundant.
                    BF: bursa of Fabricius
          Barka medium, and counterstained with methyl green.
          X 10

Fig. 28. Acid phosphatase in a 13-day bursa when follicles
          are few. Bursa plicae are seen.
          Barka medium, no counterstain.
          X 10
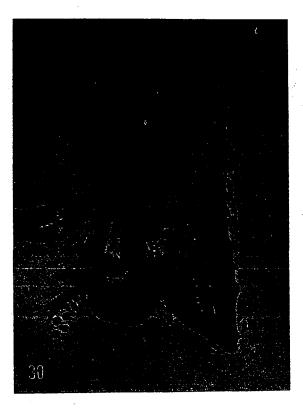
Fig. 29. Acid phosphatase in a 12-day bursa when follicles
          are not yet formed. A part of the urodeal membrane
          (unlabelled arrow) is illustrated at higher magni-
          fication in Fig. 38.
                    R: rectum   An: anus
          Preparation as in Fig. 28.
          X 10

Fig. 30. Acid phosphatase in an 11-day bursa. (This figure
          is darker than most others. The greater darkness of
          the bursa epithelium is not indicative of high acid
          phosphatase activity.)
          Section preparation as in Fig. 27.
          X 10

30

29

28

27
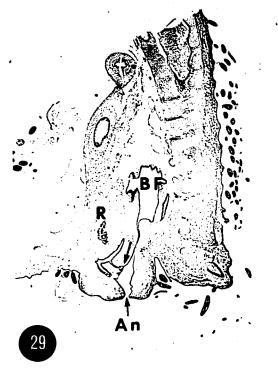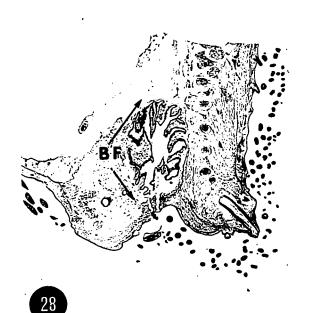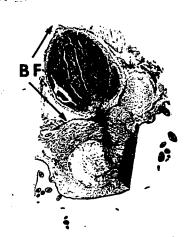
Fig. 31. A sagittal section of a 10-day embryo showing the expansion of the bursa between the rectum and the vertebral column. Intense acid phosphatase activity is noted in the urodeal membrane and the rectum. The urodeal membrane (arrow) is illustrated at higher magnification in Fig. 37. Barka medium, no counterstain.   X 10

Fig. 32. The 9-day bursa is a flattened sac just ventral to the vertebral column. Intense acid phosphatase activity occurs in the urodeal membrane (unlabelled arrow) and the rectum (R), which are shown at higher magnification in Figs. 35 and 36. Section preparation as in Fig. 31.   X 10

Fig. 33. The blind end of an 8-day bursa (B) extends dorsad toward the vertebral column.
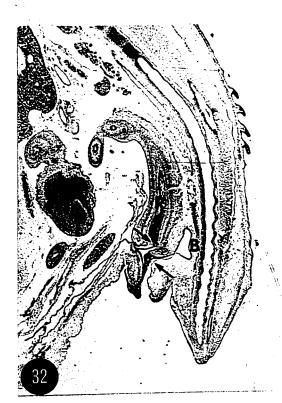
     C: cloaca   R: rectum

Frozen section, Giemsa stain.   X 10
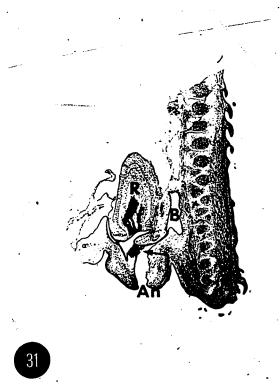
Fig. 34. At seven days the primordium of the bursa (B) extends as a blind sac away from the urodeal membrane (UM). Intense acid phosphatase activity is present in the urodeal membrane and the rectum.
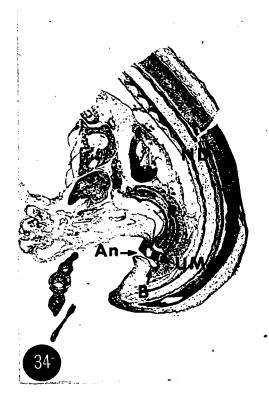
     AN: anus   ND: notochord

Section preparation as in Fig. 31.   X 10

34

33

32

31
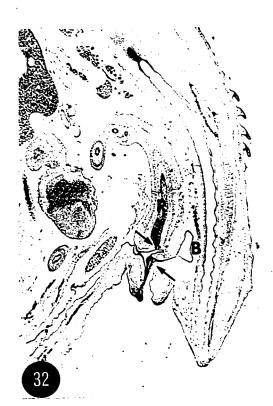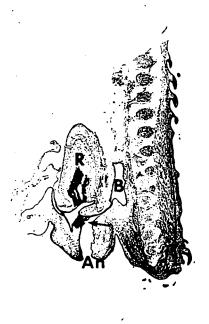
Fig. 35. Acid phosphatase in the 9-day urodeal membrane (UM).

  ME: mesenchyme

  BS: lumen of the bursa stalk

Section incubated in Barka medium for acid phos-

phatase localization, no counterstain.

X 235.

Fig. 36. Acid phosphatase in the 9-day rectum.

  R: rectum

Section preparation as in Fig. 35.
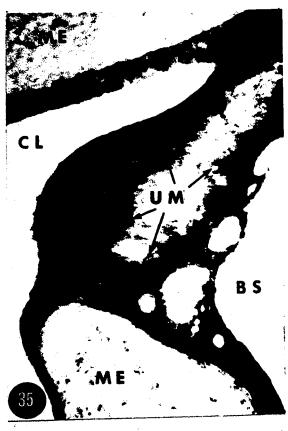
X 235

Fig. 37. Acid phosphatase in the urodeal membrane of a

10-day embryo.
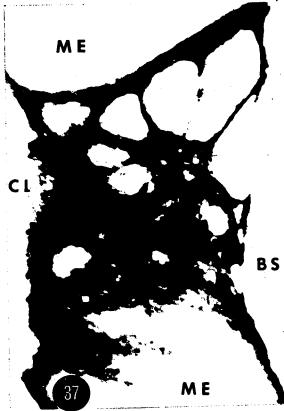
Section preparation as in Fig. 35.

X 235

Fig. 38. Acid phosphatase in the 12-day urodeal membrane.

X 620

35

36

37

38

ME

CL

UM

BS

ME

35

ME

R

CL

36

ME

CL

BS

BS

37

ME

BS

BS

38

ME
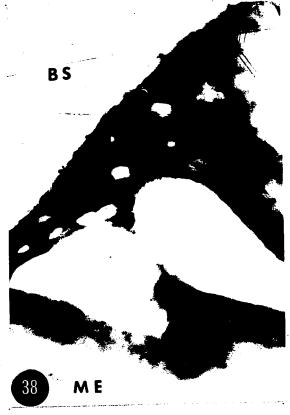
Fig. 39-42.   A series of phase contrast photomicrographs

taken from serial parasagittal sections of

a 4-day cloaca showing the cloacal fenestra

(CF).

CF: cloacal fenestra

ME: mesenchyme

UM: urodeal membrane
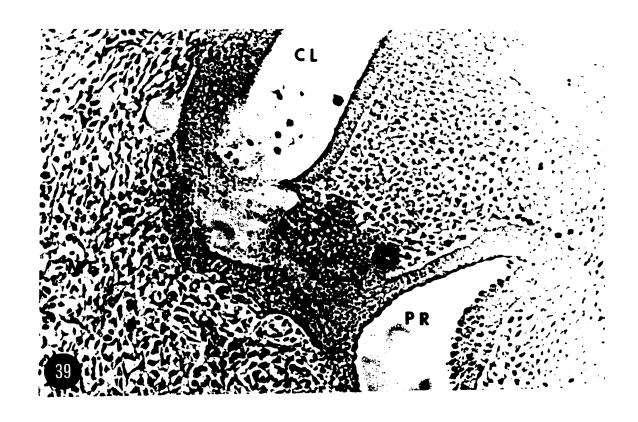
DC: degenerating cell

PR: proctodaeum

Osmium tetroxide, Araldite, and unstained.

X 198
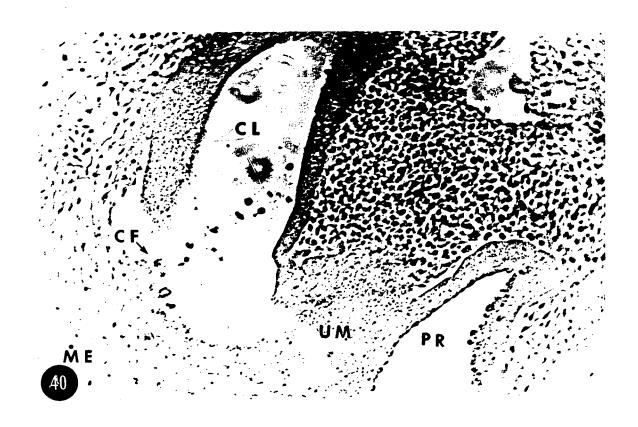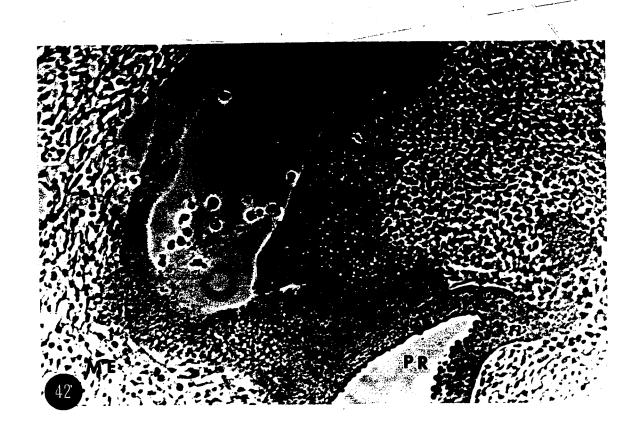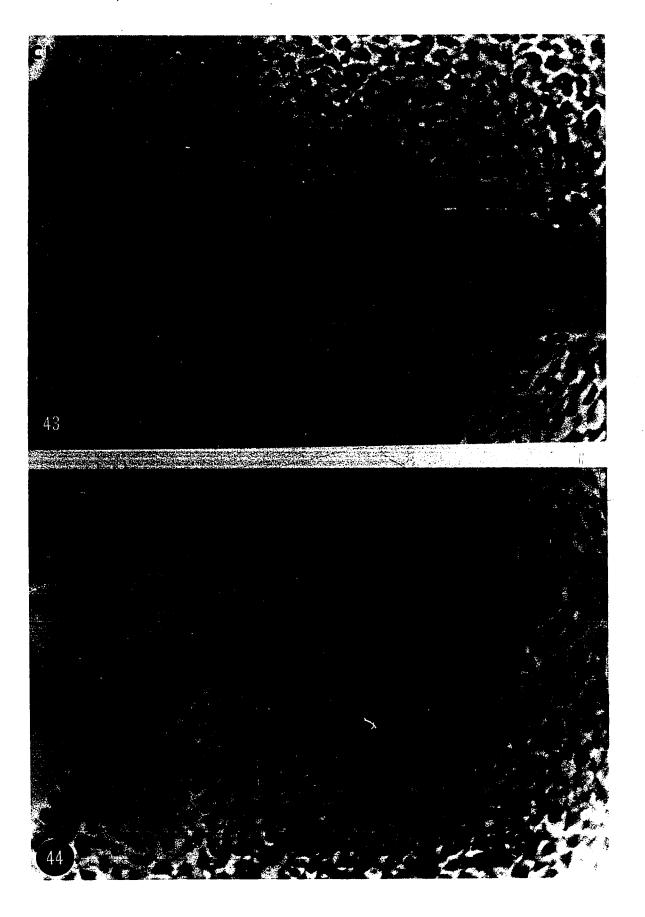
Figs. 43-44. Higher magnification of the sections follow-
ing that illustrated in Fig. 42. Note the
degenerating cells (DC) and the bursal
vesicle (BV).
Osmium tetroxide, Araldite, and unstained;
phase contrast.
X 405

43

44
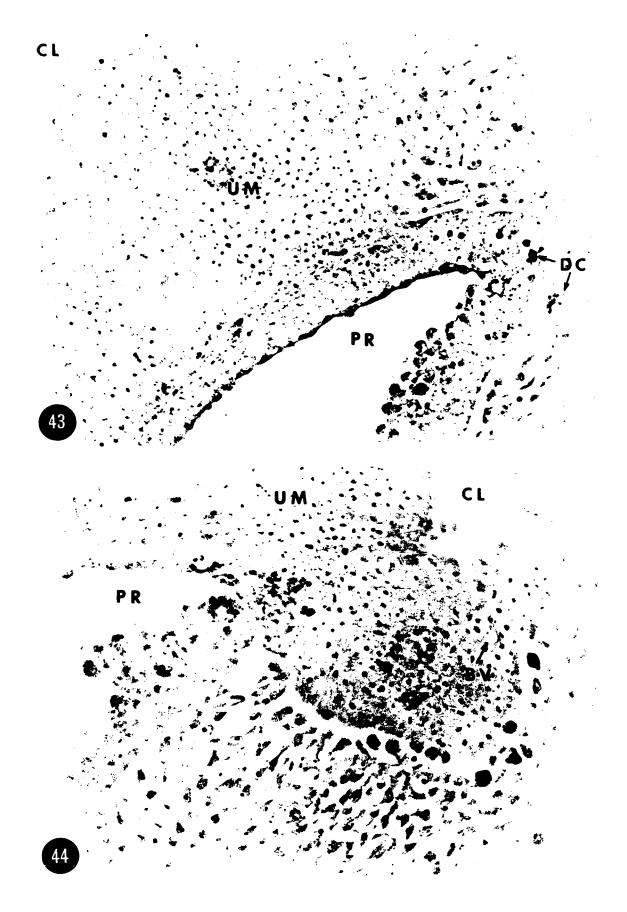
Fig. 45. A diagram of a representative sagittal section
         through the cloaca and proctodeal ectoderm of
         a 4-day chick embryo. The rectangle indicates
         the locale of a series of photomicrographs
         (Figs. 46-51).

         AM: posterior amniotic fold   DA: dorsal aorta
         ND: notochord   NT: neural tube
         X 50
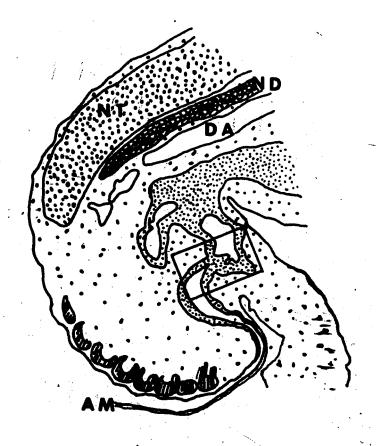
Fig. 46-51. A series of phase contrast photomicrographs
         taken from serial parasagittal sections of a
         4-day cloaca showing the contact of the ecto-
         dermal proctodeal epithelium and the endodermal
         cloacal epithelium. Note the protrusion of cells
         from the floor of the cloaca into the lumen of
         the cloaca.
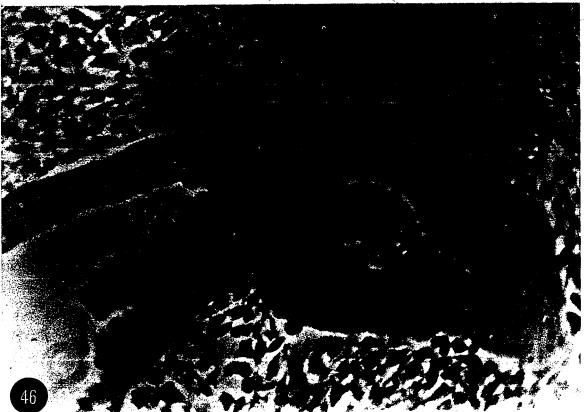
         PR: proctodaeum   CL: cloacal cavity
         AL: allantois   DC: degenerating cell
         Osmium tetroxide, Araldite, and unstained.
         X 405
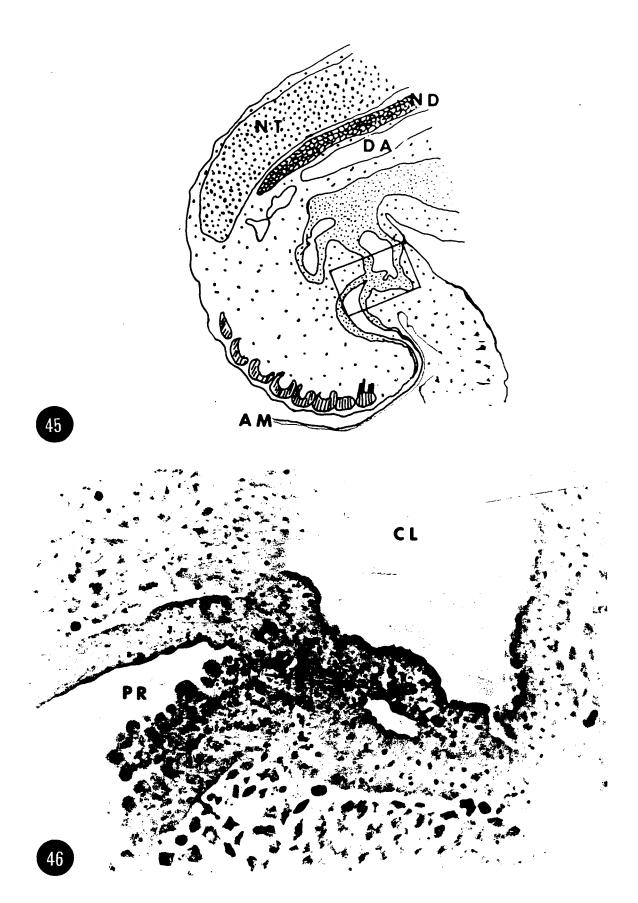
45

46

45

46

47

48

49

CL

PR

50

CL

PR

51
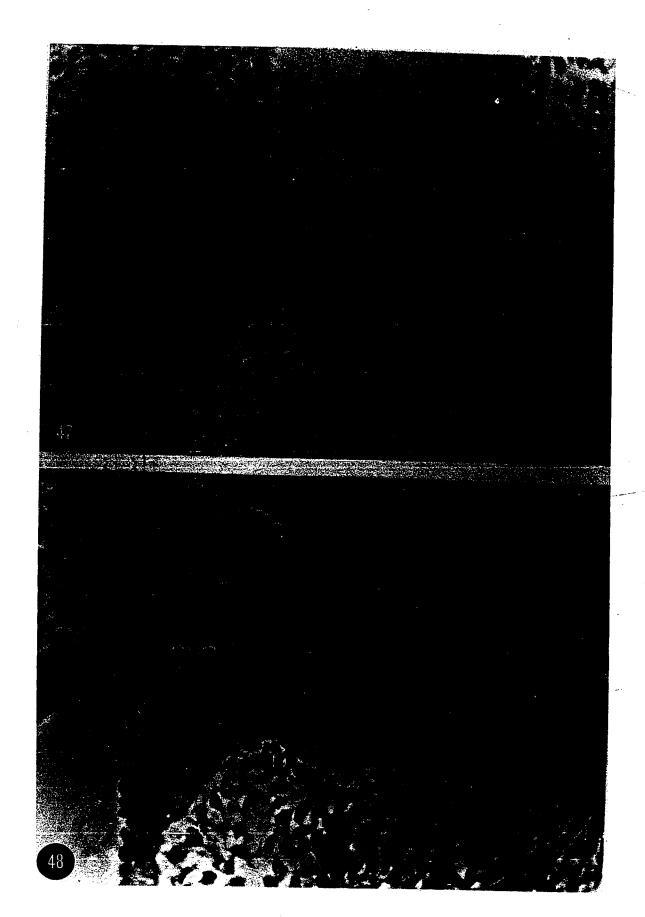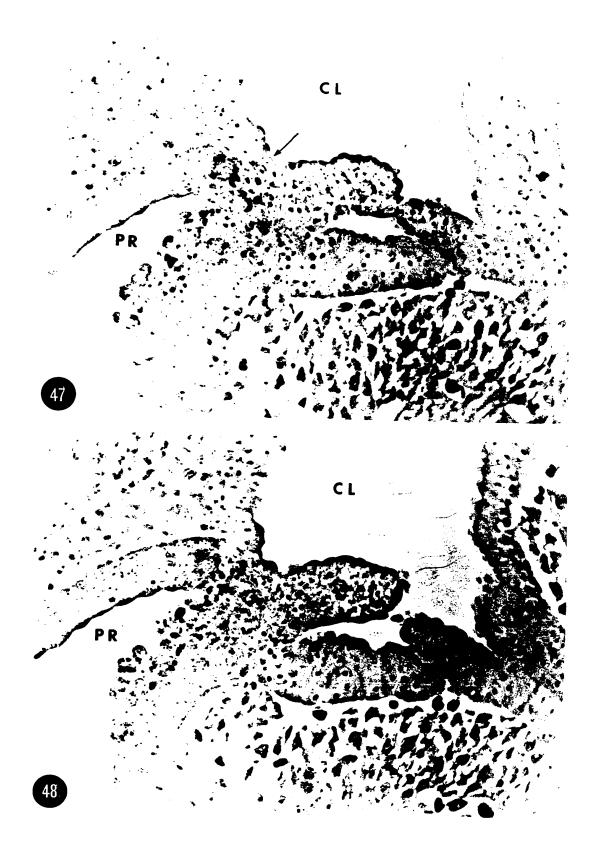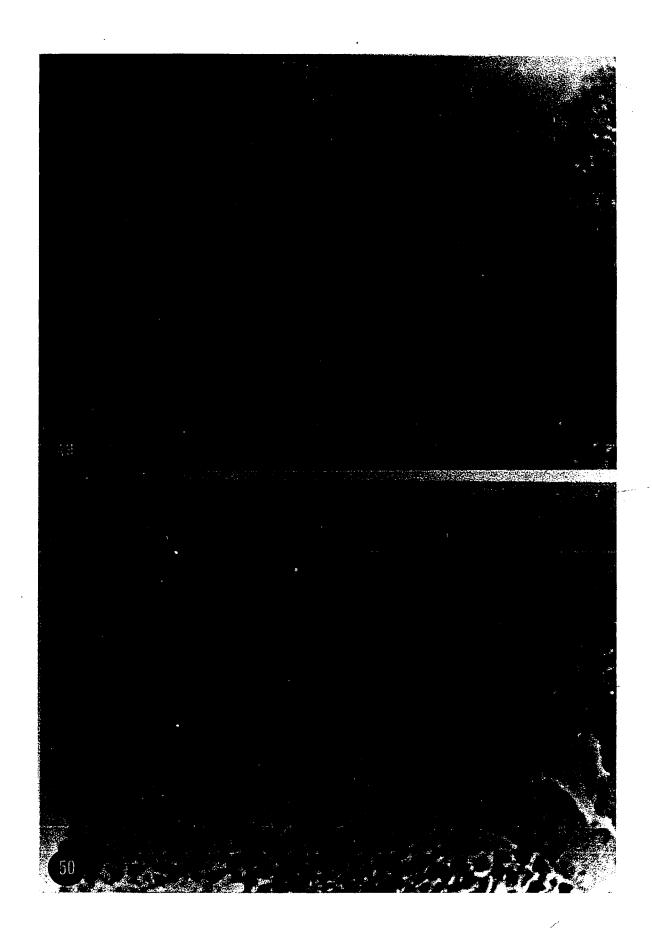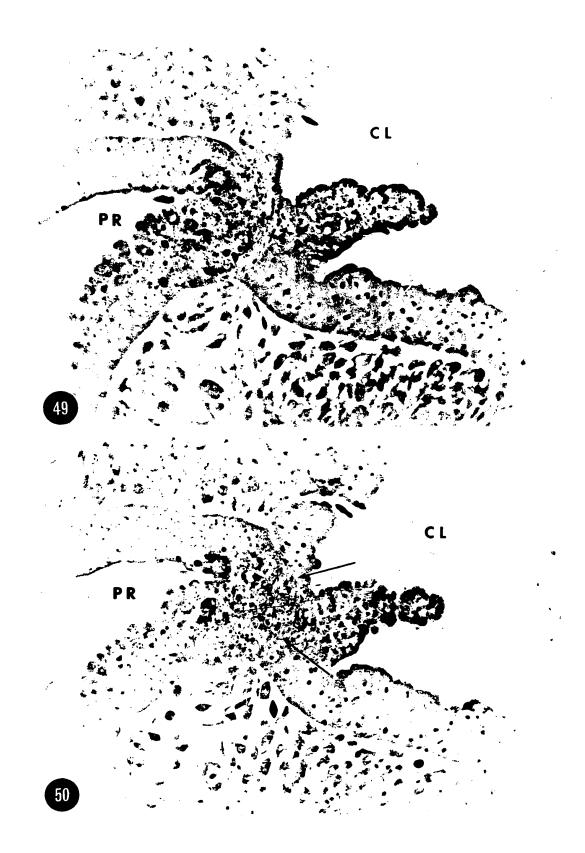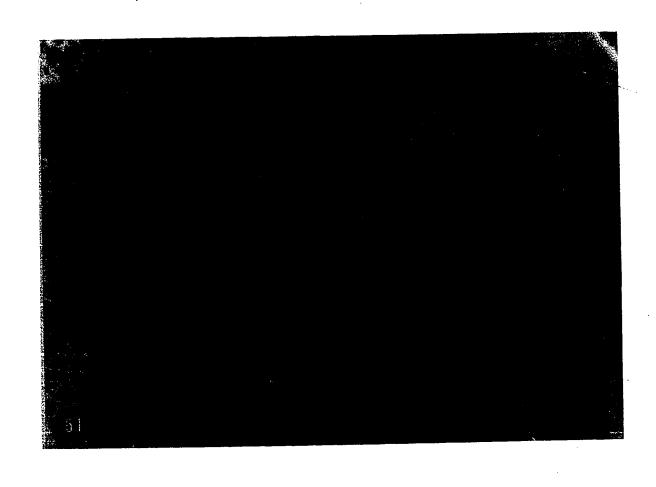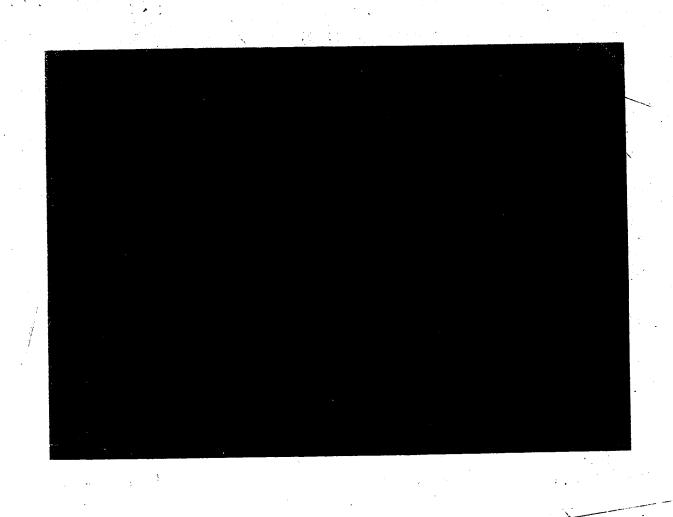
Fig. 52. A diagram of a representative sagittal section
         through a 5-day urodeal membrane. The rectangle
         indicates the location of the series of photo-
         micrographs (Figs. 53-57).

         AL:. allantois   CL: cloacal lumen
          ND: notochord   NT: neural tube
          PR: proctodaeum   UM: urodeal membrane
           R: rectum
         X 45
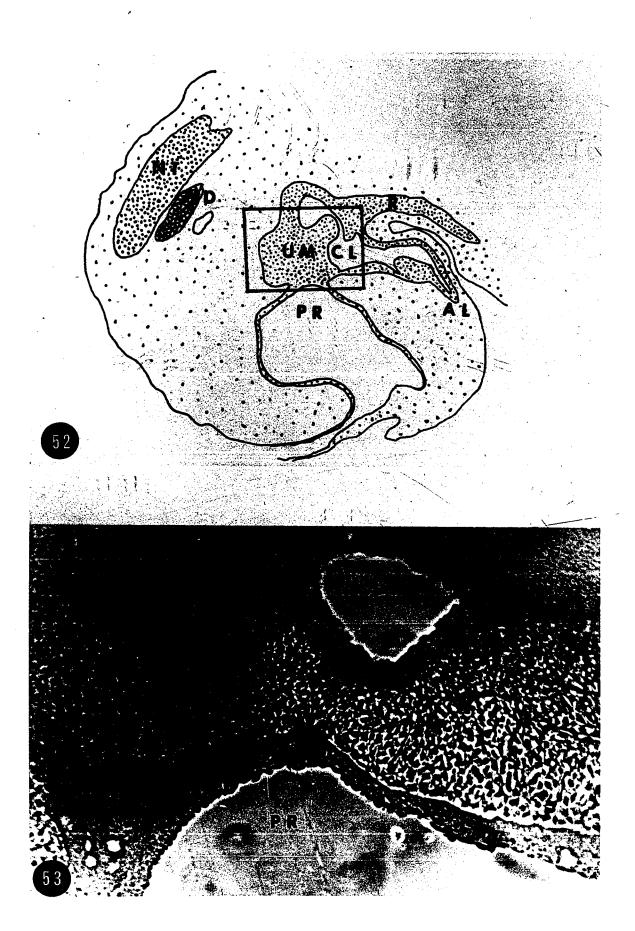
Figs. 53-57. A series of phase contrast photomicrographs
         taken from serial parasagittal sections of the
         posterior part of a 5-day chick embryo showing the
         topological relationship of the proctodeal ectoderm,
         urodeal membrane and the cloacal lining. Bursal
         vesicles are seen in the urodeal membrane.
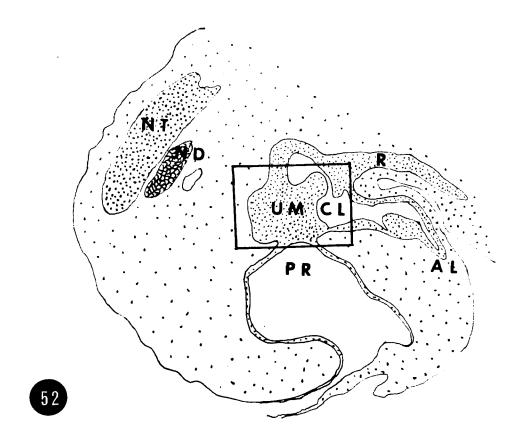
         AL: allantois   BV: bursal vesicle
         CL: cloacal lumen   ME: mesenchyme
         PR: proctodaeum   UM: urodeal membrane
         Osmium tetroxide, Araldite, and unstained.
         X 198
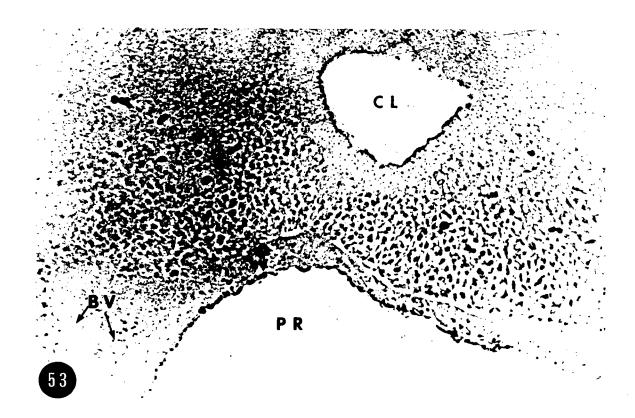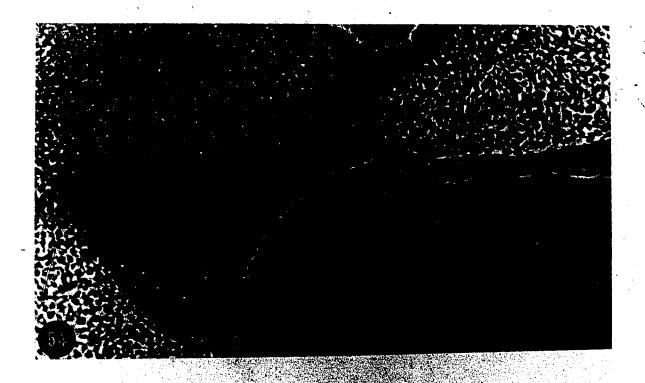
52

53

54

55

CL

ME

UM

CL

AL

PR

56

CL

AL

PR

57
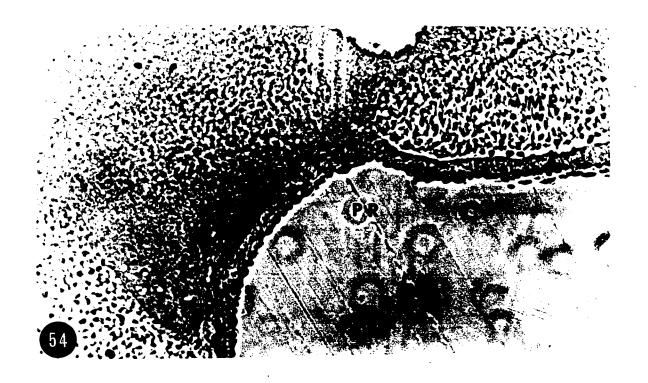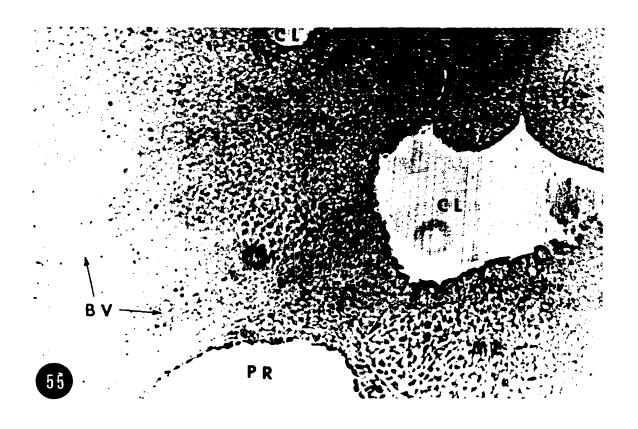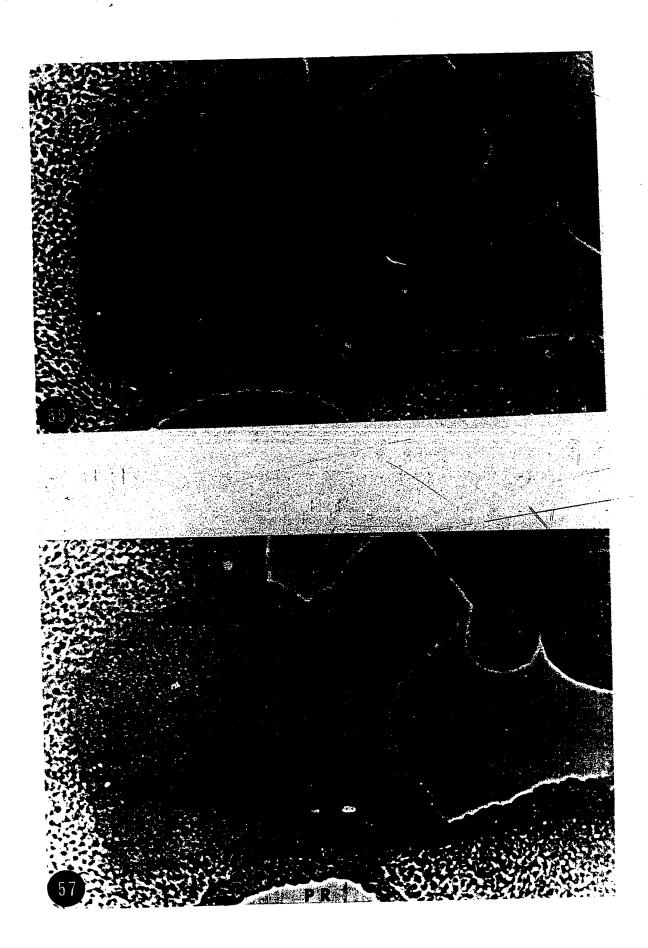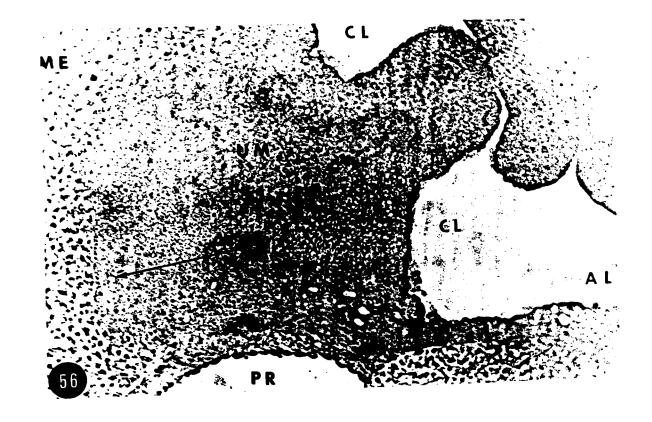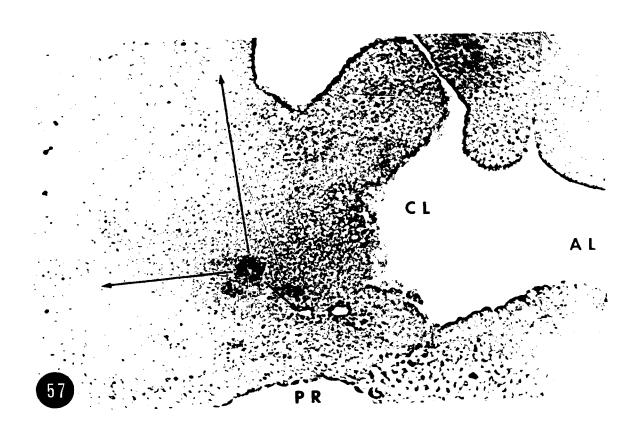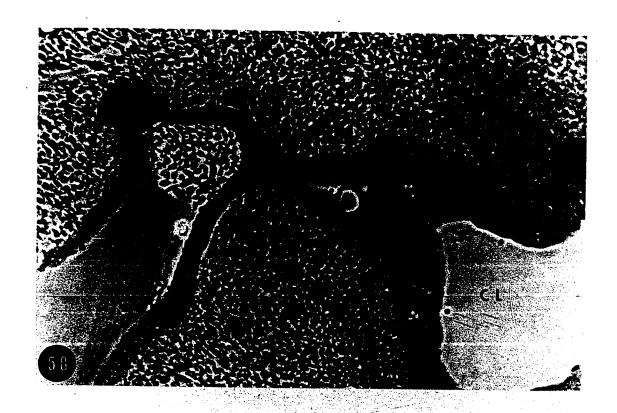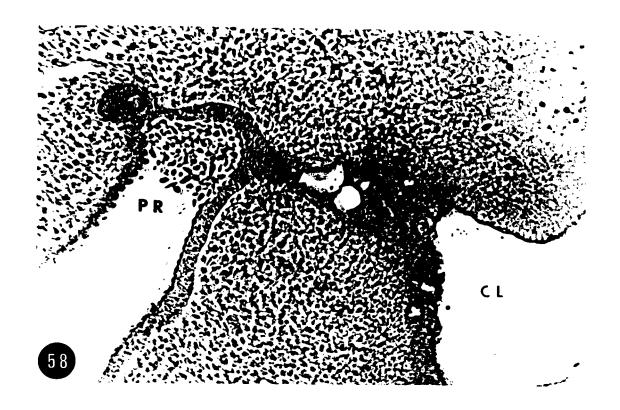
Figs. 58-63. A series of phase contrast photomicrographs
taken from serial parasaggital sections of the
posterior part of a 6-day embryo showing bursal
vesicles (BV) throughout the urodeal membrane.
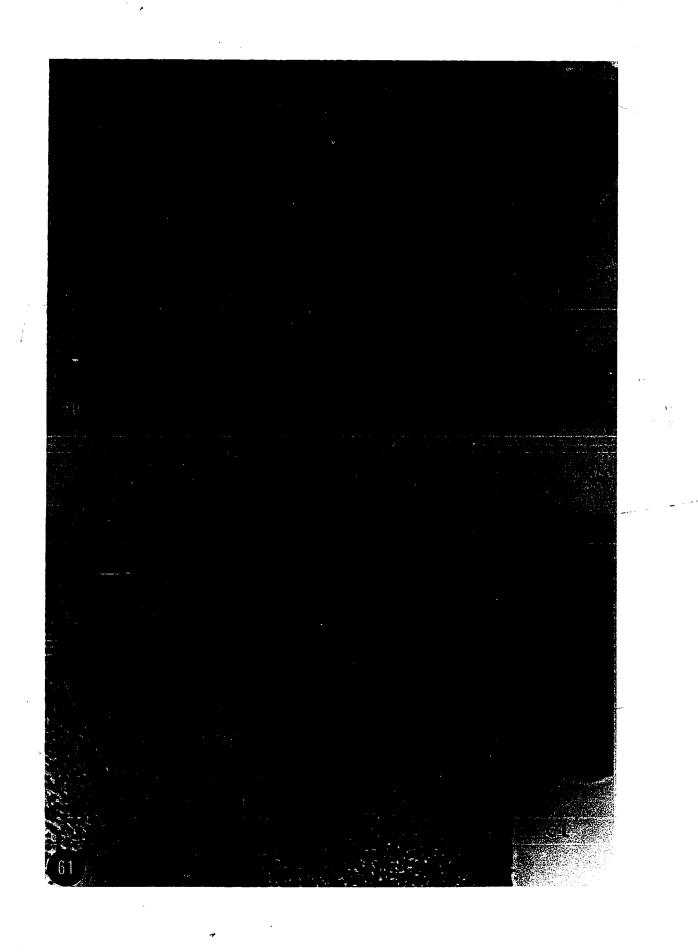
BV: bursal vesicle   CL: cloacal cavity

UM: urodeal membrane   PR: proctodaeum

Osmium tetroxide fixation, Araldite, and

unstained.

X 198

PR

CL

58

PR

CL

59

60

PR

CL

61

PR

CL

63

PR

CL

62

CL

PR

63
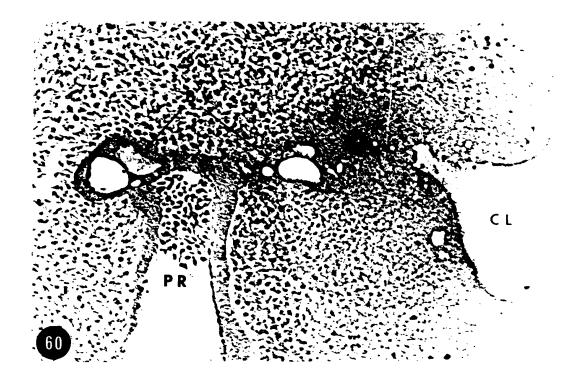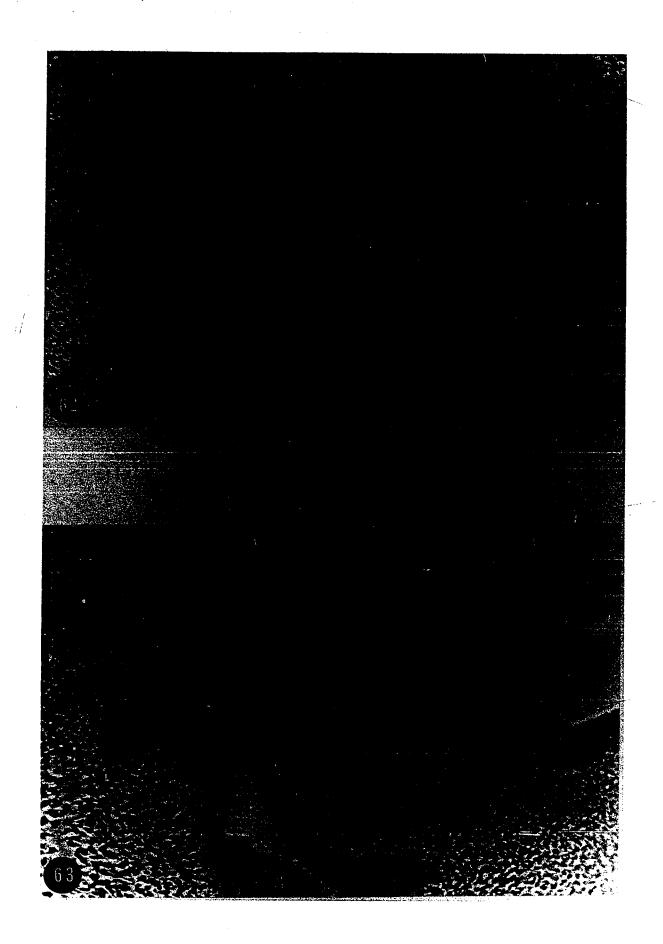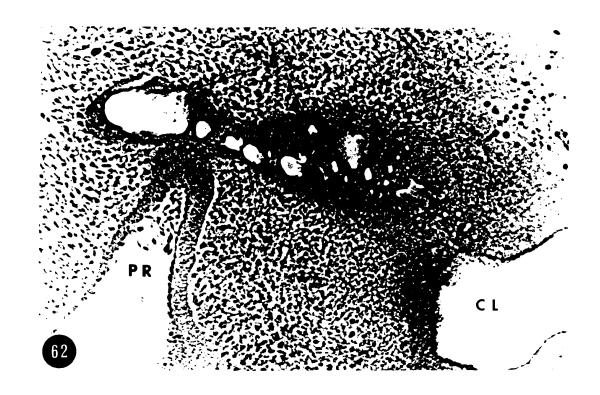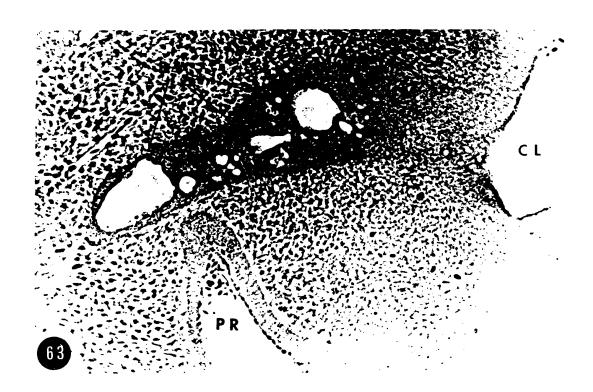
Fig. 64. Ectodermal cells of the proctodaeum. A cytolysome

(CL) is seen near the lower right corner. Note

the pinocytotic vesicles (PV), the Golgi apparatus

(G) near the cell surface, vesicular endoplasmic

reticulum and interdigitations of the cell surface

of adjoining cells.

CL: cytolysome   CM: cell membrane

G: Golgi apparatus   IS: intercellular space

L: lipid droplet   PR: proctodaeum

PV: pinocytotic vesicle

Osmium tetroxide, Araldite, and uranyl acetate.

X 22,400

64
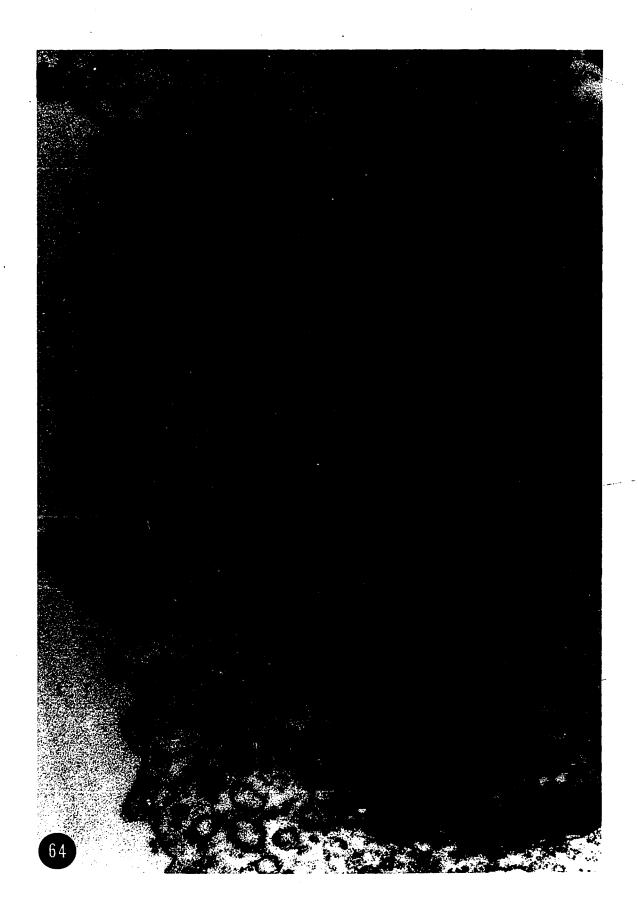
Fig. 65. Ectodermal cells of the proctodeal epithelium

showing numerous lipid droplets (L) of irregular

shape, tight junctions (TB), desmosomes (D),

Golgi apparatus (G), intercellular space (IS) and

cytolysomes (CL).

PR: proctodaeum   N: nucleus

Osmium tetroxide, Araldite, and uranyl acetate.

X 12,120

PR

D

TB

D

L

IS

D

L

65
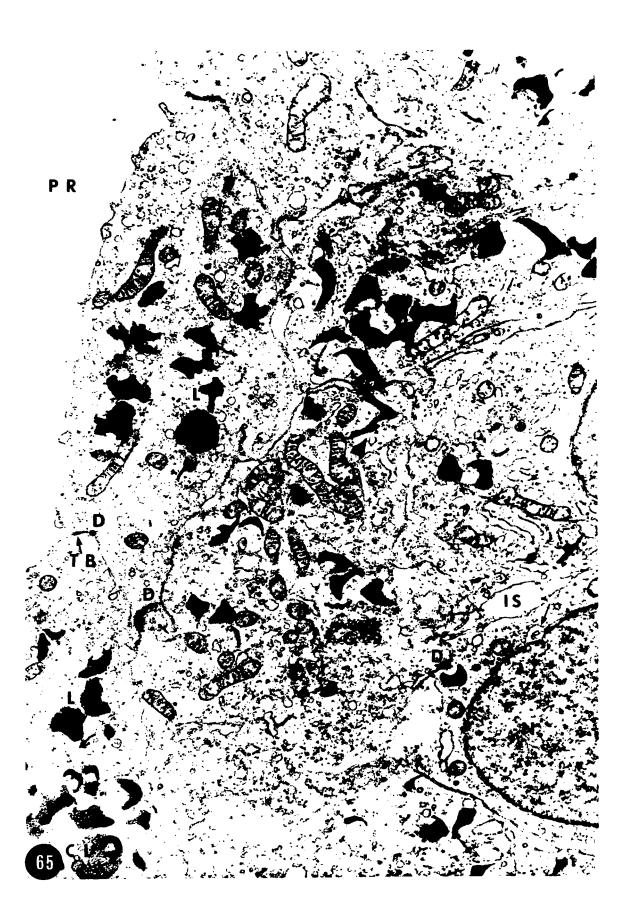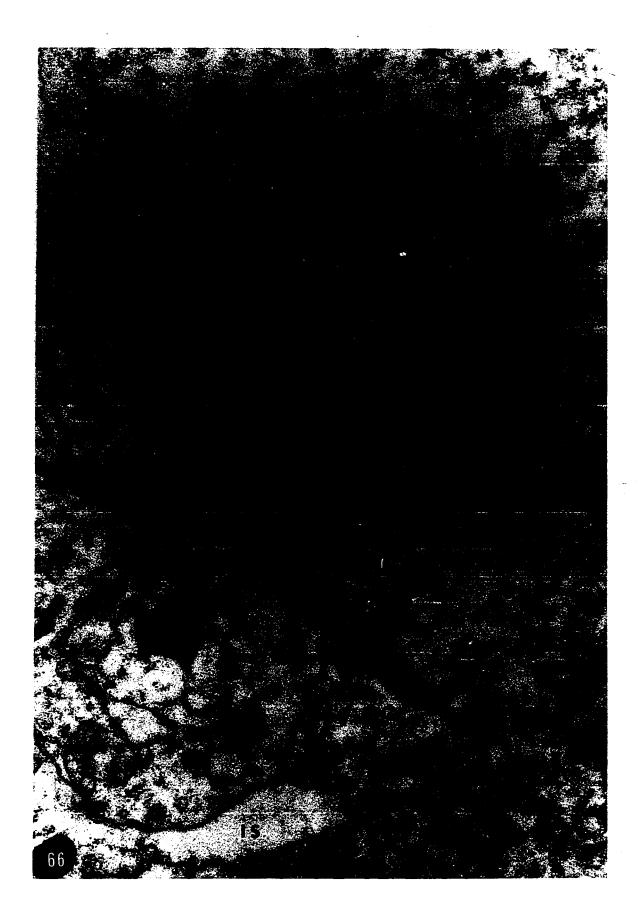
Fig. 66. A part of the urodeal membrane near the procto-

daeum showing multivesicular bodies (MVB),

Golgi apparatus (G), nuclear pores (arrows),

desmosomes (D), and an intercellular space (IS)

the border of which resembles those of bursa

vesicles. Note the sharp contrast of the parts

of the border and the diffuse character of ad-

jacent parts where cytoplasmic granules have

entered the intercellular space. The interrupted

border may be artifactual, but such interruptions

are not seen at the proctodeal and cloacal sur-

faces. The diffuse parts may be the portals

through which cytoplasmic granules contribute to

the bursa vesicles.

N: nucleus

Osmium textroxide, Araldite, and uranyl acetate.

X 26,600
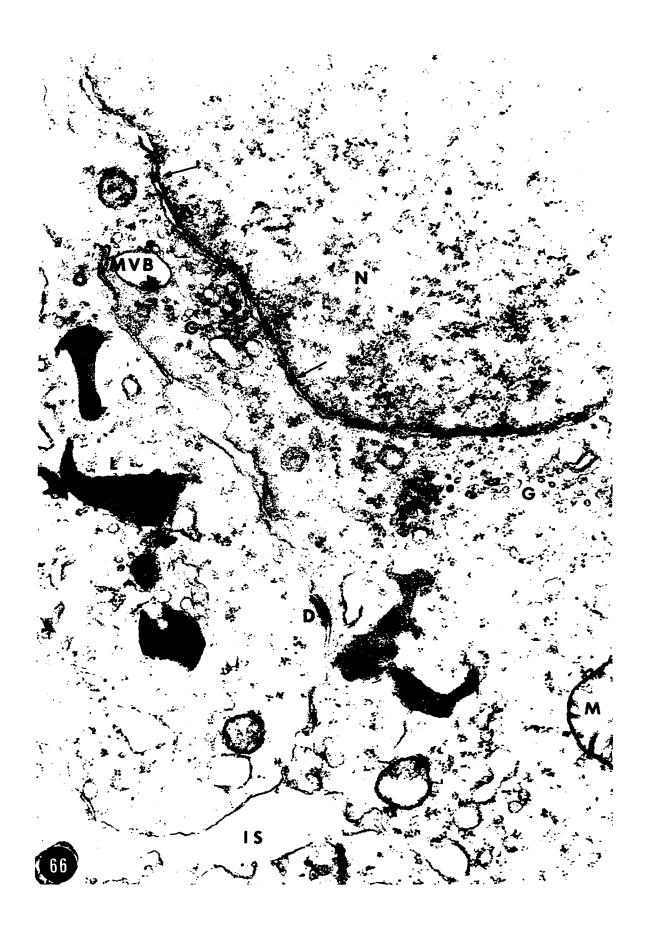
Fig. 67. An area of urodeal membrane near the proctodaeum

showing a degenerating cell (CL) surrounded by

normal cells.

CL: cytolysome   G: Golgi apparatus
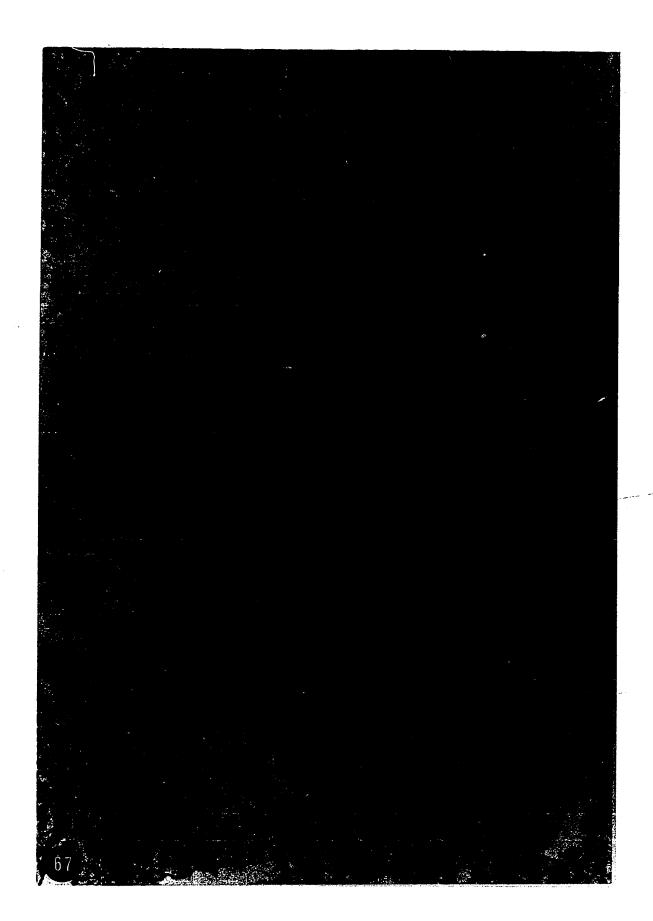
 D: desmosome   CO: Collagen-like

IS: intercellular space   material
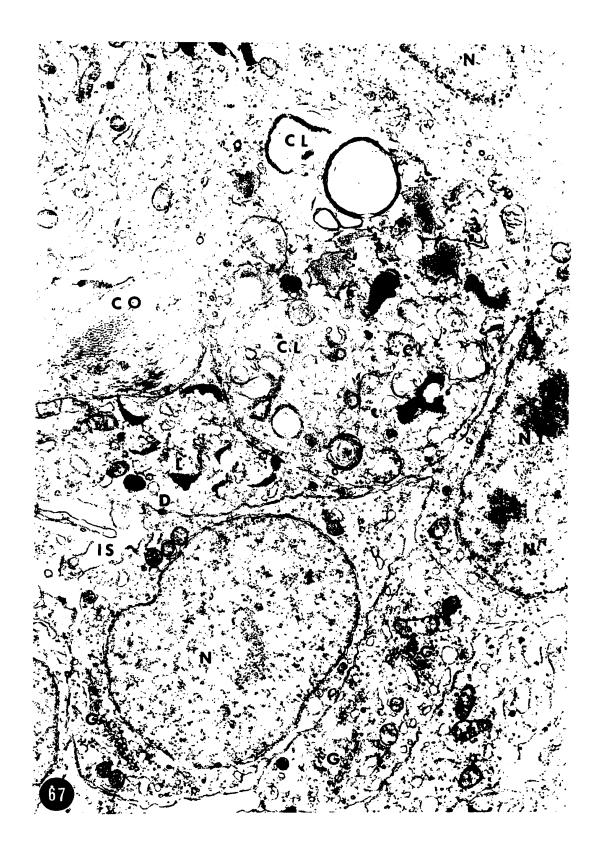
NL: nucleolus   N: nucleus

Osmium tetroxide, Araldite, and uranyl acetate.

X 14,850

Fig. 68. Epithelial cells near the proctodaeum. A degener-
ating cell is seen in the center and is surrounded
by four normal cells at four corners. Degraded
mitochondria and enlarged endoplasmic reticulum (ER)
are recognizable in the degnerating cell.
Osmium tetroxide, Araldite, and unstained.
X 16,800

68

68
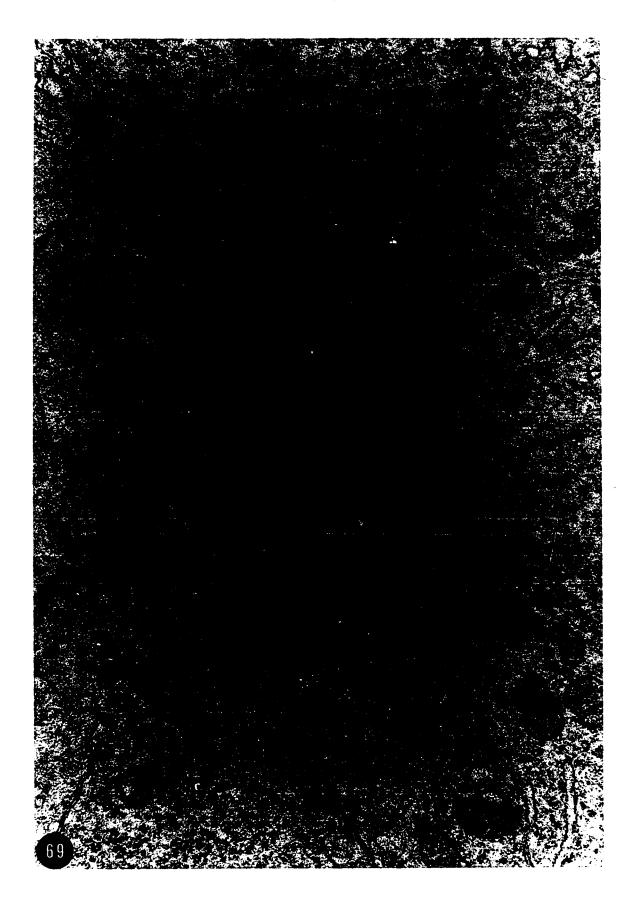
Fig. 69. An area of the urodeal membrane showing numerous
         aggregations of ribosomes (R), granular endoplasmic
         reticulum, multivesicular bodies (MVB), and dis-
         tended intercellular spaces (IS).
         Osmium tetroxide, Araldite, and uranyl acetate.
         X 24,960

MVB

IS

N

M

R

M

69
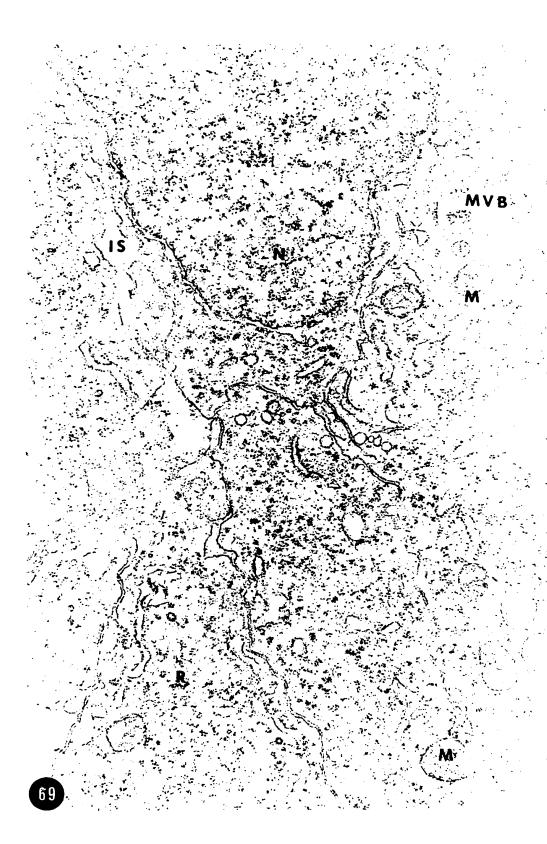
Fig. 70. Part of Fig. 71 enlarged to show multivesicular

bodies (MVB), numerous ribosomes (R), and

irregular lipid droplets (L). The fusion of a

Golgi veiscle with the limiting membrane of the

multivesicular body is indicated by an arrow.

Note the close attachment of the cell contain-

ing large MVB with the cell below it. The

lower cell has either been damaged during fixa-

tion or naturally in the region of attachment.

There is a band of amorphous material extending

from D to the right of R. The limiting membrane

of the MVB nearest this diffuse area is ruptured,

perhaps artifactually. The proximity of these

two unusual alterations in an area which other-

wise seems to be moderately well fixed suggests

that the MVB of the superior cells may have con-

tributed to the alteration of the lower cell.

Osmium tetroxide, Araldite, and uranyl acetate.

X 22,400
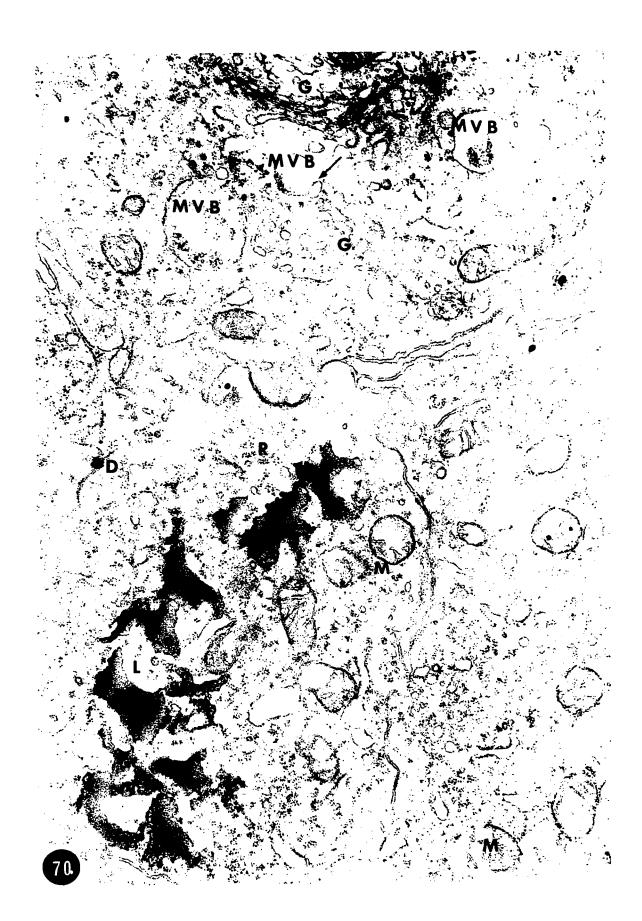
Fig. 71. An area of the urodeal membrane. Part of a bursal
          vesicle (BV) is seen at the lower left corner.
          Note the extensions of some cells.(arrows).
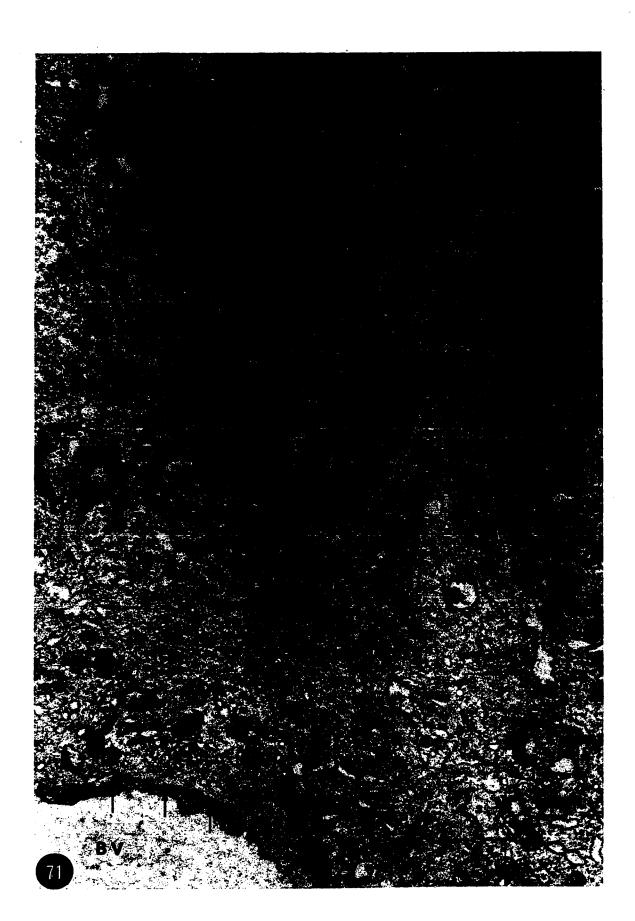
     D: desmosome   L: lipid droplet

     N: nucleus

Osmium tetroxide, Araldite, and uranyl acetate.

X 13,938
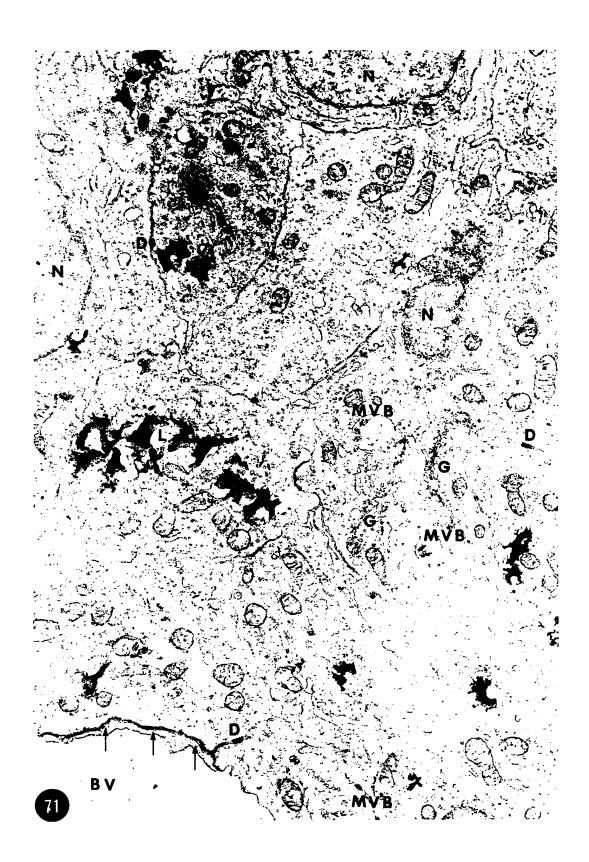
Fig. 72.   Part of a bursal vesicle and adjacent cells.

Granular material is present in the bursal vesicle

(BV). The plasma membrane facing the bursal

vesicle has alternate dense and diffuse parts which

resemble the alternate dense and diffuse parts of

the border of some intercellular spaces (Fig. 66).

The outer membrane of the nuclear envelope comes so

close to the cytoplasmic membrane that it may almost

appear continuous with it (arrows).

Osmium tetroxide, Araldite, and uranyl acetate.

X 27,600
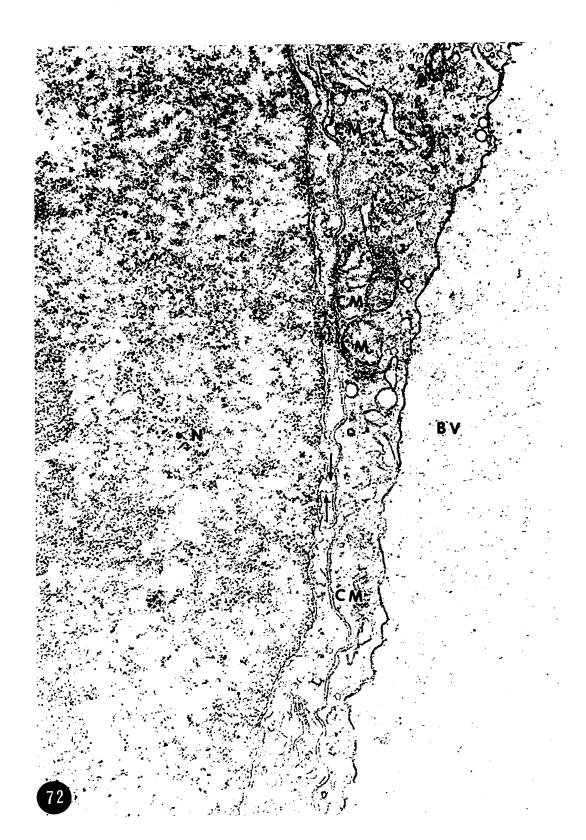
Fig. 73.   A part of the urodeal membrane and the cloaca.
The oblique or cross section of the tight junc-
tion of cells near the bursa vesicles is shown in
the upper center between two thick arrows. The
perpendicular view of the tight junction of the
bursa vesicle is indicated by thin arrows as seen
in the lower center. The tight junction also ap-
pears between cells facing the cloacal lumen.
The cytoplasm adjacent to tight junctions shows a
slight condensation. The plasma membrane facing
the cloacal lumen is darker than the rest of the
plasma membrane except the junctional complex of
the epithelial cells.
Osmium tetroxide, Araldite, and unstained.
X 9,000

Insert: A higher magnification of a plasma mem-
brane at the cloacal lumen (CL).   It shows the
asymmetrical unit membrane. The darker and thicker
line of the unit membrane is facing the cloacal
lumen, the light and thin line faces the cyto-
plasm.
Uranyl acetate.
X 100,000

73

CL

BV

CL

73
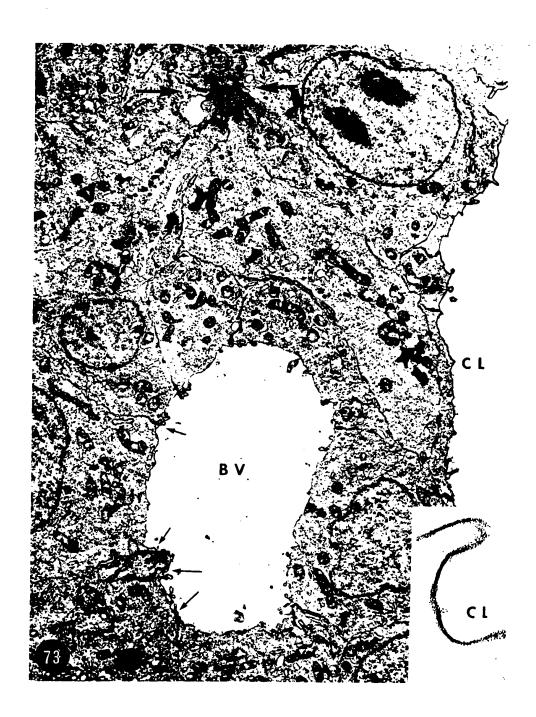
Fig. 74. Cells of the urodeal membrane, near the lumen of

the cloaca, showing interdigitations and numerous

clusters of ribosomes.

D: desmosome   CM: cell membrane
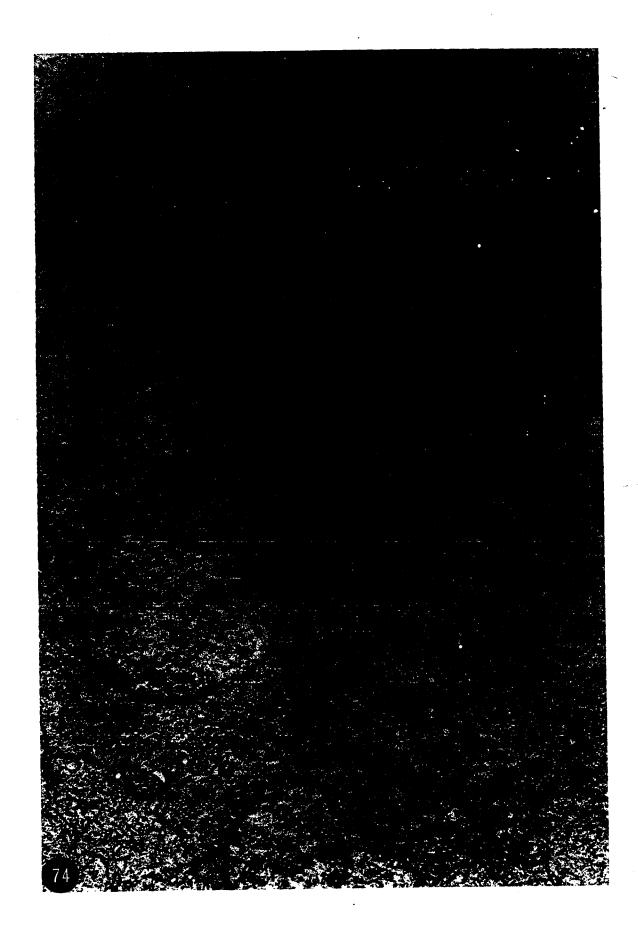
G: Golgi apparatus   M: mitochondrion

MVB: Multivesicular body   N: nucleus

NL: nucleolus

Osmium tetroxide, Araldite, and uranyl acetate.

X 11,363

74
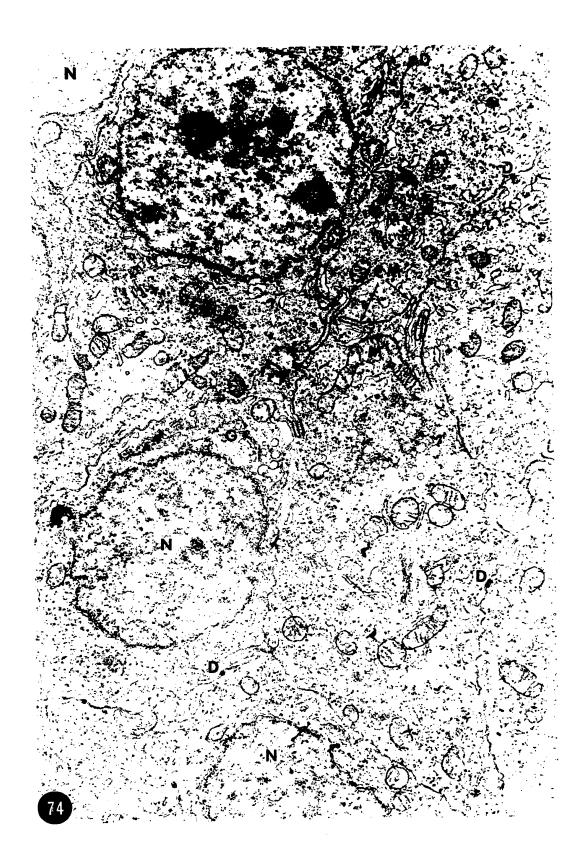
Fig. 75. Part of a cell of the urodeal membrane, near the

lumen of the cloaca, showing a cytolysome (CL)

and clusters of ribosomes (R).

Osmium tetroxide, Araldite, and uranyl acetate.

X 45,000
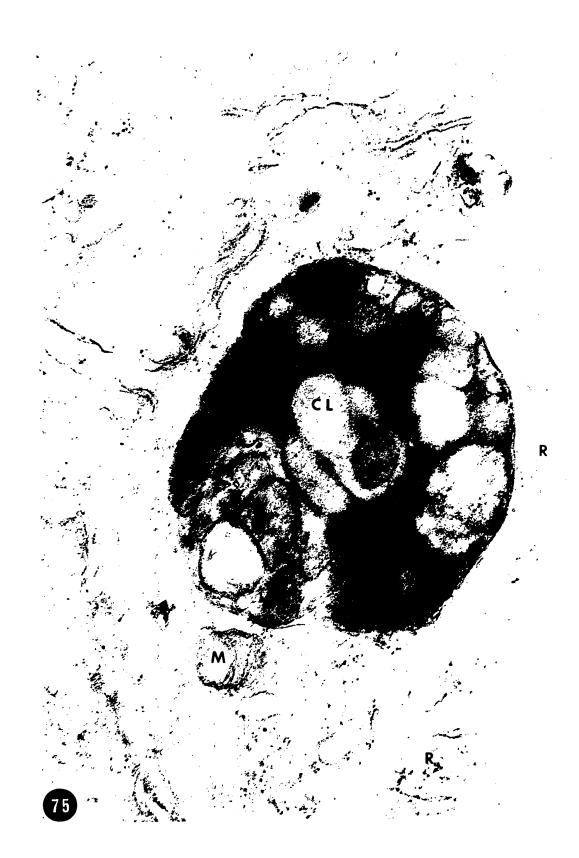
Fig. 76. Cells of the urodeal membrane adjacent to the
mesenchyme. Note the elongate form of the cells.
Swelling of the nuclear envelope is seen (thick
arrow). Small vesicles seem to pinch off from
the outer membrane of the nuclear envelope (thin
arrow). This is an unstained section. The ap-
pearance of ribosomes is not so distinct as that
seen in stained sections.

BM: basement membrane   NL: nuceolus
 D: desmosome   M: mitochondrion
MB: microbody   L: lipid droplet
 N: nucleus   MVB: multivesicular
                                 body
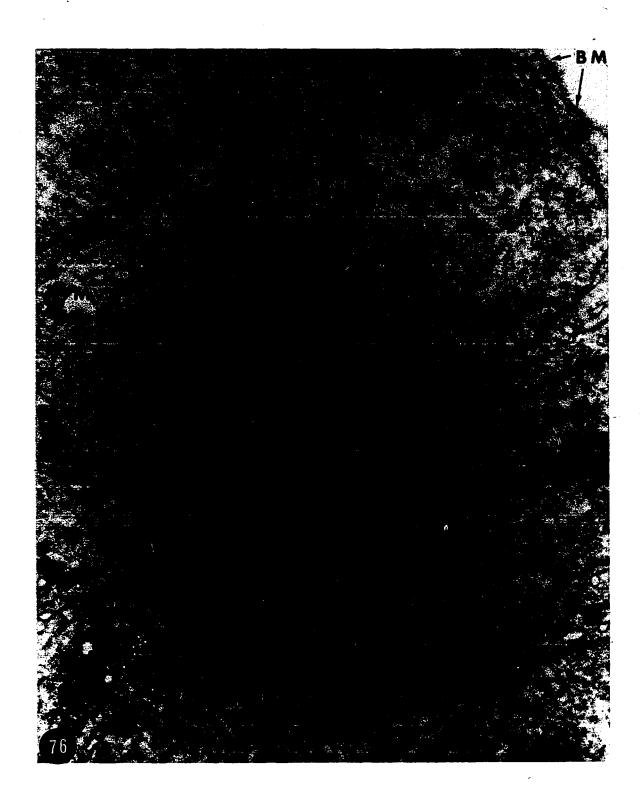
Osmium tetroxide, Araldite, and unstained.

X 14,640

BM

N

MVB

N

MVB

L

M

D

N

MB

MVB

M

N

76
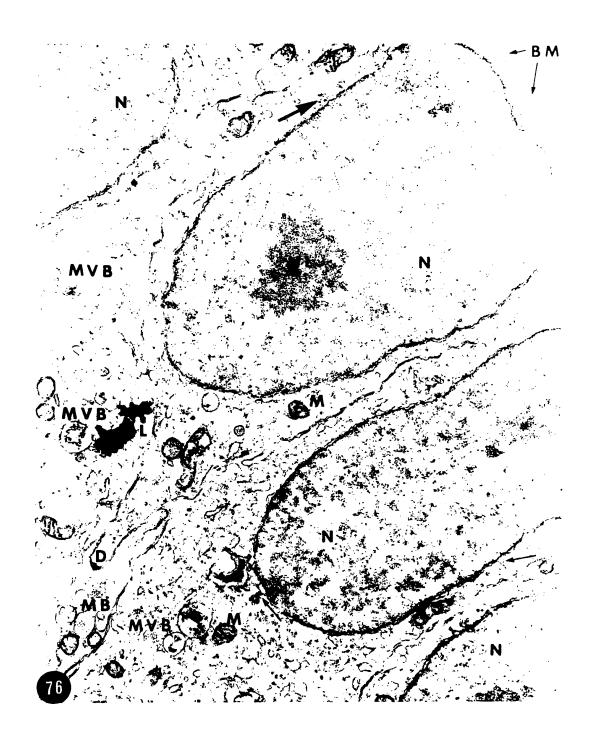
Fig. 77.   A frontal section of a 13-day embryo showing the
           thymus lying along both sides of the neck.   The
           acid phosphatase activity is low; the darkness of
           the thymus is due to the counterstain.
           Barka medium and counterstained with methyl green.
           X 10
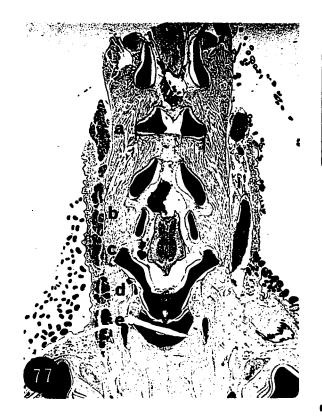
Fig. 78.   Part of the thymus illustrated in Fig. 77 showing
           scattered punctate acid phosphatase (see arrows).
           X 250

77

78

Fig. 79. The neck region of a 12-day embryo showing the thymus
          lying along the neck (a-f). Part of the thymus in-
          dicated by an arrow is illustrated at higher magni-
          fication in Fig. 80.
          Barka medium, no counterstain.
          X 10
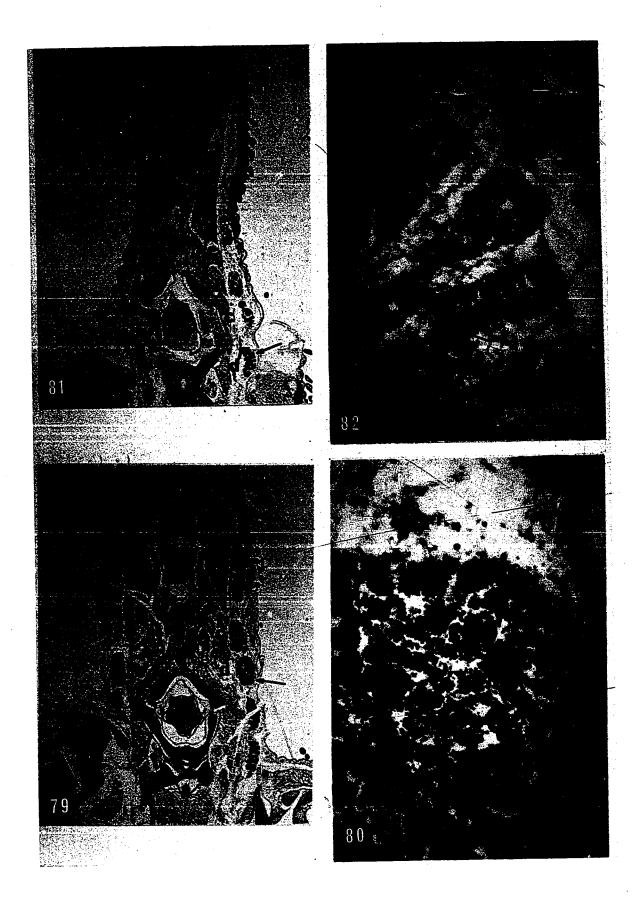
Fig. 80. Part of the thymus shown in Fig. 79 illustrating
          punctate acid phosphatase activity in the mesenchyme
          and very little in the thymus.
          X 250

Fig. 81. A frontal section of the neck region of an 11-day
          embryo to show the thymus lying along the neck
          (a-d). Part of the thymus indicated by an arrow
          is illustrated at higher magnification in Fig. 82.
          Barka medium, no counterstain.
          X 10

Fig. 82. Part of the thymus shown in Fig. 81 illustrating
          punctate acid phosphatase in the mesenchyme and
          very little in the thymus.
          X 250

81

82

79

80

81

a

b

c

d

82

a

b

c

d

e

f

79

80

Fig. 83. A frontal section of the neck of a 10-day embryo
         showing three lobes of the thymus (a-c). Part of
         the thymus indicated by an arrow is shown at higher
         magnification in Fig. 84.
         Barka medium, no counterstain.   X 10

Fig. 84. Part of the thymus shown in Fig. 83 illustrating
         punctate acid phosphatase in the mesenchyme and
         very little in the thymus (see arrows).
         X 250

Fig. 85. A frontal section of the neck region of an 8-day
         embryo to show the lobulation of the thymus (a-e).
         One lobe of the thymus indicated by an arrow is
         shown at higher magnification in Fig. 86.
         Barka medium, no counterstain.
         X 10

Fig. 86. Part of the thymus shown in Fig. 85 illustrating
         punctate acid phosphatase in the mesenchyme and
         very little in the thymus. The figure shows the
         thymus at an incipient stage of lymphopoiesis when
         it has just begun to lobulate. The upper lobules
         appear more epithelial and the lower appear more
         lymphoidal.
         X 250

85

86

83

84

85

86

83

84
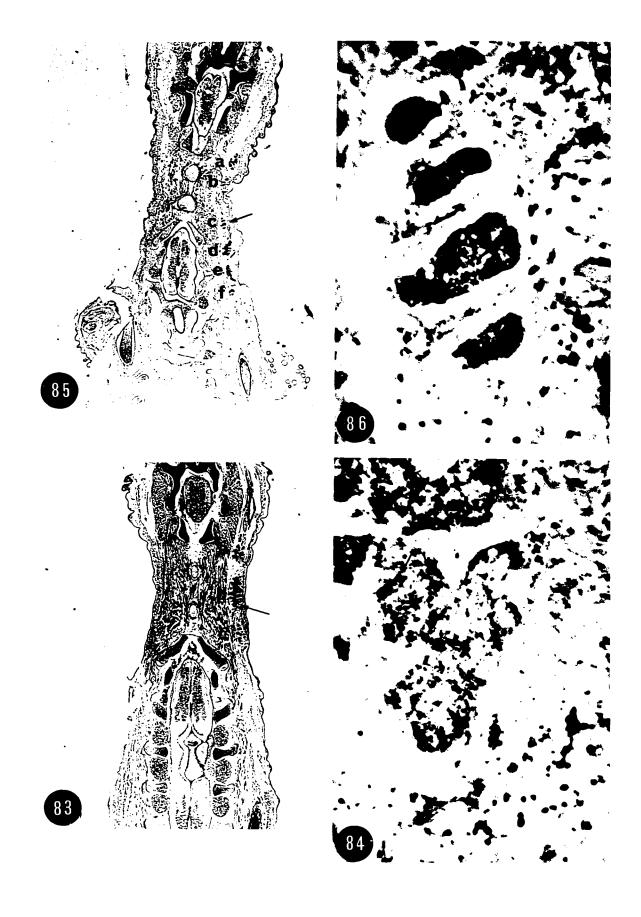
Fig. 87.   A frontal section of the neck region of the 7-day
            embryo showing the slender thymus primordium (in-
            dicated by two arrows) which is illustrated at
            higher magnification in Fig. 88.
            Frozen section and methylene blue staining.
            X 10

Fig. 88.   A part of Fig. 87 showing the slender thymus pri-
            mordium (TH) at higher magnification.
            X 250.

Fig. 89.   A frontal section of the 6-day embryo showing the
            thymus primordia (arrow) which is illustrated at
            higher magnification in Fig. 90.
            Barka medium, no counterstain.
            X 10

Fig. 90.   Thymus III (TH3) and Thymus IV (TH4) show intense
            acid phosphatase activity. Punctate activity is
            present in the mesenchyme.
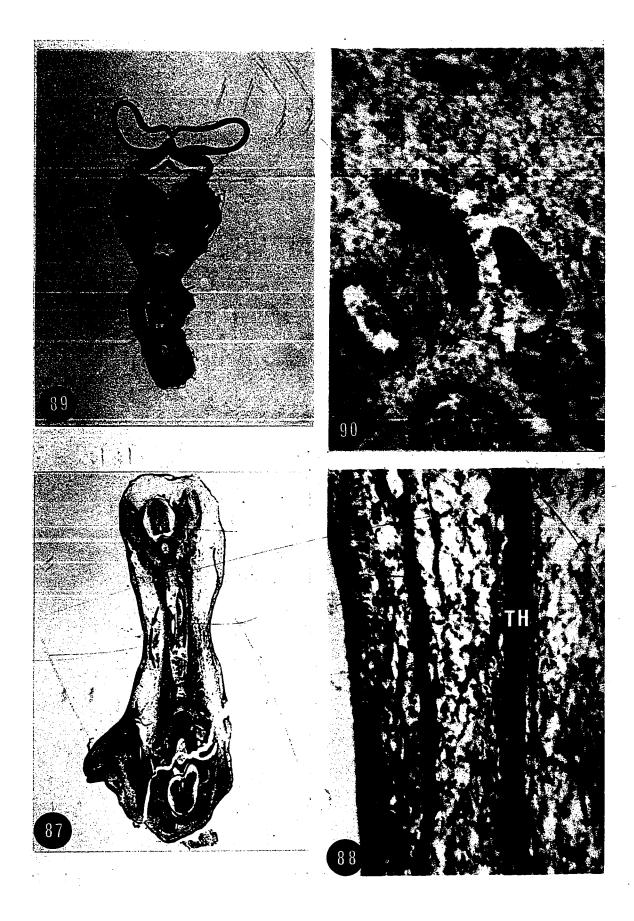
                        AA3:   third aortic arch
                        AA4:   fourth aortic arch
                        TH3:   Thymus III
                        TH4:   Thymus IV
                         NG: nodosal ganglion

            X 250

89

90

87

TH

88

89

TH 3

TH 4

A A

NG

AA4

90

87

TH

88
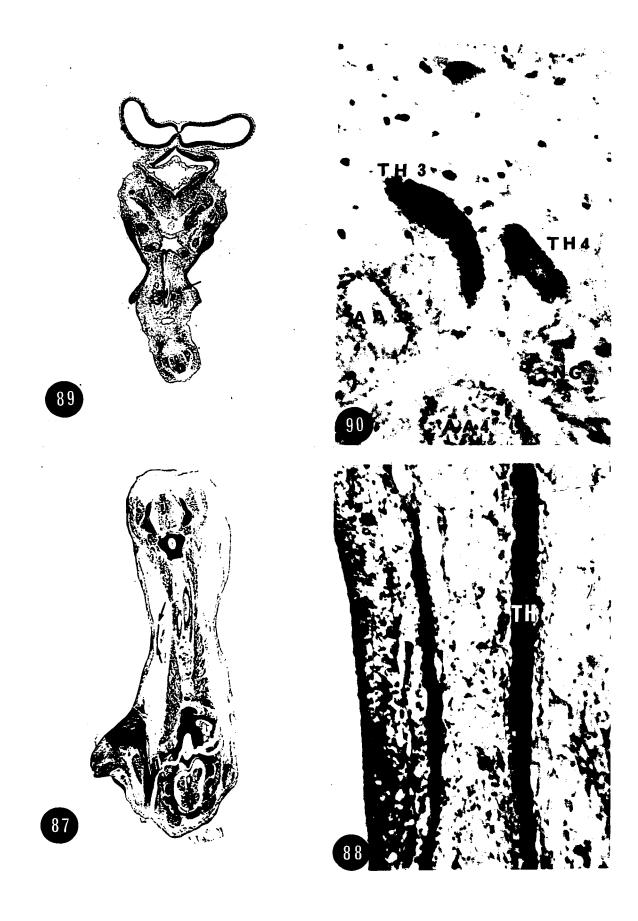
Fig. 91.   A diagram of a representative section through

the branchial region of a 5-day embryo.   The

series of photomicrographs of Figs. 92-94 are

taken from the area indicated by the rectangle.

DA: dorsal aorta   PX: pharynx

N: nodose ganglion   ND: notochord

V: jugular vein
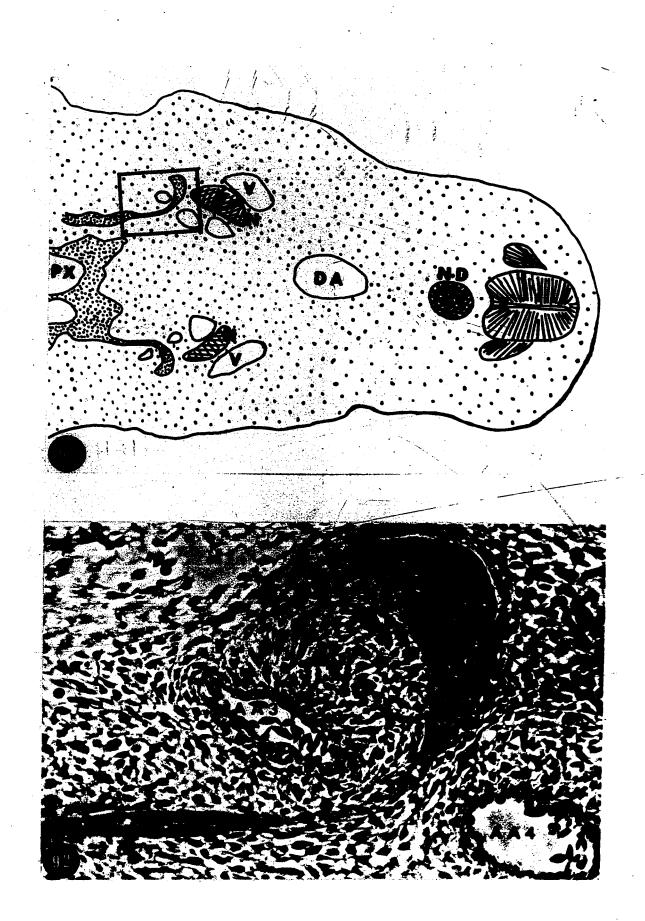
X 60
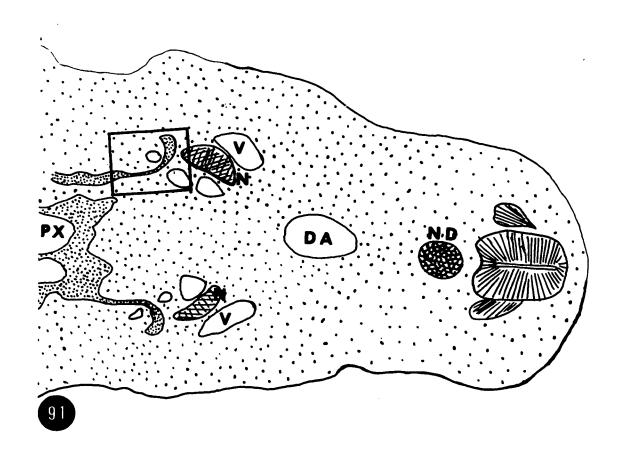
Figs. 92-94.   A series of phase contrast photomicrographs

taken from serial frontal sections through the

branchial region of a 5-day chick embryo, arranged

in a dorsoventral sequence.   Visible parts of the

thymus primordium are a dorsolateral part (TH3)

of the third pharyngeal pouch, and its appended

ectoderm, and a dorsolateral part (TH4) of the

fourth pharyngeal pouch.   The epithelial tissue

above the arrows is branchial ectoderm.

AA3:   third aortic arch
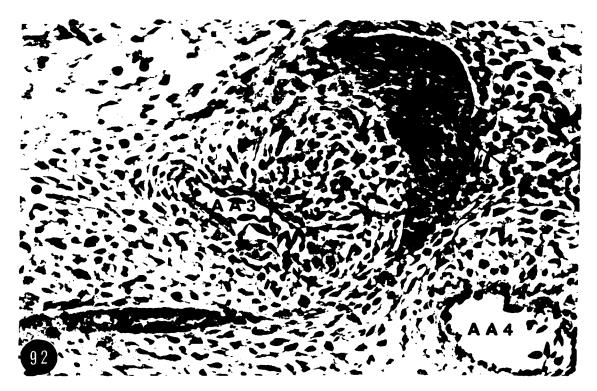
AA4:   fourth aortic arch

X 405

PX   DA   N·D

93

94
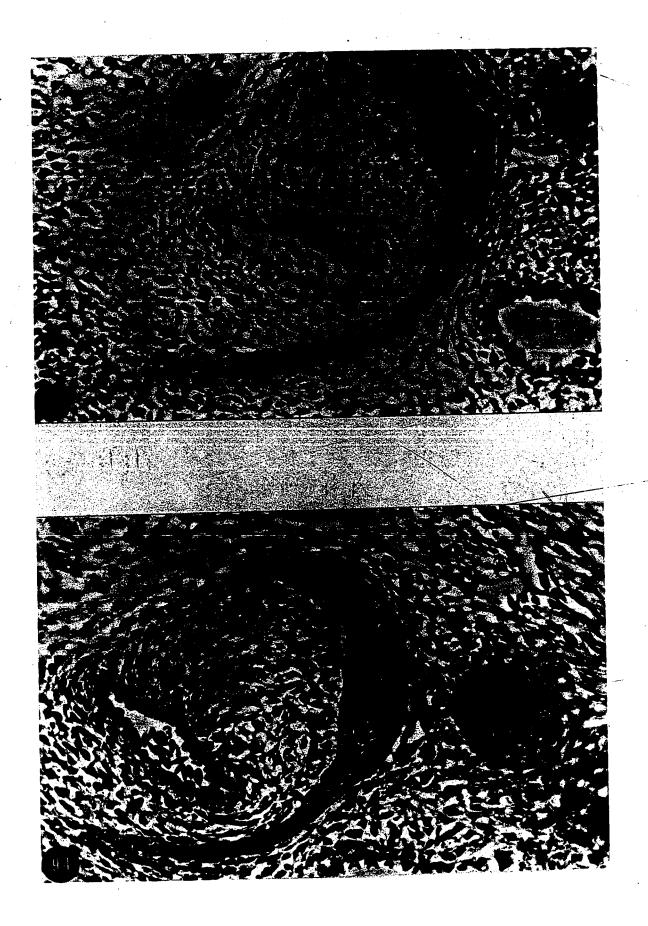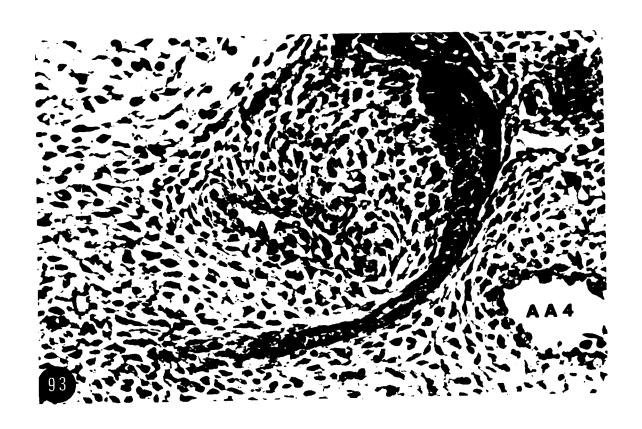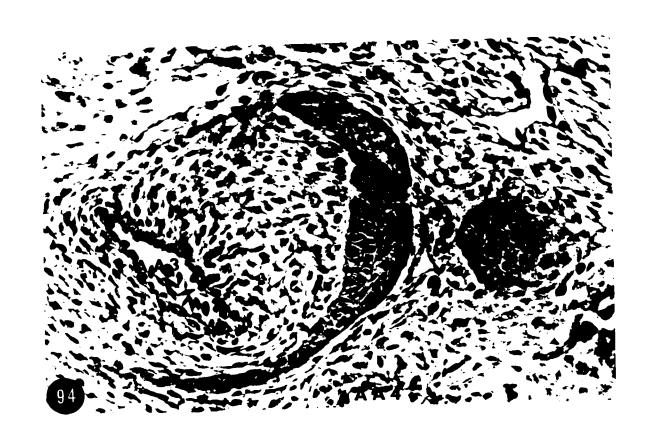
Fig. 95.   A diagram of a representative frontal section

through the branchial region of a 11-4 hour

embryo.   The rectangle indicates the location

of the series of photomicrographs, Figs. 96-

98, and 102-108.

                              DA: dorsal aorta

                              PX: pharynx

                               V: jugular vein

X 40

Figs. 96-98.   Phase contrast photomicrographs taken in

dorsoventral sequence.   The endodermal primor-

dium of Thymus III is seen in Fig. 96.   The

lumen of a third pharyngeal pouch extends into

the dorsal protrusion of the pouch (PH3) (Figs.

97 and 98).

                     AA3:   third aortic arch

                     PH3:   Pahryngeal Pouch III
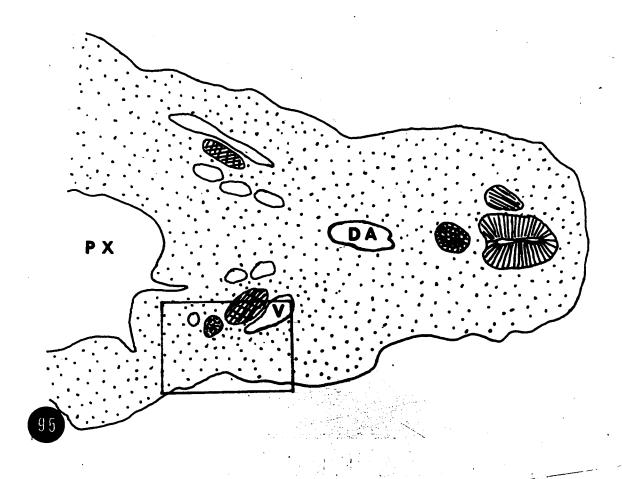
                      NG: nodosal ganglion
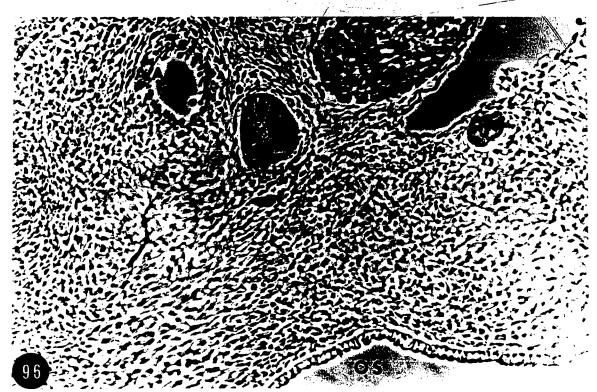
                     TH3:   Thymus III
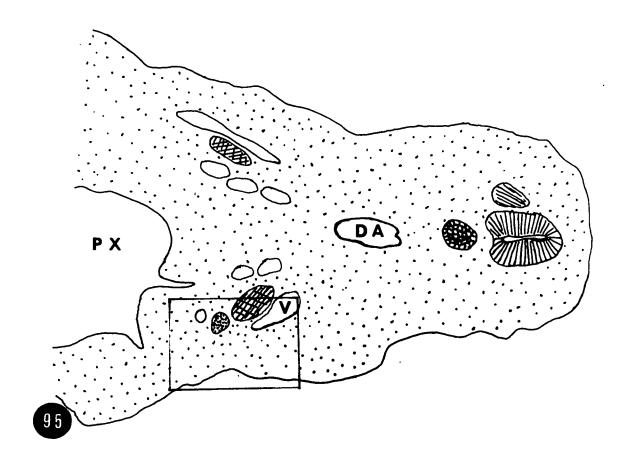
                      OS: external body surface

                       V: jugular vein

X 198

PX

DA

V

95

96

95

PX

DA

V

96

AA 3

V

OS

97

PX

V

OS

98

97
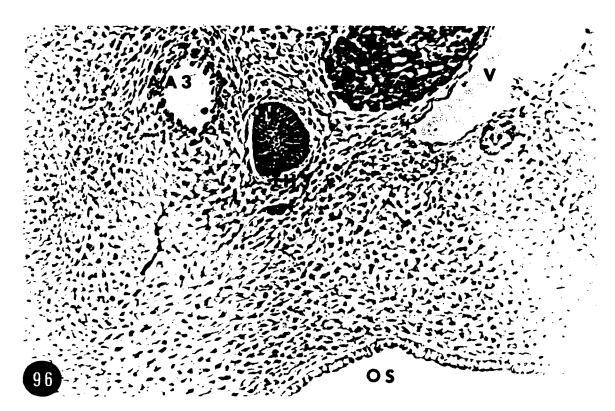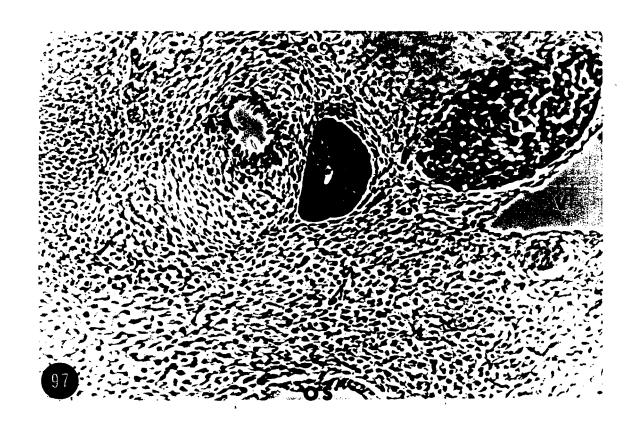
98
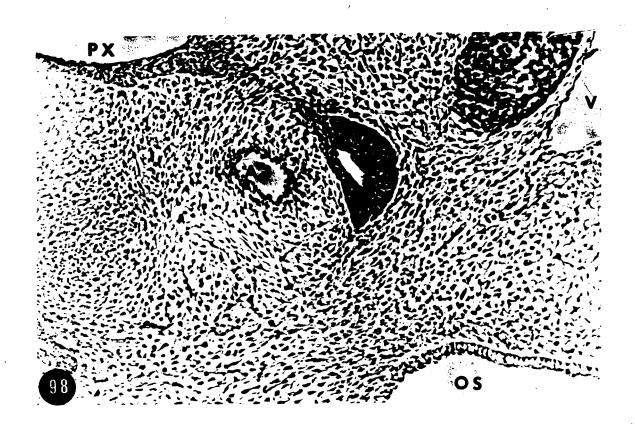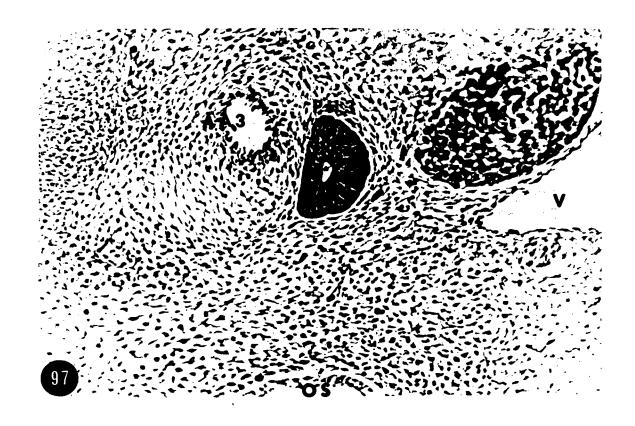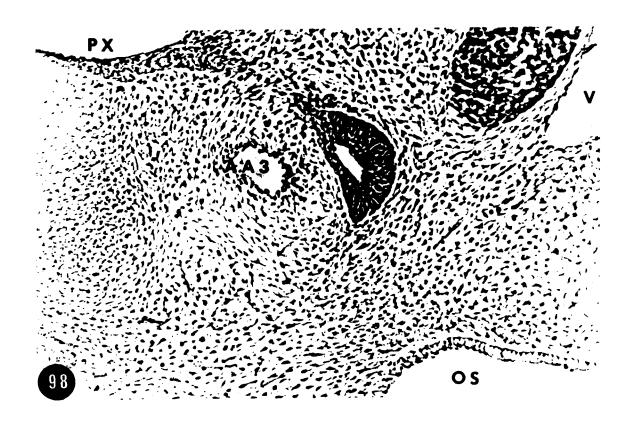
Figs. 99 and 100. Pharyngeal Pouch III at the base of the
endodermal primordium of the thymus of a 5-day
embryo. Acid phosphatase activity is intense
in the epithelial cells, and forms a band around
the lumen (white arrows). Intensely reactive
extrusions (black arrows) are thought to repre-
sent debris and dead epithelial cells.
Barka medium, no counterstain.
X 580

Fig. 101. Pharyngeal Pouch III of a 5-day embryo in
contact with its Ectobranchial Groove III
(ED3). Both epithelia have high activity.
Barka medium, no counterstain.
X 580

ED 3

ME

PH 3

101

Figs. 96-98 and 102-108.   A series of phase contrast photo-
micrographs taken from serial frontal sections of
the branchial region of a 114 hour embryo,
arranged in a dorso-ventral sequence.   The pri-
mordium of Thymus III is seen in Fig. 96.   The
lumen of the third pharyngeal pouch extends into
the dorsal protrusion of the pouch (PH3) (Figs.
97 and 98).   The contact of the dorsal part of
the third pharyngeal pouch (PH3) and the third
ectobranchial duct (ED3) is shown in Fig. 103.
Figs. 104 and 105 show the solid form of the
ventral part of the third pharyngeal pouch (PH3)
in contact or fusing with the ectobranchial duct.
Figs. 106-108 show the dorsal part of the fourth
pharyngeal pouch coming into contact with the
fourth ectobranchial duct.   Many degenerating cells
are recognizable in the branchial ectoderm and the
pouch.

AA3:   third aortic arch
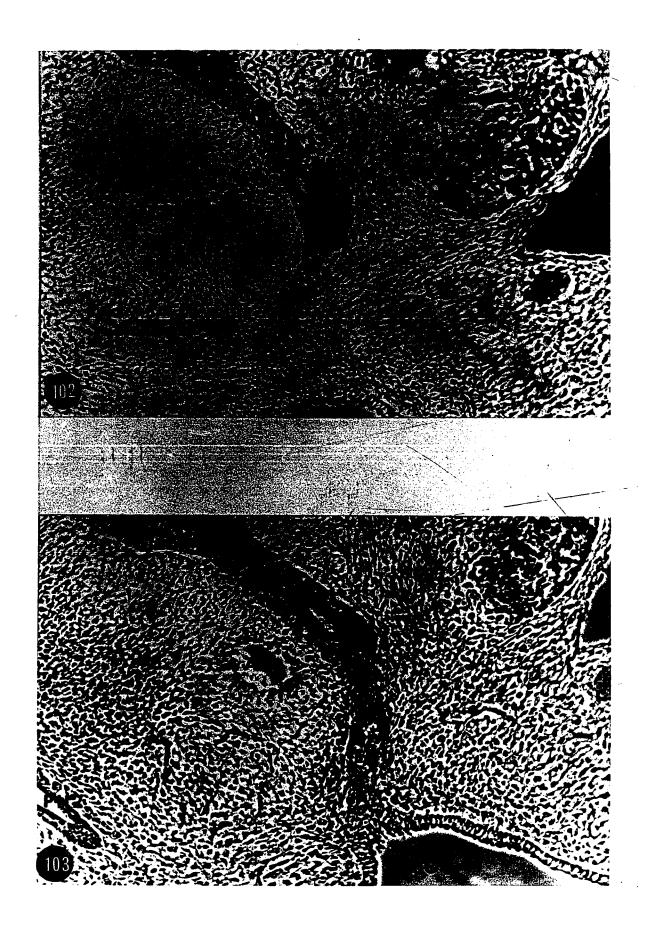
NG: nodosal ganglion
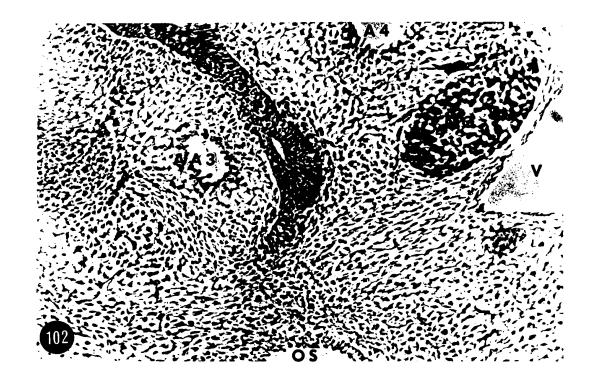
OS: outside the body surface
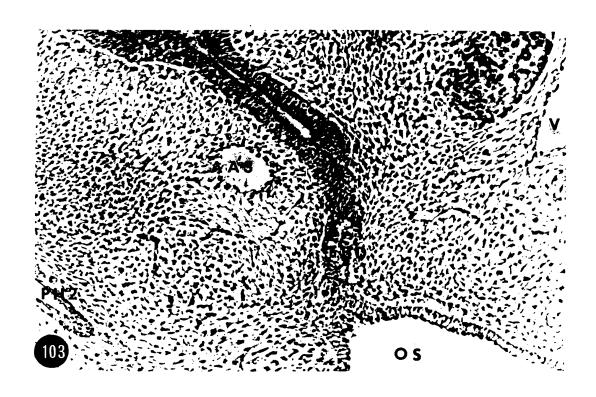
PH3:   third pharyngeal pouch
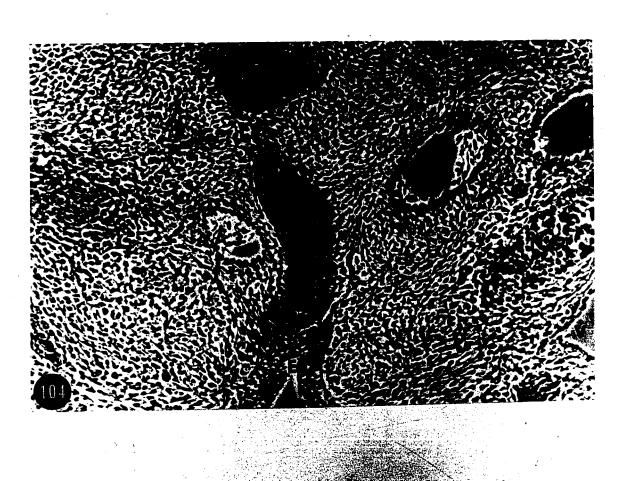
TH3:   Thymus III

V: jugular vein

X 198

104

105

106

107
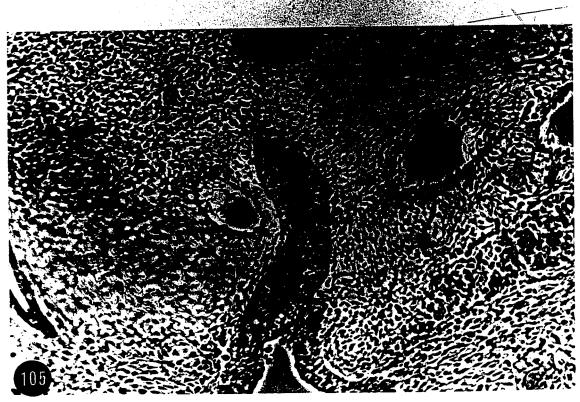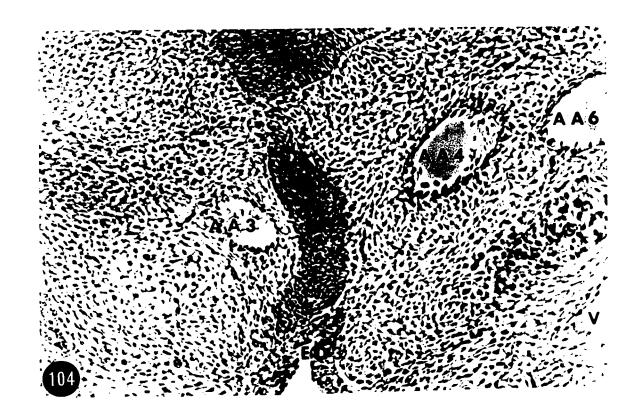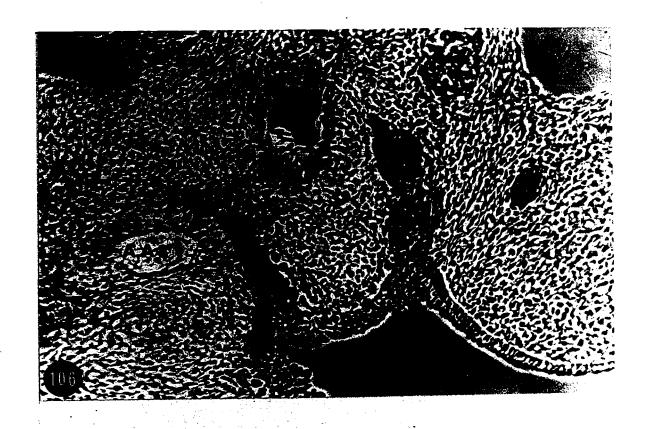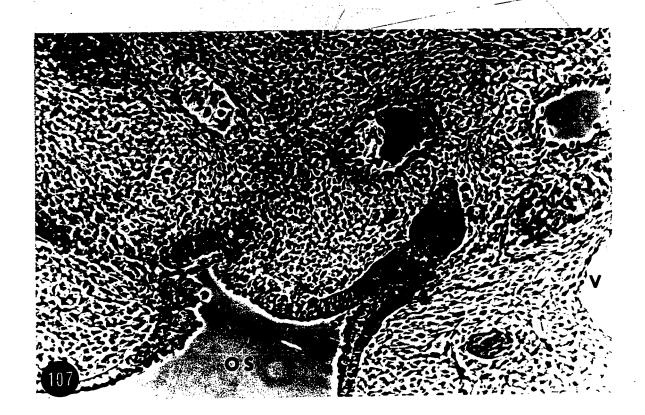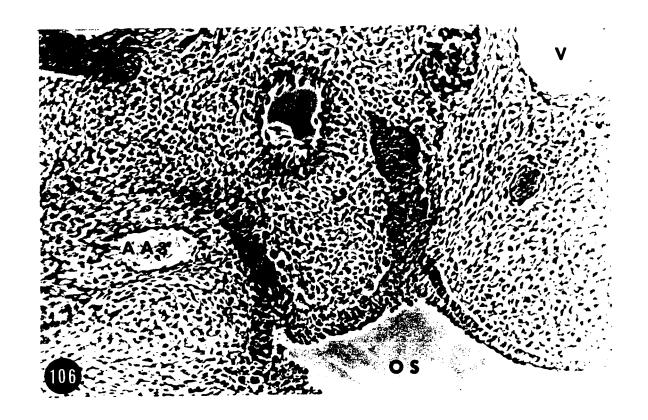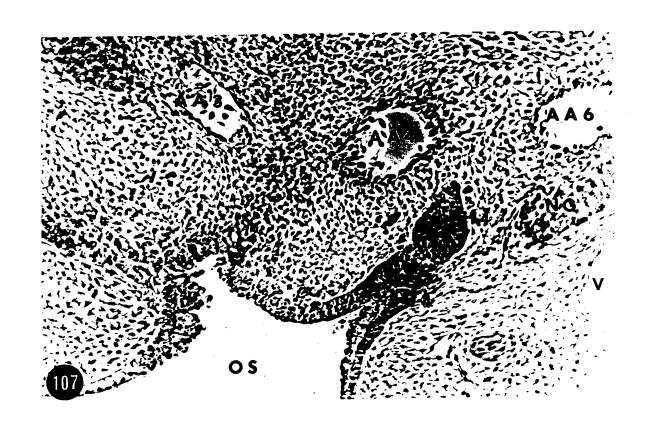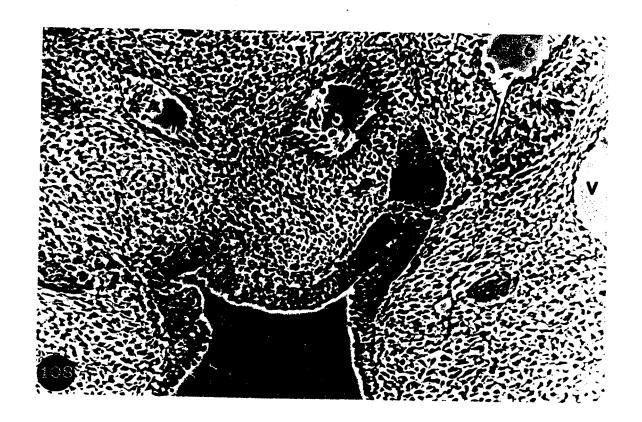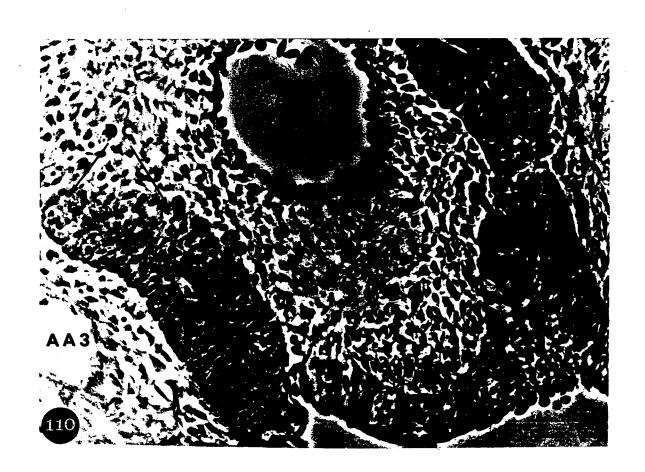
Fig. 110. Higher magnification of the section preceding
           that illustrated in Fig. 106. Pharyngeal
           Pouch III (PH3) extends to the superficial
           branchial ectoderm and the Pharyngeal Pouch
           IV (PH4) contacts the Ectobranchial Duct IV
           (ED4). The epithelia contain many degenerat-
           ing cells.
           X 405

Fig. 111.   Acid phosphatase activity in Thymus III of a
            5-day embryo. The mesenchyme has yellowish
            background stain.
            Barka medium, no counterstain.
            X 600

Fig. 112.   Acid phosphatase activity in the ectoderm on
            the medial side of the hyoid arch, an area
            which undergoes degeneration. The ectoderm
            on the lateral side of the hyoid arch contains
            little activity.
            Barka medium, no counterstain.
            X 110
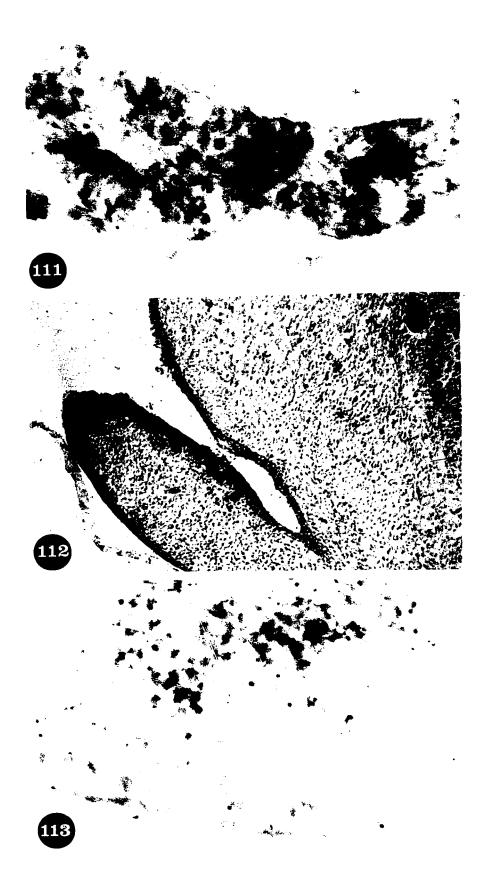
Fig. 113.   Acid phosphatase in the urodeal membrane, an
            area which undergoes degeneration. Three bursa
            vesicles are seen at the right hand side of
            the figure, and the cloacal lumen is seen in
            the upper left hand corner.
            Barka medium, no counterstain.
            X 600

111

112

113

111

112

113
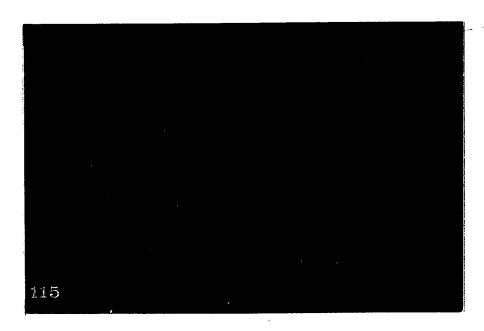
Fig. 114. The anterior part of a 5-day embryo vitally
stained to detect degeneration. Degenerating
cells are distributed in the branchial region
(thin arrows) and in the upper edge of the
forelimb (thick arrow). The head of the
embryo lies to the right of the figure, the
dorsal side of the embryo to the top. Part
of the branchial region indicated by thin ar-
rows is shown at higher magnification in Fig.
145.

    H: heart   E: eye
Nile blue sulfate.
X 42

Fig. 115. Part of the branchial region shown in Fig. 114
to illustrate the distribution of degenerating
cells at the dorsocaudad edge of the hyoid
arch (thin arrow) and in the third and fourth
branchial grooves (thick arrows).

                  Hy: hyoid arch
X 175

114

115
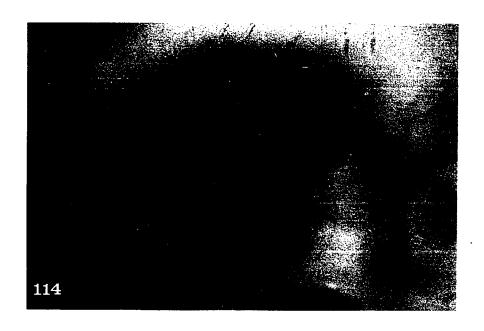
Fig. 116. A montage of several electron micrographs
where the lateral extension of the ventral
part of Pharyngeal Pouch III (upper left
corner) meets the branchial surface. The
demarcation between these two parts is not
clear. Two types of cells are noticed,
light (LC) and dark cells (DC). Cytolysomes
(CL) and cell debris are numerous, both in the
epithelial and mesenchymal cells (ME).
Glutaraldehyde-osmium tetroxide, Araldite,
and uranyl acetate.
X 3000

116

116
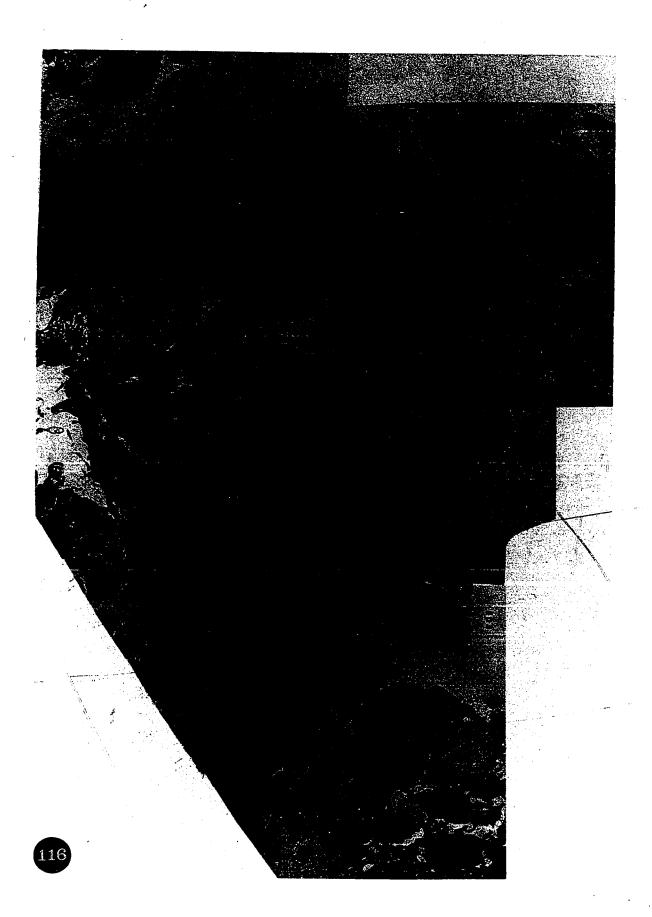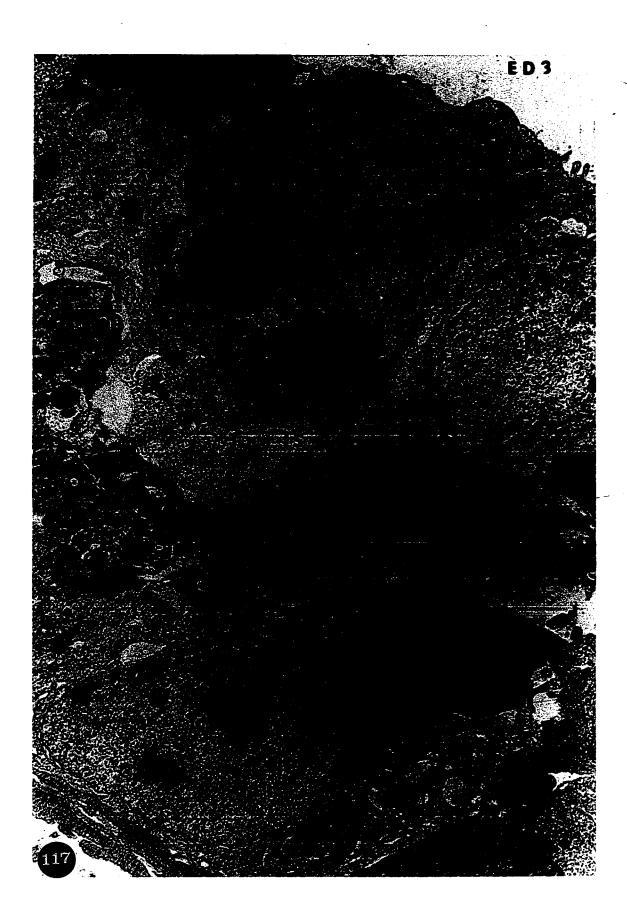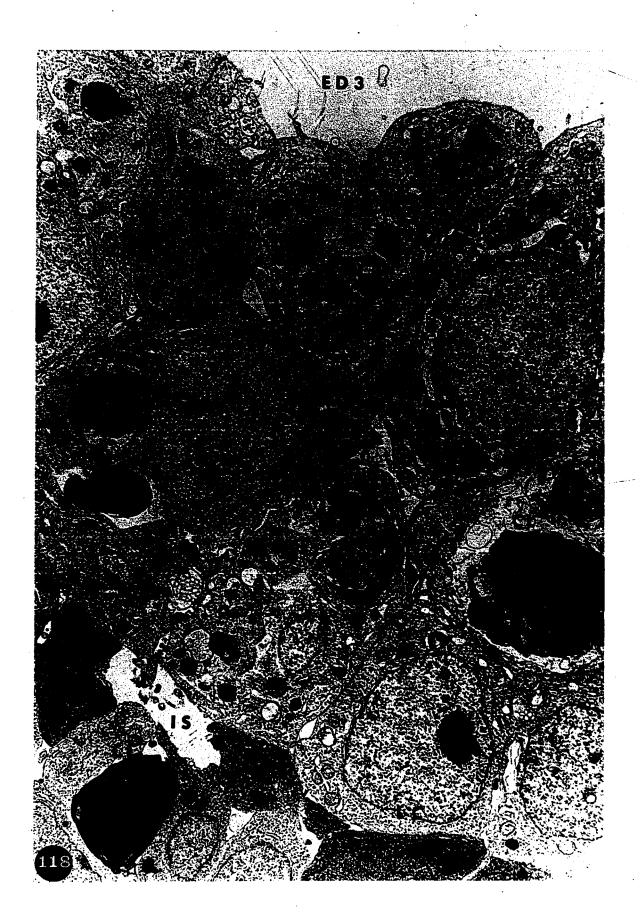
Fig. 117-119. Parts of Fig. 116 shown at higher magnifi-

cation. A myeloid membrane (MM) is seen in the

intercellular space but continuous with the

plasma membrane (Fig. 117). Large intercellular

spaces (IS) and numerous cytolysomes (CL) of

different sizes and forms are noticed. Note

the light (LC) and dark cells (DC).
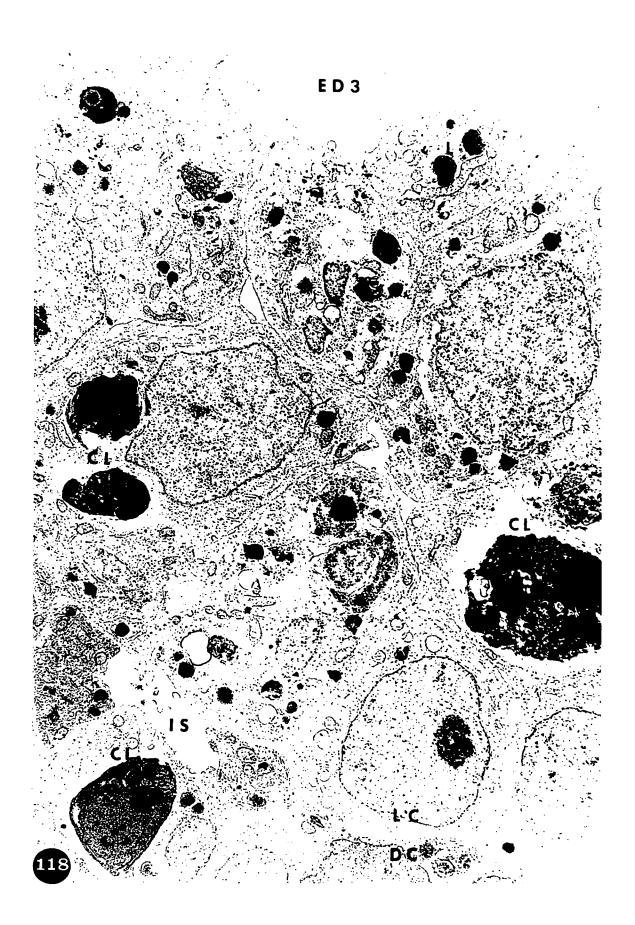
ED3: Branchial Groove III   N: nucleus

Glutaraldehyde-osmium tetroxide, Araldite,

and uranyl acetate.

X 10,138

ED 3

ED 3

CL

CL

IS

CL

L·C

DC
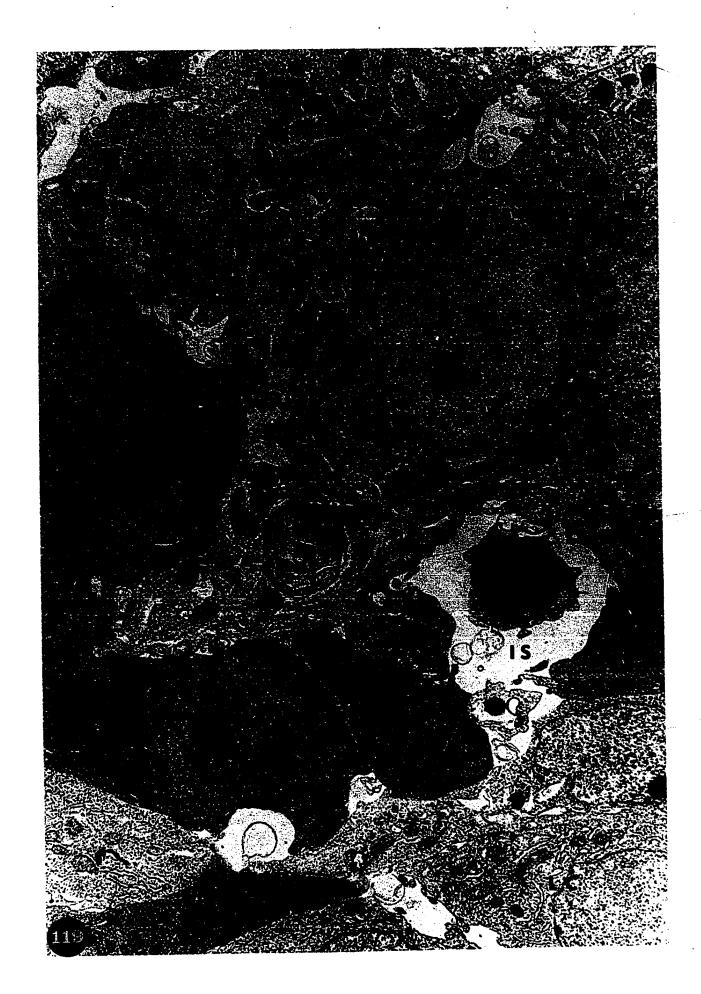
118
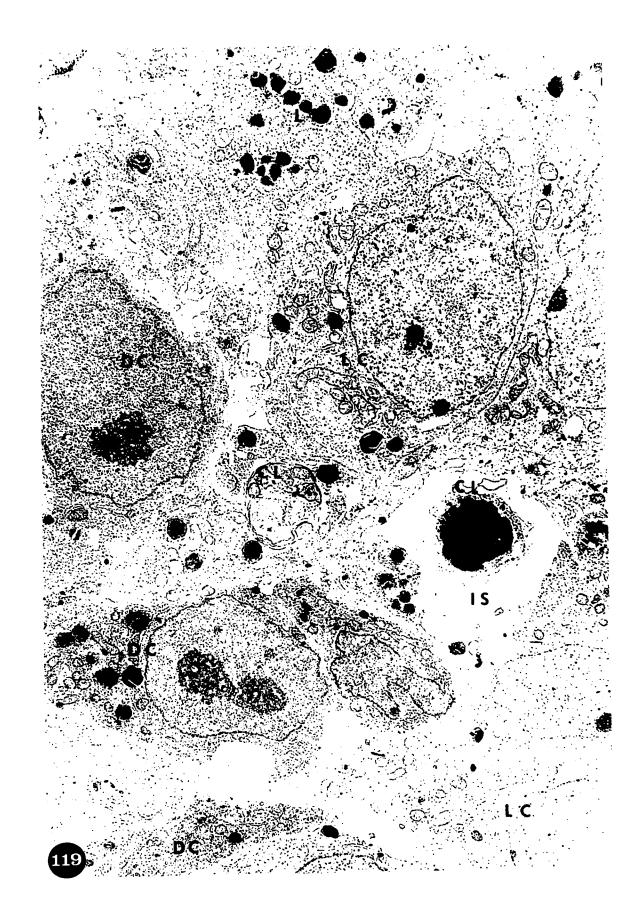
Fig. 120. Parts of light and dark cells in the area of
contact of the Pharyngeal Pouch III and the
Branchial Groove III. Myeloid membranes (MM)
associated with the cytolysome (CL) are found
in both light and dark cells. Lipid droplets
(L) in dark cells contain structures similar
to the cristae of mitochondria, but those of
light cells are more homogeneous. This may
represent a transfer of lipid from the degen-
erating structures of dark cells to light
cells.
Glutaraldehyde-osmium tetroxide, Araldite,
and uranyl acetate.
X 21,000

120
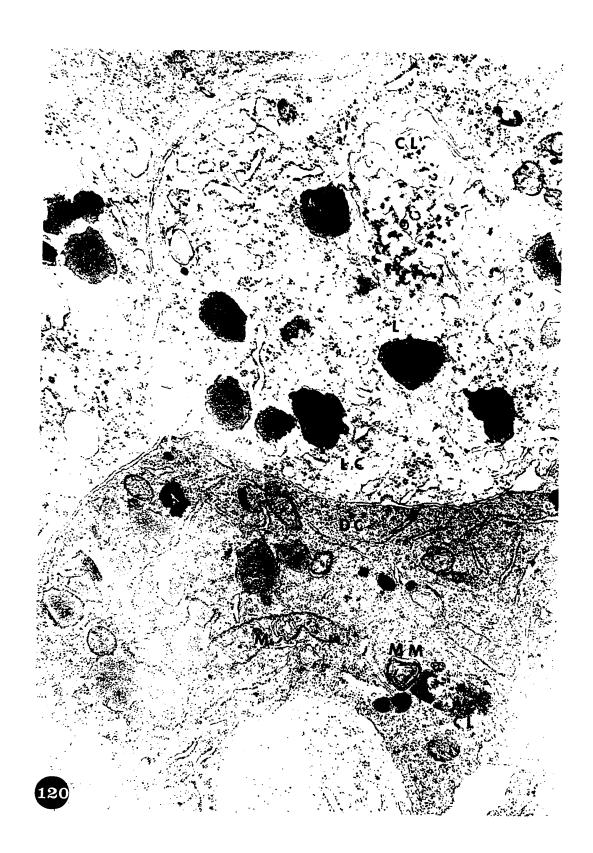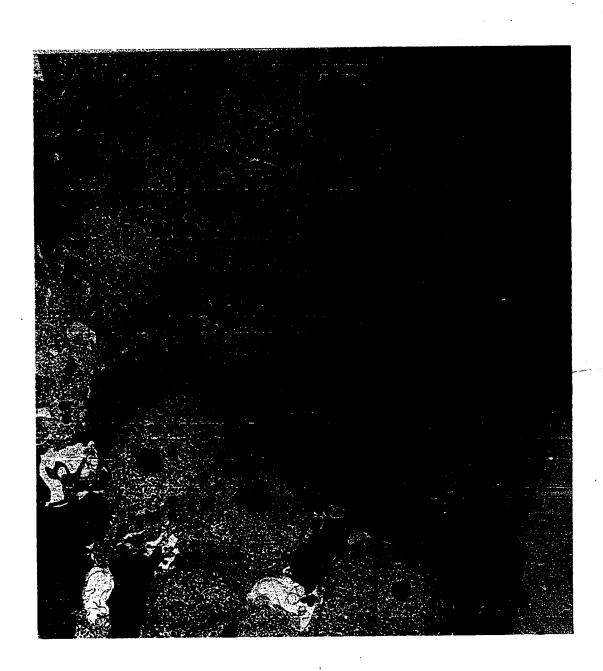
Fig. 121. Lateral part of Branchial Membrane III of a

5-day embryo showing cell debris (CL) and a

mixture of dark and light cells. The light

cells are larger than the dark cells, which

seem crenated or partly dehydrated. Similar

groups of light and dark cells are seen at the

branchial surface. The two types of cells

seem to occur in the vicinity of the contact

between ectoderm and endoderm, but have not

been seen in the deeper parts of Branchial Mem-

brane III. The Branchial Groove is to the top

of the figure, the mesenchyme is to the lower

right.

Glutaraldehyde-osmium tetroxide, Epon, and

uranyl acetate.

X 9,600

CL

121
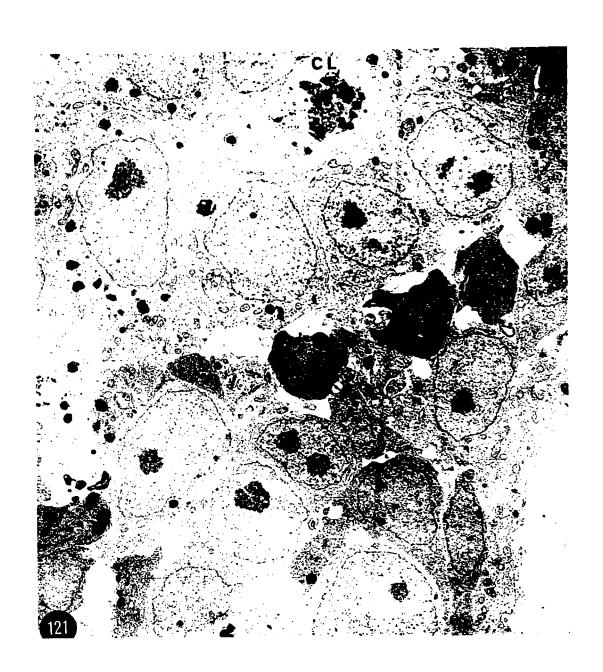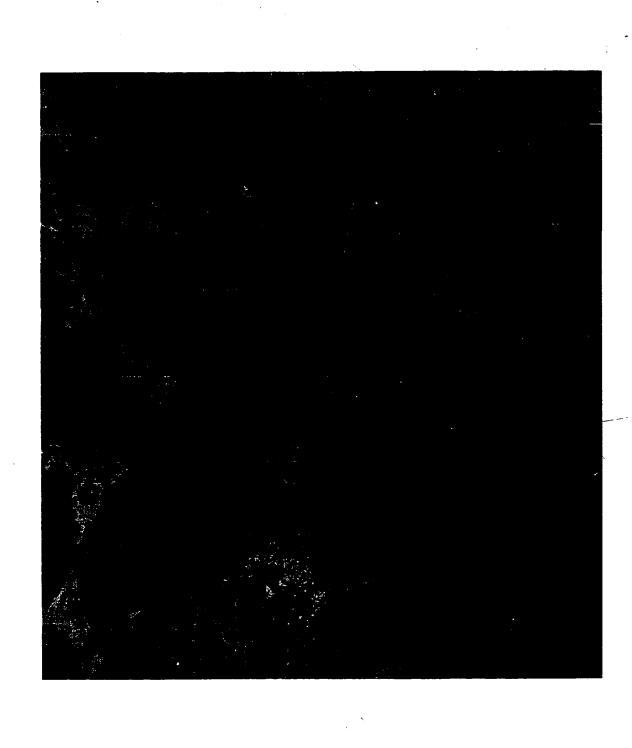
Fig. 122. Part of Thymus III of a 5-day embryo showing

thymus cells near the dorsal tip of the

thymus, and the incomplete basement membrane

surrounding the thymus (thin arrow). One of

the thymus cells has a nuclear whorl (thick

arrow). These are common in thymus cells, but

have not been seen in the adjacent mesenchyma.

Glutaraldehyde-osmium tetroxide, Epon, and
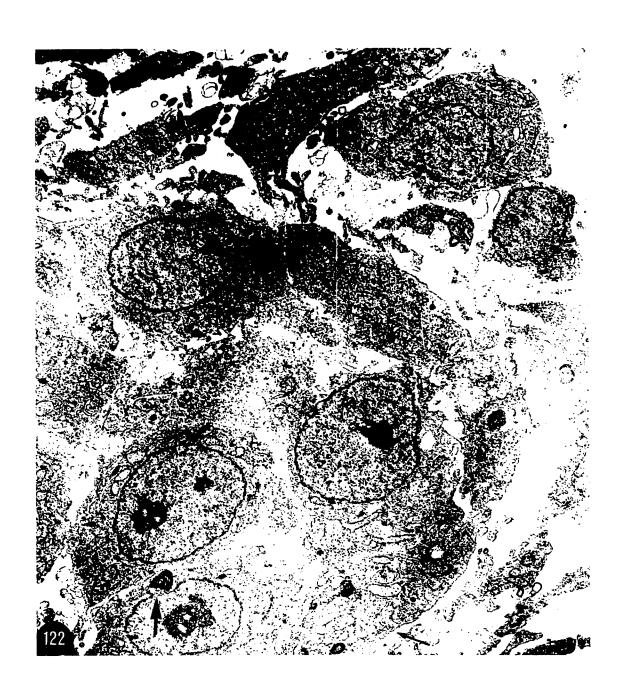
uranyl acetate.

X 10,800

Fig. 123. Part of Thymus III of a 5-day embryo showing

cell debris (D) in the upper center and a

clump of cell debris in the mesenchyme

probably phagocyted by a mesenchymal cell.

Glutaraldehyde-osmium tetroxide, Epon, and

uranyl acetate.

X 12,600

D

ME

123
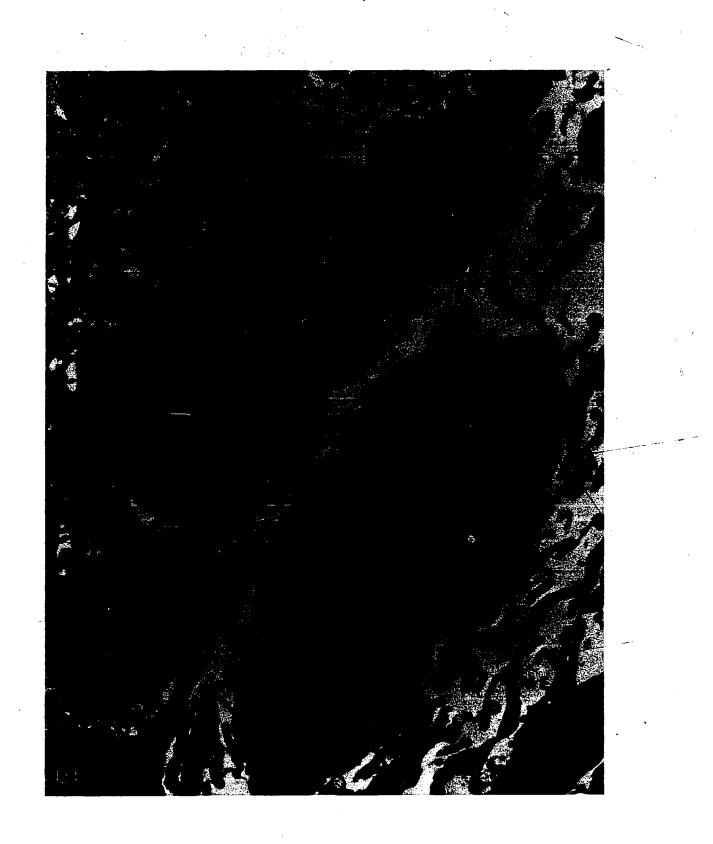
Fig. 124. Part of Thymus III of a 5-day embryo showing

three cytolysomes, differing in appearance

and size.

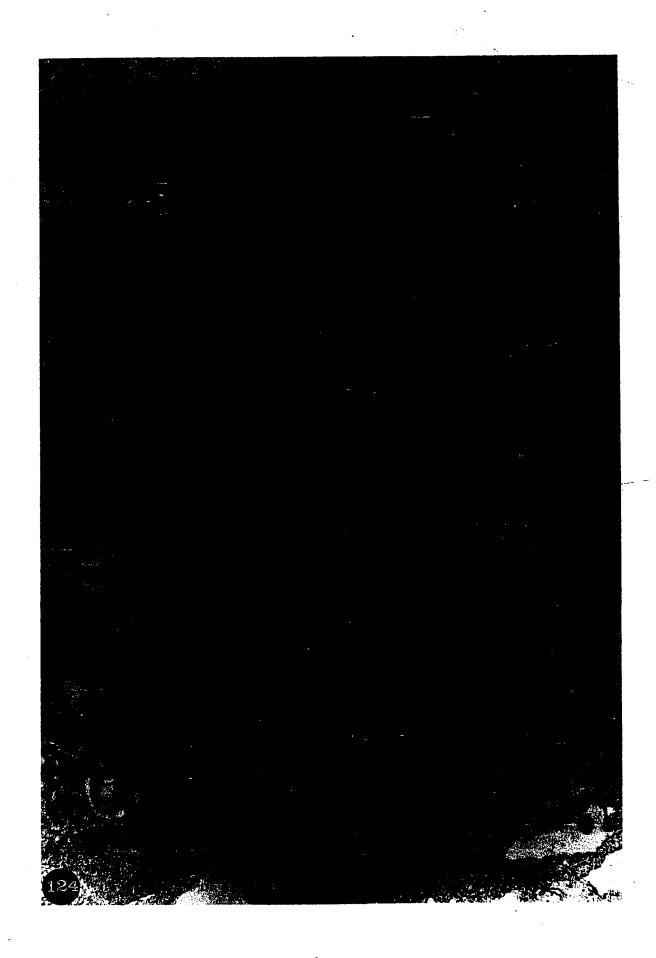Glutaraldehyde-osmium tetroxide, Araldite,

and uranyl acetate.

X 17,200

124

IS

N

2

M M

3

IS

124

Fig. 125. Part of Thymus III of a 5-day embryo showing
a thymus cell and a mesenchymal cell (ME)
just outside the thymus. A basement membrane
is not visible.
Glutaraldehyde-osmium tetroxide, Epon,
and uranyl acetate.
X 35,000

125

M

Fig. 126.   A mesenchymal cell near Thymus III containing

            cell debris (CL).

                    IS: intercellular space

                     M: mitochondrion

                     N: nucleus

            Glutaraldehyde-osmium tetroxide, Araldite,

                and uranyl acetate.

            X 17,200

126

N

Cl

M

I S

126
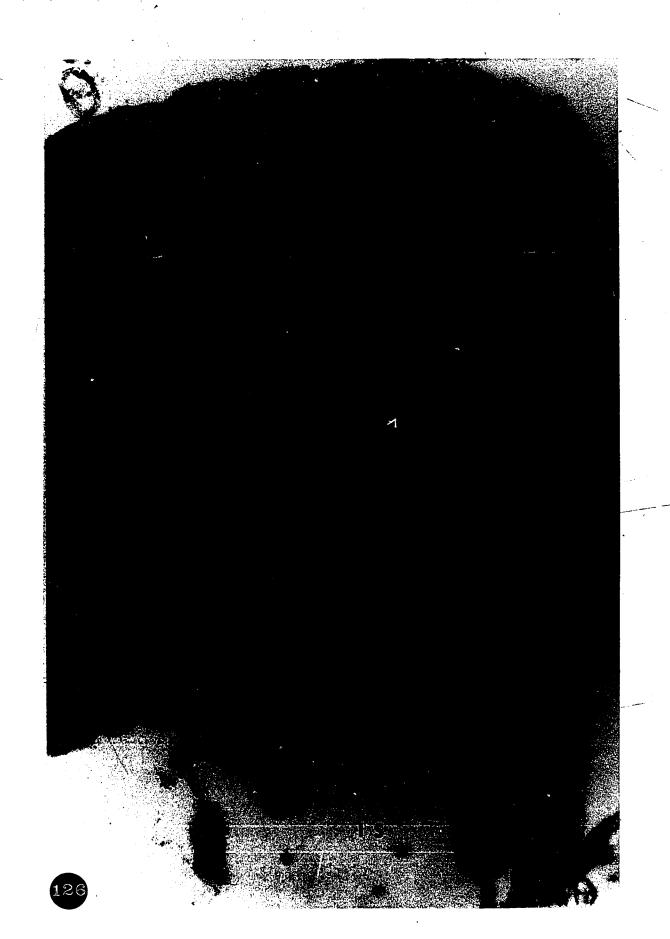
Fig. 127. Part of a cell from Thymus III of a 5-day
embryo showing nuclear whorls and an altered
mitochondrion (M). The presence of several
nuclear pores (NP) indicates that the nuclear
envelope has not been grossly damaged during
fixation and preparation. The contrast
between the whorls and the remainder of the
nuclear envelope suggests that the whorls
represent focal degradations or instability
of parts of the nuclear envelope.
Glutaraldehyde-osmium tetroxide, Araldite,
and uranyl acetate.

X 30,000
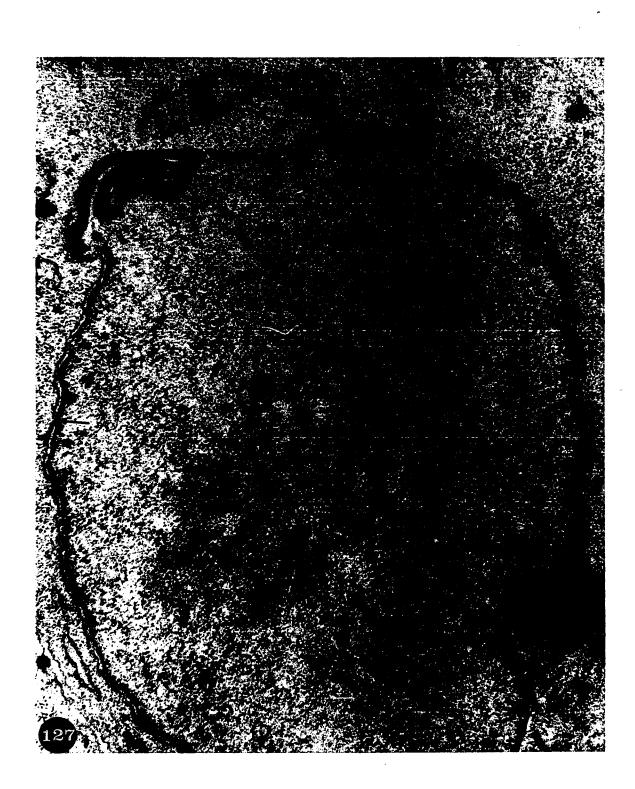
Fig. 128. A thymus cell of a 5-day embryo showing a

myelin figure which protrudes into the inter-

cellular space. The proximate part of the

nuclear envelope is diffuse and the base of

the myelin figure does not contain polyribo-

somes. This suggests that the myelin figure

is a protrusion of the nuclear envelope al-

though a direct connection cannot be seen.

N: nucleus   NP: nuclear pore

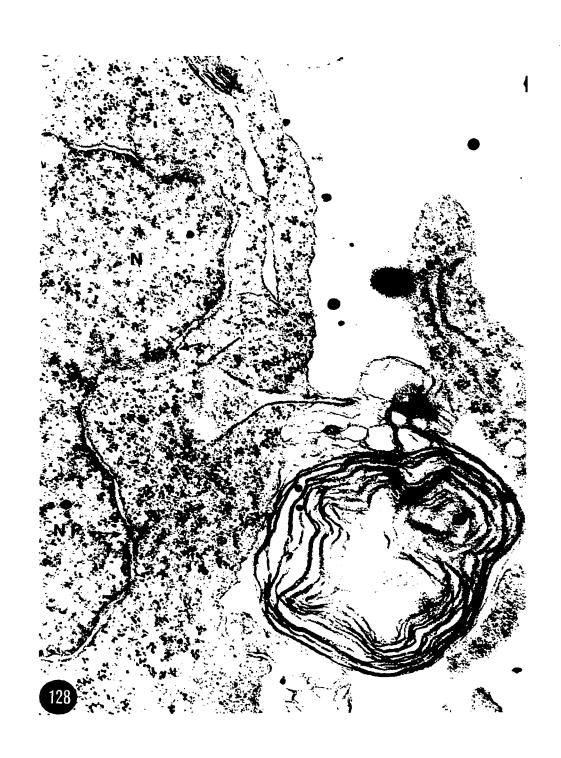Glutaraldehyde-osmium tetroxide, Araldite,
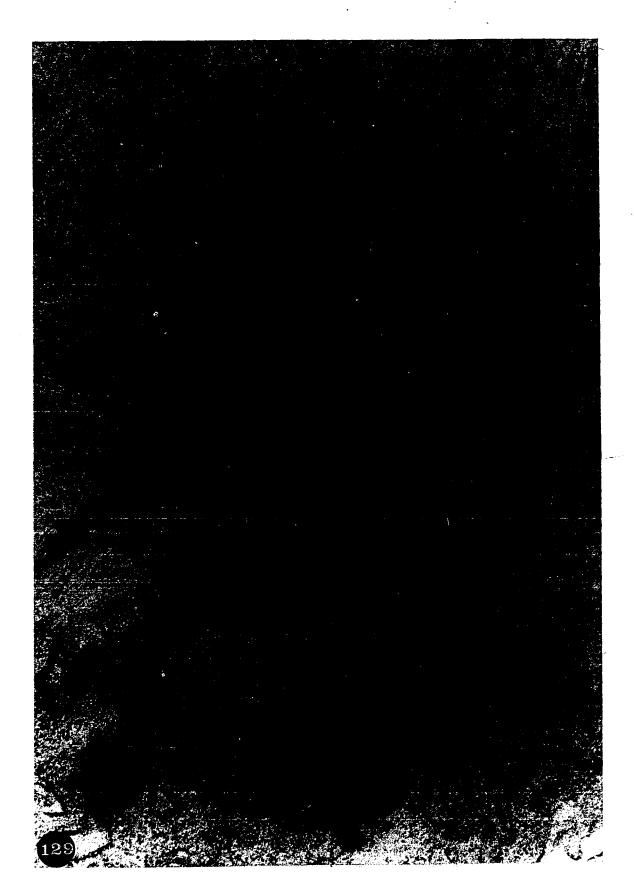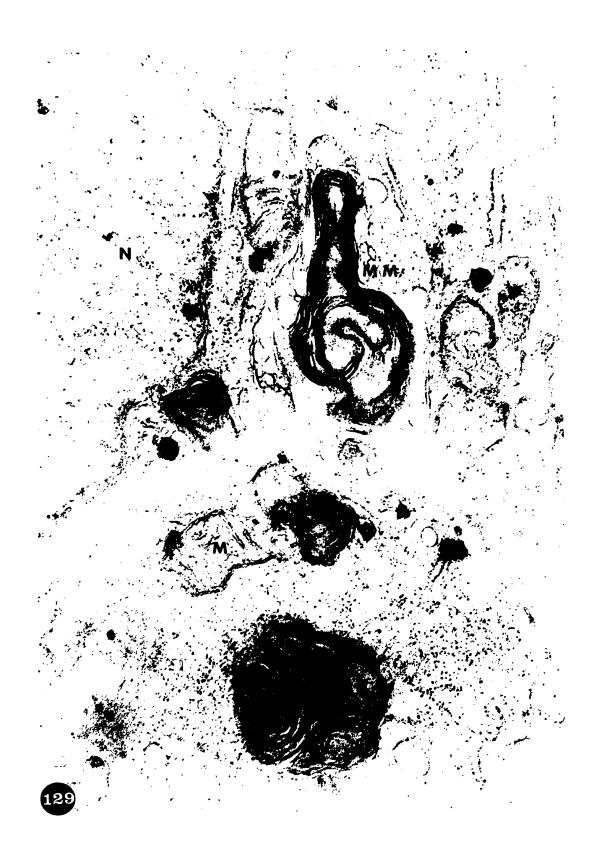
and uranyl acetate.

X 35,200

Fig. 129. Part of Thymus III of a 5-day embryo showing
myelin membranes (MM) in association with a
mitochondrion (M), the nuclear envelope, and
the plasma membrane.

N: nucleus

Glutaraldehyde-osmium tetroxide, Araldite,
and uranyl acetate.

X 32,500

Fig. 130. Thymus cells of a 5-day embryo showing myelin

membranes in association with a mitochondrion (M)

and the endoplasmic reticulum (ER). Loosely

packed myelin membranes (LMM) are present at the

intercellular space (IS) and the plasma membrane.

The nuclear envelope is not connected to the

cytoplasmic myelin figure.

Glutaraldehyde-osmium tetroxide, Araldite,

and uranyl acetate.

X 32,500

Fig. 131. Part of an endodermal cell from the dorsal part
of the Pharyngeal Pouch III showing myelin
membranes (MM) in continuity with the Golgi
membrane (G) and with the endoplasmic reticulum
(ER).

ME: mesenchymal cell

IS: intercellular space

M: mitochondrion

Glutaraldehyde-osmium tetroxide, Araldite, and
uranyl acetate.

X 32,500

131

ME

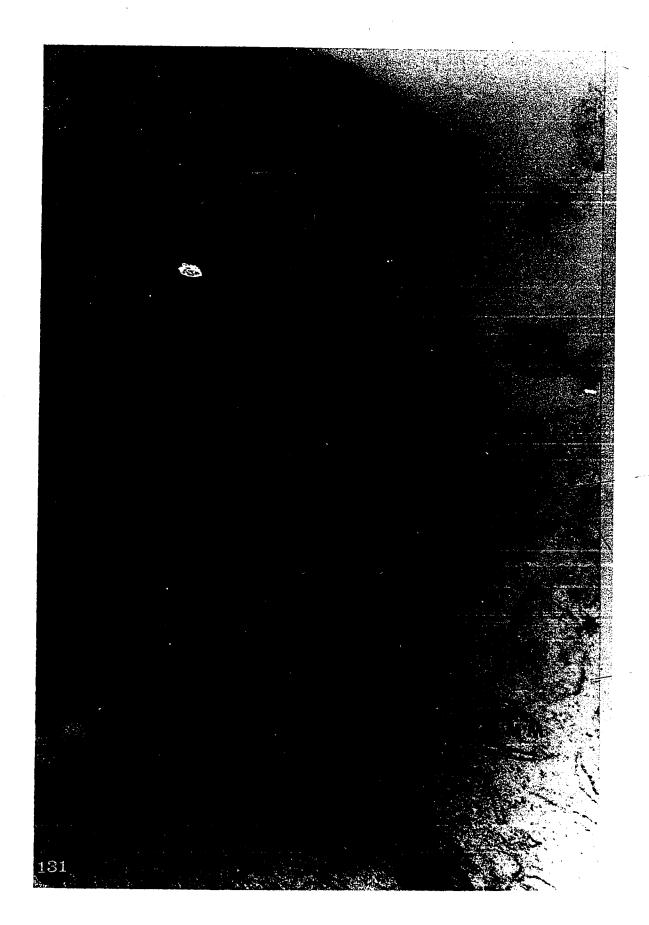ME

IS

M

MM

G

MM

ER

ER

MM

ER

MM

131

Fig. 132. Part of an endodermal cell from the dorsal part

of the Pharyngeal Pouch III at the top, and

part of a mesenchymal cell at the bottom. The

endoplasmic reticulum (ER) of the mesenchymal

cell approaches and may contact the plasma

membrane (arrow). Tubular endoplasmic reticulum

is common in the mesenchymal cells. An indenta-

tion of the nucleus (IN) of the endodermal cell
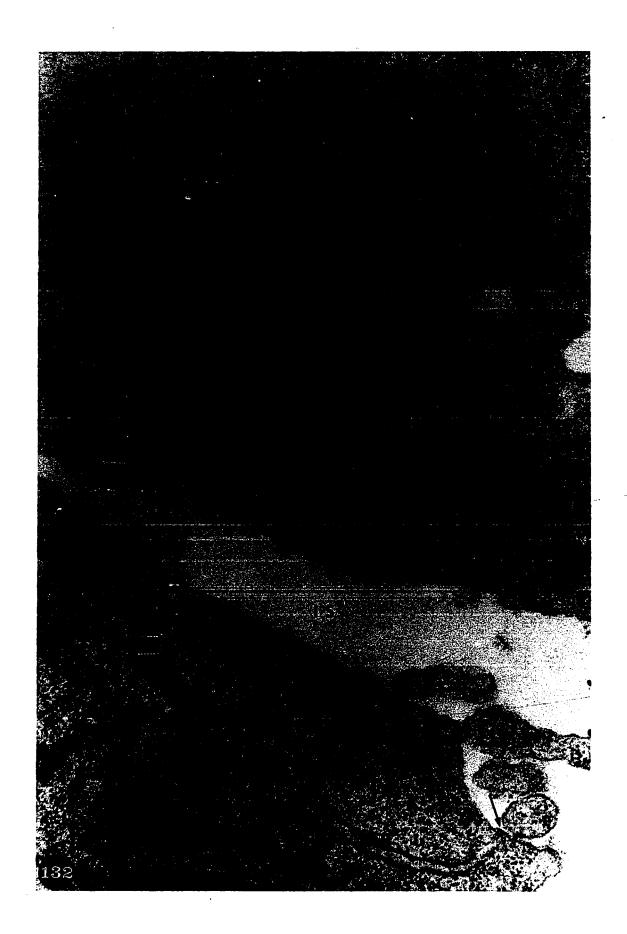
is noted.

    IS: intercellular space

    M: mitochondrion

    N: nucleus

Glutaraldehyde-osmium tetroxide, Araldite, and

uranyl acetate.
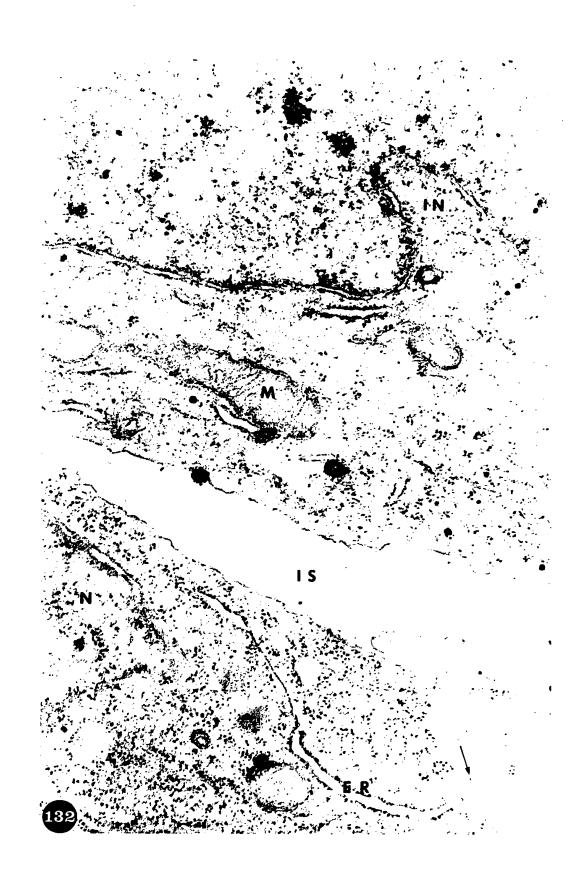
X 30,000

Fig. 133.   A frontal through section of Thymus IV of a
            5-day embryo showing Feulgen-positive pyknotic
            debris (arrows). The pyknotic debris is darker
            than normal nuclei.
            Feulgen reaction for DNA, counterstained with
            luxo fast blue.
            X 580

Fig. 134.   Branchial Groove IV (ED4) of a 5-day embryo
            showing Feulgen-positive pyknotic debris
            (arrows) in the ectodermal epithelium.
            Feulgen reaction for DNA, counterstained with
            luxo fast blue.
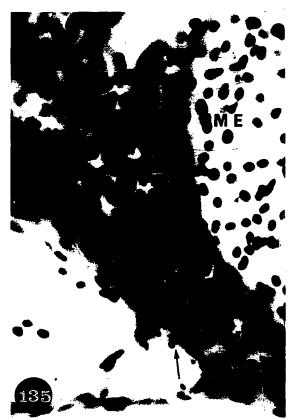   X 580

Fig. 135.   Part of the urodeal membrane of a 9-day embryo
            to show the Feulgen-positive pyknotic nuclei
            (arrows).
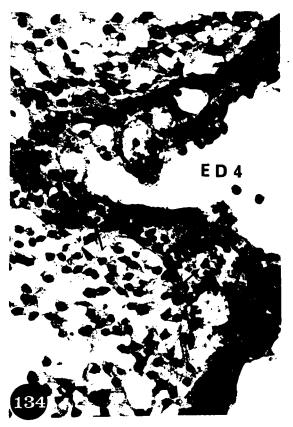   Feulgen reaction for DNA, counterstained with
            luxo fast blue.
            X 580

ED 4

ME

133

124

135

133

ED 4

134

ME

135

Figs. 136-141. Representative serial paraffin sections of

Thymus III of a 5-day embryo showing Colcemid-

arrested metaphases (long arrows) and pyknotic

debris (short arrows). Arrested metaphases are
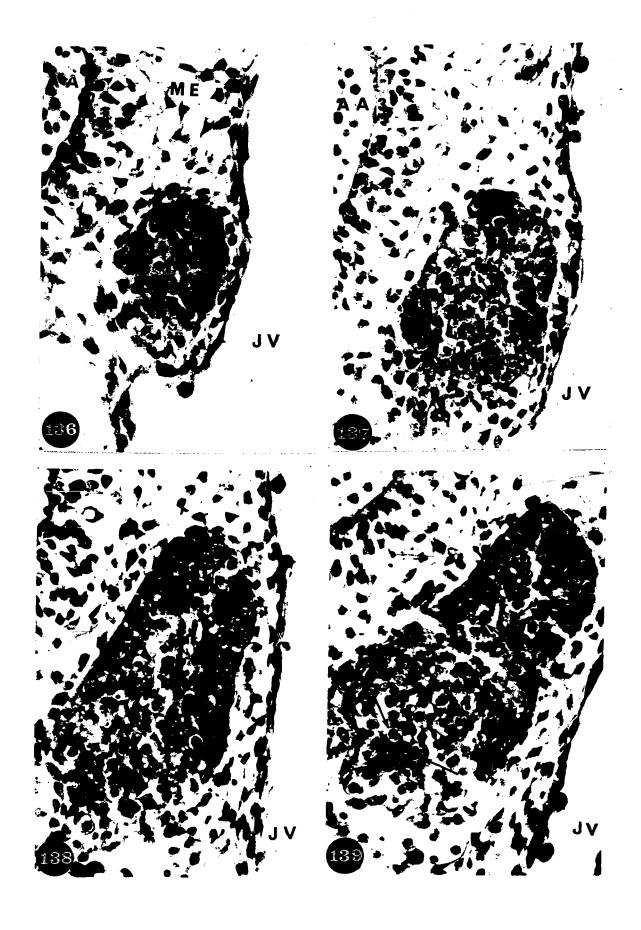
also seen in the mesenchyme.

AA3: third aortic arch

ME: mesenchyme

JV: jugular vein

Colcemid treatment for six hours before killing,

formalin-calcium, stained with Erhlich haema-

toxylin.

X 580

A   ME

JV

136

AA

JV

JV

137
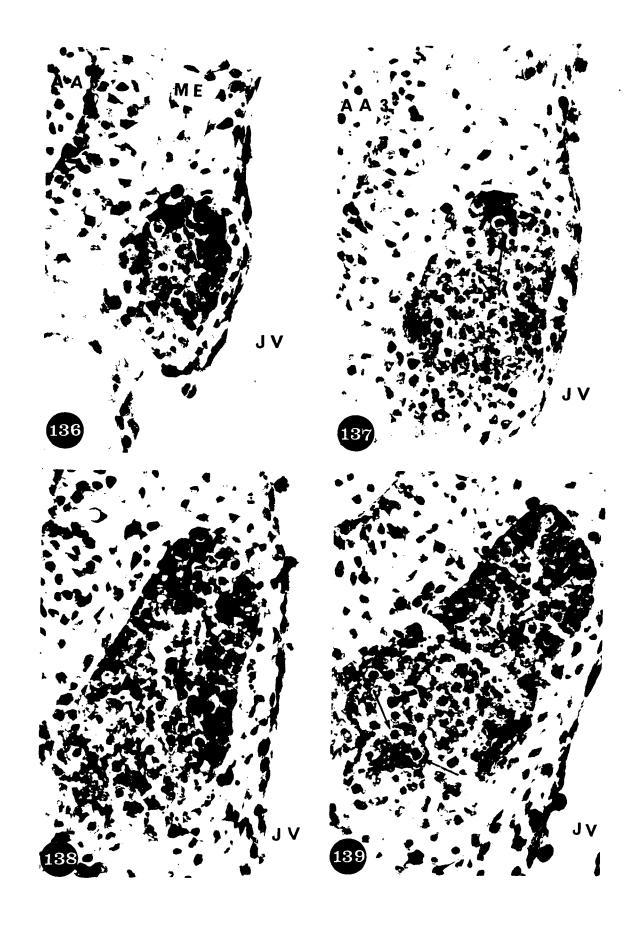
JV

138

JV

139

136

137

138

139

Fig. 142. Pharyngeal Pouch IV (PH4) of a 5-day embryo showing arrested metaphases along the lumen of the pouch after Colcemid treatment. Sections stained with Erhlich haematoxylin. X 580

PH 4

A A

140

141

PH 4

A A

142